

18th INTERNATIONAL SHIP AND
OFFSHORE STRUCTURES CONGRESS

09-13 SEPTEMBER 2012
ROSTOCK, GERMANY

VOLUME 1



COMMITTEE III.1

ULTIMATE STRENGTH

COMMITTEE MANDATE

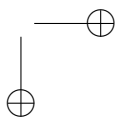
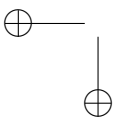
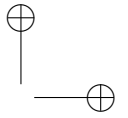
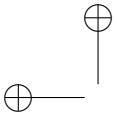
Concern for the ductile behaviour of ships and offshore structures and their structural components under ultimate conditions. Attention shall be given to the influence of fabrication imperfections and in-service damage and degradation on reserve strength. Uncertainties in strength models for design shall be highlighted.

COMMITTEE MEMBERS

Chairman: Jeom K. Paik
Hadi Amlashi
Bart Boon
Kim Branner
Piero Caridis
Purnendu Das
Masahiko Fujikubo
Chien-Hua Huang
Lennart Josefson
Patrick Kaeding
Chang-Wook Kim
Guy Parmentier
Ilson P. Pasqualino
Cesare M. Rizzo
Suhas Vhanmane
Xiaozhi Wang
Ping Yang

KEYWORDS

Ultimate strength; ultimate limit states; ultimate limit state design; buckling collapse; load-carrying capacity; fabrication-induced initial imperfections; in-service damage and degradation; reserve strength; uncertainties; strength model.



CONTENTS

| | | |
|-------|--|-----|
| 1 | Introduction | 289 |
| 2 | Fundamentals for Ultimate Limit State-based Design and Safety Assessment | 290 |
| 2.1 | Types of Limit States | 290 |
| 2.2 | Factors Affecting Nonlinear Structural Consequences | 290 |
| 2.3 | Ultimate Limit State Criterion | 291 |
| 2.4 | Format Types for Structural Design and Safety Assessment | 291 |
| 3 | Rules and Guidelines | 293 |
| 3.1 | International Association of Classification Societies (IACS) | 293 |
| 3.2 | Classification Societies | 294 |
| 3.2.1 | American Bureau of Shipping (ABS) | 294 |
| 3.2.2 | Bureau Veritas (BV) | 297 |
| 3.2.3 | Det Norske Veritas (DNV) | 300 |
| 3.2.4 | Germanischer Lloyd SE (GL) | 302 |
| 3.2.5 | Registro Italiano Navale (RINA) | 302 |
| 3.3 | Other Regulatory Agencies | 302 |
| 4 | Definition of Parameters and their Uncertainties | 302 |
| 4.1 | Introduction | 302 |
| 4.2 | Physical Aspects | 303 |
| 4.3 | Modelling Uncertainties | 306 |
| 4.4 | Ageing and In-service Damage Effects | 307 |
| 4.5 | Conclusions on Practical Aspects in Ultimate Strength Assessment | 308 |
| 5 | Recent Advances | 308 |
| 5.1 | Components | 308 |
| 5.1.1 | Plates | 308 |
| 5.1.2 | Stiffened Panels | 310 |
| 5.1.3 | Shells | 312 |
| 5.1.4 | Composite and Sandwich Panels | 314 |
| 5.1.5 | Tubular Members and Joints | 317 |
| 5.1.6 | Influence of Fabrication-related Initial Imperfections | 320 |
| 5.1.7 | Influence of In-service Damage | 322 |
| 5.2 | Systems | 324 |
| 5.2.1 | Ship-shaped Structures | 324 |
| 5.2.2 | Other Marine Structures | 326 |
| 5.2.3 | Influence of Fabrication-related Initial Imperfections | 326 |
| 5.2.4 | Influence of In-service Damage | 327 |
| 6 | Benchmark Studies | 327 |
| 6.1 | Candidate Methods | 327 |
| 6.2 | Target Structures | 328 |
| 6.2.1 | Plates | 328 |
| 6.2.2 | Stiffened Panels | 329 |
| 6.2.3 | Hull Girders | 329 |
| 6.3 | Modelling Techniques | 331 |
| 6.3.1 | Plates | 331 |
| 6.3.2 | Stiffened Panels | 331 |
| 6.3.3 | Hull Girders | 334 |
| 6.4 | Results and Observations | 334 |
| 6.4.1 | Plates | 334 |

| | | |
|-------|--|-----|
| 6.4.2 | Stiffened Panels | 335 |
| 6.4.3 | Hull Girders | 345 |
| 7 | Conclusion and Recommendations | 351 |
| 8 | Acknowledgements | 352 |
| 9 | References | 352 |

1 INTRODUCTION

The basic strength members in ships and offshore structures include support members (e.g., stiffeners, plate girders), plates, and stiffened panels. During their lifetime, the structures that are constructed using these members are likely subjected to various types of loading or deformation that is for the most part operational but may, in some cases, be extreme or even accidental. The sources of such loading and deformation include fabrication-related initial imperfections (e.g., initial distortions, welding residual stress, softening in the heat-affected zone of welded aluminium structures); abnormal waves/winds/currents; dynamic pressure loads arising from sloshing, slamming or green water; low temperature in Arctic operations; cryogenic conditions resulting from liquefied natural gas cargo; ultra-high pressure in ultra-deep waters; elevated temperature due to fire; blast loads due to explosion; impact loads associated with collision, grounding or dropped objects; and age-related degradation such as corrosion, fatigue cracking and local denting damage.

Figure 1 illustrates the various types of phenomena that may occur in ships and offshore structures while they are in service (Paik, 2011). Each of these phenomena occurs in different scenarios with different mechanisms, but it is interesting to mention that all of them commonly give rise to nonlinear structural consequences that involve both geometric and material nonlinearities. For the robust design of ships and offshore structures, therefore, it is essential to accurately and efficiently identify the nonlinear structural consequences associated with such phenomena.

In the past, criteria and procedures for the structural design of ships and offshore platforms were primarily based on allowable stresses and simplified buckling checks for structural components. However, it is now well recognised that ultimate limit state-based approaches are much better methodologies for structural design and strength

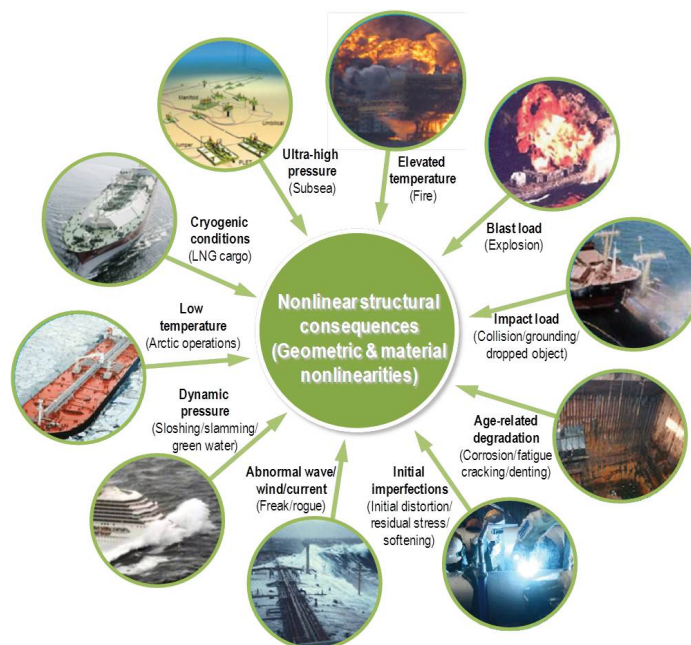


Figure 1: Various types of phenomena causing nonlinear structural consequences in ships and offshore structures (Paik, 2011)

assessment than the traditional working stress-based approaches, as the latter are typically formulated as a fraction of material such as yield strength. This situation exists because it is difficult to determine the true margin of structural safety using linear elastic methods alone when the remaining ultimate limit states are unknown. It follows that determining the true ultimate limit state is of crucial importance to obtain consistent measures of safety that can form a fairer basis for comparisons of structures of different sizes, types, and characteristics. The ability to correctly assess the true margin of safety would also inevitably lead to improvements in related regulations and design requirements (Paik and Thayamballi, 2003).

To obtain a safe and economic structure, ultimate limit state-based capacity and structural behaviour under known loads must be accurately assessed. The structural designer can perform a relatively refined structural safety assessment even in the preliminary design stages if there are simple expressions available for accurately predicting the ultimate limit state behaviour. A designer may even desire to do this not only for the intact structure, but also for structures with premised or accidental damage as a way of anticipating their damage tolerance and survivability.

This report presents advances and possible future trends in ultimate strength computation methods for ship and offshore structural components and their system structures. Papers published since the ISSC 2009 Congress are mainly discussed here, but older publications are also included if they are considered to present fundamental and important findings in line with the mandate of the present Committee.

2 FUNDAMENTALS FOR ULTIMATE LIMIT STATE-BASED DESIGN AND SAFETY ASSESSMENT

2.1 *Types of Limit States*

A limit state is defined as the condition beyond which a structural member or entire structure fails to perform its designated function. Four types of limit states are relevant here (Paik and Thayamballi, 2003; ISO, 2007), namely

- Ultimate limit state (ULS)
- Serviceability limit state (SLS)
- Fatigue limit state (FLS)
- Accidental limit state (ALS)

ULS is the collapse of a structure due to a loss of structural capacity in terms of stiffness and strength that typically arises from the buckling and plastic collapse of structural components. SLS represents failure in normal operations due to a deterioration in routine functionality. Typical examples of SLS include local damage, unacceptable deformation, and excessive vibration and noise that affect the proper functioning of structural elements or equipment. FLS is the fatigue cracking of structural details as the result of stress concentration and damage accumulation under repeated loading actions. ALS is the excessive structural damage that results from accidents such as collisions, grounding, explosions, and fire – all of which affect the safety of the structure, the environment, and the personnel. This report discusses ULSs.

2.2 *Factors Affecting Nonlinear Structural Consequences*

Nonlinear structural consequences involving ultimate limit states can be represented as a function of various factors, namely

$$\text{Nonlinear structural consequences} = f(a,b,c,d,e,f,g,h) \quad (1)$$

where,

- a = geometrical factors associated with buckling, large deflection, crushing, or folding,
- b = material factors associated with yielding/plasticity, ductile/brittle fracture, rupture, or cracking damage,
- c = fabrication-related initial imperfections such as initial distortion, residual stress, and softening,
- d = load types/components (quasi-static),
- e = dynamic factors (strain rate sensitivity, inertia effect) associated with freak/rogue/abnormal waves and the impact pressure actions that arise from sloshing, slamming, or green water; overpressure actions arising from explosions; and impacts due to collisions, grounding, or dropped objects,
- f = temperature factors such as low temperatures associated with cold water operation and/or low-temperature cargo and high temperatures due to fire and explosions,
- g = age-related deterioration such as corrosion and fatigue cracking, and
- h = human factors related to unusual operations in terms of ship speed (relative to the maximum permitted speed or acceleration), ship heading, and loading conditions.

2.3 Ultimate Limit State Criterion

The design condition of a structure can be expressed as follows (Paik and Thayamballi, 2003).

$$G = C_d - D_d \geq 0 \quad (2)$$

where G = a performance function, C_d = the design value of capacity (strength), and D_d = the design value of demand (load).

In ULS-based design and safety assessment, capacity is the ultimate strength and demand represents extreme actions or action effects such as those in the most unfavourable conditions to which the structure may be subjected. In accidental condition, capacity represents the residual ultimate strength of structures with damages caused by the corresponding accident.

2.4 Format Types for Structural Design and Safety Assessment

Two types of format for design or safety assessment are usually applied to ensure that a structure has an adequate degree of safety and reliability against ULSs (Paik and Thayamballi, 2003), namely

- Partial safety factor format
- Probabilistic format

The partial safety factor format considers the effects of uncertainties in the following form.

$$C_d = C_k/\gamma_C, D_d = \gamma_D D_k \quad (3)$$

where C_k and D_k = the characteristic values of capacity and demand, respectively, and γ_C and γ_D = the partial safety factors associated with the uncertainties of capacity and demand, respectively.

Substituting equation (3) into equation (2) yields

$$G = \frac{C_k}{\gamma_C} - \gamma_D D_k \geq 0 \quad (4)$$

The measure of structural adequacy is determined as follows.

$$\eta = \frac{C_d}{D_d} = \frac{1}{\gamma_C \gamma_D} \frac{C_k}{D_k} \quad (5)$$

where η is a measure of structural adequacy. To ensure safety, η must be greater than 1. This report focuses on defining C_k for ship and offshore structures including plates, stiffened panels, and hull girders.

The probabilistic format, in contrast, is more rigorous when considering the effects of uncertainties. The performance function of equation (2) can be rewritten as a function of the basic variables, $x_1, x_2, \dots, x_i, \dots, x_n$, as follows (Paik and Thayamballi, 2007).

$$G(x_1, x_2, \dots, x_i, \dots, x_n) = 0 \quad (6)$$

When $G > 0$, the structure is in the desired state. When $G \leq 0$, it is in an undesired state. Based on the first-order approximation, equation (6) can be written using the Taylor series expansion as follows.

$$G \cong G(\mu_{x_1}, \mu_{x_2}, \dots, \mu_{x_i}, \dots, \mu_{x_n}) + \sum_{i=1}^n \left(\frac{\partial G}{\partial x_i} \right)_{\bar{x}} (x_i - \mu_{x_i}) \quad (7)$$

where μ_{x_i} = the mean value of variable x_i ; \bar{x} = the mean values of the basic variables $(\mu_{x_1}, \mu_{x_2}, \dots, \mu_{x_i}, \dots, \mu_{x_n})$; and $(\partial G / \partial x_i)_{\bar{x}}$ = the partial differentiation of G with respect to x_i at $x_i = \mu_{x_i}$.

The mean value of function G is then given by

$$\mu_G = G(\mu_{x_1}, \mu_{x_2}, \dots, \mu_{x_i}, \dots, \mu_{x_n}) \quad (8)$$

where μ_G = the mean value of function G .

The standard deviation of function G is calculated by

$$\sigma_G = \left[\sum_{i=1}^n \left(\frac{\partial G}{\partial x_i} \right)_{\bar{x}}^2 \sigma_{x_i}^2 + 2 \sum_{i>j} \left(\frac{\partial G}{\partial x_i} \right)_{\bar{x}} \left(\frac{\partial G}{\partial x_j} \right)_{\bar{x}} \text{covar}(x_i, x_j) \right]^{1/2} \quad (9)$$

where σ_G = the standard deviation of G ; σ_{x_i} = the standard deviation of variable x_i ; $\text{covar}(x_i, x_j) = E[(x_i - \mu_{x_i})(x_j - \mu_{x_j})]$ = the co-variation of x_i and x_j ; and $E[\]$ = the mean value of $\[\]$.

When the basic variables, $x_1, x_2, \dots, x_i, \dots, x_n$, can be considered independent of one another, $\text{covar}(x_i, x_j) = 0$. In this case, equation (9) can then be simplified to

$$\sigma_G = \left[\sum_{i=1}^n \left(\frac{\partial G}{\partial x_i} \right)_{\bar{x}}^2 \sigma_{x_i}^2 \right]^{1/2} \quad (10)$$

The so-called reliability index for this case can be defined using the first-order second-moment method (FOSM), as follows.

$$\beta = \frac{\mu_G}{\sigma_G} \quad (11)$$

where β = the reliability index. To ensure safety, the reliability index must be greater than the target reliability index.

For a function, G , of two parameters, C_d and D_d that are considered to be statistically independent, with mean μ_G and standard deviation σ_G , the reliability index, β , can be obtained as follows.

$$\beta = \frac{\mu_C - \mu_D}{\sqrt{\sigma_C^2 + \sigma_D^2}} \quad (12)$$

where μ_C and μ_D = the mean values of C_d and D_d , respectively, and σ_C and σ_D = the standard deviations of C_d and D_d , respectively.

In this regard, it is clear that the primary tasks that need to be accomplished by the structural design criterion of Equation (2) are how to determine C_k , D_k , γ_C , and γ_D for the partial safety factor design format, and μ_C , μ_D , σ_C , and σ_D for the probabilistic design format. The present Committee is concerned with the determination of these values in conjunction with the ultimate limit state design.

3 RULES AND GUIDELINES

3.1 International Association of Classification Societies (IACS)

The criteria for buckling and ultimate strength can be found in Section 10 of the IACS Common Structural Rules (CSR) for Double Hull Oil Tankers (2010a), which apply to double hull oil tankers of 150 m length and upward. These criteria are applied to local supporting members, primary support members, and other structures such as pillars, corrugated bulkheads, and brackets.

The characteristic buckling strength is to be taken as the most unfavourable/critical buckling mode for each structural element. Some of the different buckling modes considered include the uniaxial and biaxial buckling of plate, the column buckling of stiffeners, the torsional buckling of stiffeners, and the buckling of the web plate of primary support members.

These prescriptive buckling requirements augment various baseline assumptions and limitations. Namely, the structural elements are expected to comply with certain stiffness and proportion requirements specified in the rules, which include plate panel proportions, local support members, web and flange plates, pillars and brackets, stiffness of stiffeners, and the spacing between flange supports or tripping brackets. For corrugated bulkheads, local flange/web buckling, unit corrugation buckling, and overall buckling failure mode under axial compression and lateral pressure are to be checked.

To assess the buckling of plates and stiffened panels subject to combined stress fields, the advanced buckling assessment method is to be followed because it considers effects such as nonlinear geometrical behaviour, inelastic material, initial imperfections, welding residual stresses, interactions between structural elements, simultaneous acting loads, and boundary conditions. A more detailed description of this methodology can be found in Appendix D of the CSR for Double Hull Oil Tankers.

The buckling and ultimate strength checks for bulk carriers is detailed in Section 3, Chapter 6 of the CSR for Bulk Carriers (2010b), which applies to the hull structures of single-side skin and double-side skin bulk carriers with a length $L \geq 90$ m. The structural elements are verified at the elementary plate panel level and the partial and total panel levels (lateral buckling mode and torsional buckling mode). Corrugated watertight bulkheads are to be checked against shear buckling in flooded conditions.

Harmonized CSR for both tankers and bulk carriers are under development, and the first draft is scheduled for review about 1st July 2012.

3.2 *Classification Societies*

3.2.1 *American Bureau of Shipping (ABS)*

In addition to the IACS Common Structural Rules for Double Hull Oil Tankers (ABS, 2010a) and Bulk Carriers (2010b), the ABS published Rules for Building and Classing Steel Vessels (ABS, 2011b) (referred to hereafter as “ABS Steel Vessel Rules”), a Guide for Building and Classing Floating Production Installations (ABS, 2009), a Guide for Building and Classing Floating Offshore Liquefied Gas Terminals (ABS, 2010), a Guide for Building and Classing Drillships (ABS, 2011a), and a Guide for the Buckling and Ultimate Strength Assessment of Offshore Structures (ABS, 2004) (referred to hereafter as “ABS Buckling Guide”) – all of which provide buckling and ultimate strength criteria for the classification of different types of ships and offshore structures other than those specified in the CSR Rules.

The criteria given in these rules/guides correspond to either the serviceability (buckling) limit state or the ultimate limit state for structural members and panels. A working stress method is adopted, where uncertainties in loads and resistances are inherently incorporated into the maximum strength allowable utilization factors. The process for the buckling and ultimate strength assessment of stiffened panels consists of three levels, namely plate panels, stiffened panels, and girders and webs, which correspond to different failure modes.

The buckling and ultimate strength of each level is expected to be greater than its preceding level to avoid the collapse of the entire structure. This is achieved, to a certain degree, through buckling control concepts that serve as the assumptions and limits of the strength criteria in the rules/guides as an effectiveness assurance and should generally be followed in design. Examples include: the buckling strength of stiffeners is generally to be greater than that of the plate panels they support; the stiffness of stiffeners with the associated effective plating is not to be less than certain values for them to provide adequate lateral stability; moments of inertia for main supporting members with their associated effective plating are to be sufficient to prevent out of plane buckling; tripping brackets are to be installed to prevent the torsional instability of deep girders and webs with wide flanges; and proportional limits are to be provided to prevent the local instability of stiffener face plates and webs.

Plates

According to the ABS rules/guides, the buckling of plate panels is acceptable as long as the ultimate strength check is satisfied because the plate panels can sustain further loading until the ultimate strength is reached. However, a buckling check is necessary to establish the attached plating width for a stiffened panel check, with the full width used for plating that does not buckle and the effective width applied if it does buckle.

Details of buckling and ultimate strength criteria for plates subject to in-plane and lateral pressure loads can be found in the various ABS rules and guides mentioned above.

Stiffened Panels

The failure modes of stiffeners include beam-column buckling, torsional-flexural buckling, and local flange/web plate buckling. Buckling state limits for a stiffened panel are considered its ultimate state limits because the compressive strength decreases quickly if any of these types of buckling occur.

Strong Supporting Members

In general, girders are designed to be stocky (the column slenderness ratio is not greater than 0.5) so that lateral buckling can be disregarded along with torsional buckling if the appropriate tripping brackets are provided. Otherwise, the girder is to be checked against the various failure modes.

Corrugated Panels

Corrugated panels are “self-stiffened” panels with failure modes that can include flange/web plate buckling, unit corrugation buckling, and entire corrugation buckling (overall buckling) depending on the panel configuration and loading type. The buckling strength is the least value obtained from these three failure modes, considering any load type and combination.

Cylindrical Shells

A fabricated steel cylindrical shell is an important type of compression element used in offshore structures. It is stiffened against buckling by ring and/or stringer stiffeners. The criteria for calculating the buckling of ring and/or stringer stiffened cylindrical shells subject to axial loading, bending moment, radial pressure or a combination of these loads are presented in the ABS Buckling Guide (ABS, 2004).

Five failure modes are considered in the ABS Buckling Guide (ABS, 2004):

- Local shell or curved panel buckling (i.e., the buckling of the shell between adjacent stiffeners). The stringers remain straight and the ring stiffeners remain round.
- Bay buckling (i.e., the buckling of the shell plating together with the stringers, if present, between adjacent ring stiffeners). The ring stiffeners and the ends of the cylindrical shells remain round.
- General buckling, (i.e., the buckling of one or more ring stiffeners together with the attached shell plus stringers, if present).
- Local stiffener buckling (i.e., the torsional/flexural buckling of stiffeners, ring, or stringer or the local buckling of the web and flange). The shell remains undeformed.
- Column buckling (i.e., the buckling of the cylindrical shell as a column).

A higher level of failure usually leads to more severe consequences than the preceding level. Therefore, the similar buckling control requirements regarding stiffness and shell plate proportions, rings, and stringers mentioned previously are necessary to better assure the safety of the stiffened cylindrical shells.

Individual Structural Members

Individual structural members include tubular and nontubular members with uniform geometric properties along their entire lengths that are made of a single material and are used widely in offshore topside structures and various platforms for supporting major equipment. The buckling behaviour of the structural members is influenced by a variety of factors, including sectional shape, material characteristics, boundary conditions, loading types and parameters, and fabrication methods. The four different failure modes consist of flexural buckling, torsional buckling, lateral-torsional buckling and local buckling and all four are taken into account. The loading application includes any of following loads and load effects:

- Axial force in the longitudinal direction
- Bending moment

- Hydrostatic pressure
- Combined axial tension and bending moment
- Combined axial compression and bending moment
- Combined axial tension, bending moment, and hydrostatic pressure
- Combined axial compression, bending moment, and hydrostatic pressure

The individual members are categorized into compact and noncompact sections. If an individual member is from the noncompact section, the local buckling strength is to be assessed and the effect of local buckling must be taken into account when determining the critical buckling stress of the member.

Tubular Joints

The failure mode of a tubular joint depends on the joint configuration, joint geometry, and loading conditions. These failure modes include:

Local failure of the chord:

- Plastic failure of the chord wall in the vicinity of the brace.
- Cracking that leads to a rupture of the brace from the chord.
- Local buckling in the chord's compression areas.

Global failure of the chord:

- Ovalization of the chord cross-section.
- Beam bending failure.
- Beam shear failure between adjacent braces.

In addition, a member can fail away from the brace-chord joint due to chord or brace overloading. These failure modes can be established by following the approach described in the ABS Buckling Guide (ABS, 2004).

Ultimate strength criteria are provided for the following loads and load effects:

- Axial load in a brace member,
- In-plane bending moment in a brace member,
- Out-of-plane bending moment in a brace member,
- Axial load in a chord member,
- In-plane bending moment in a chord member,
- Out-of-plane bending moment in a chord member, and
- Combinations of the abovementioned loads and load effects.

Hull Girder

The vertical ultimate hull girder strength for either hogging or sagging conditions within the $0.4L$ amidship region is to satisfy the limit state as specified below in the partial factor format: $\gamma_s M_s + \gamma_w M_w \leq M_u / \gamma_u$, where M_s , M_w , and M_u are the permissible still-water bending moment, the vertical wave-induced bending moment, and the hull girder ultimate strength, respectively and γ_s , γ_w , and γ_u are the corresponding load or safety factors.

The hull girder's ultimate strength, M_u , is calculated using the incremental-iterative approach. This approach assumes that the hull transverse section remains plane during each curvature increment, and that the hull structure exhibits elasto-plastic behaviour. To calculate the ultimate strength, the hull transverse section is divided into a set of individual elements that include a plate element, a stiffener element, an element consisting of a stiffener with an associated effective width of plating, and a corner element consisting of a plate's intersection with a web plate.

The elements, while considered to be acting independently, are combined to provide the ultimate strength resistance of the hull's transverse cross-section. Each element, when compressed beyond its buckling limit, has reduced strength according to its buckling and ultimate strength characteristics. All relevant failure modes for individual structural elements such as plate buckling, beam-column buckling, torsional stiffener buckling, local stiffener buckling and their interactions must be considered to identify the weakest inter-frame failure mode. Each failure mode can be described by the load-end shortening curve, as stated in various ABS rules/guides. Numerical calculations (Sun and Wang, 2005a, 2005b; Wang *et al.*, 2011) show that the results are in good agreement when this and other methods are applied.

Buckling Analysis by Finite Element Method

In addition, the ABS Buckling Guide (2004) provides guidance for applying a buckling analysis using the finite element method (FEM) as an alternative to the formulations presented in the guide. The key issues in an FEM analysis such as the determination of the loads and boundary conditions, the development of the mathematical model, the choice of element types, the design of the mesh, solution procedures and verification and validation, are outlined in the guide.

3.2.2 Bureau Veritas (BV)

In ship assessment the ultimate strength assessment requirements consist of checking the structural strength under the worst, extreme quasi-static loading conditions (BV, 2011). For offshore floating units (BV, 2010), the requirements for resisting quasi-static loading are joined by a requirement that the unit structure be able to resist some of the impact conditions defined in the rules. Safety factors are applied to loads and strength as well to take into account the uncertainties regarding parameters and the lack of accuracy that results from simplified approaches.

Ship Structure

The BV assessment approach for ultimate strength is based on a multilevel analysis of plates, stiffened panels, and the hull girder.

When plates do not fulfil the strength criteria, provided that the plate strength failure alone does not lead to adverse consequences, the residual strength of the plate is taken into account in the stiffened panel strength. In the process of ship or floating offshore structures assessment, ultimate strength analyses are carried out after the yielding criteria have been assessed and before fatigue assessment.

Plates and Shells

The first step consists of assessing that the plates fulfil the yield stress requirements. Then a critical stress is defined, depending on the elastic buckling stress and yield stress for the different loading conditions, compression, bending, and shear along with combined compression, bending, and shear. When compression forces are unidirectional a factor F is defined. Pt B Ch 7 Sec 1 5.4.4 (BV, 2011) is used to combine criteria between compression and shear. When compression is biaxial, the criterion requires that the sum of the ratio of acting compressive stress divided by the critical stress corresponding to the direction affected by a power equal to 1.9, and the ratio of acting shear stress divided by the shear critical buckling stress also affected with a power equal to 1.9. A similar approach is provided for a curved shell.

Stiffened Panels

Pt B Ch 7 Section 2 (Ordinary Stiffeners) considers the strength of stiffened plates against buckling (BV, 2011). Again, the assessment of yielding criteria is required before carrying out buckling assessments. The strength of a stiffened panel involves the participation of the web flange and attached plate.

If the plate between stiffeners fulfils the buckling criteria it is considered as participating in the inertia of the equivalent beam, plate, and stiffener. If not, the partial participation of the attached plate is assumed by correcting the effective plate width with the effective plate width depending on the stiffened panel buckling mode being considered. Three buckling modes are considered: bending, torsional, and web buckling. For each buckling mode a buckling stress formula is provided, and the stress that results from the loads applied to the structure only takes into account the effective attached plate being considered for that particular buckling mode. A critical buckling stress c is then defined as the minimum value of all buckling mode stress affected by an elasto-plastic correction when c is beyond half of the yield stress.

For ordinary stiffeners contributing to the hull girder's longitudinal strength, the applied compression stress is corrected to be homogeneous with the critical buckling stress.

Pillars

Pillars are also to be checked against buckling failure with the effect of load eccentricity and moment combination taken into account in the checking criteria according to Pt B Ch 7 Section 3 6.3.1 (BV, 2011).

Hull Girder

The ultimate strength assessment of the hull girder is required for ships with a length of more than 170 m and the ultimate strength of the hull girder is given in terms of the bending moment capacity M versus the curvature χ . The procedure is given in Pt B Ch 6 Appendix 1 (BV, 2011) following a Smith method, as illustrated in Figure 2.

The bending moment capacity M versus the curvature χ curve is obtained by means of an incremental iterative approach. The main longitudinal parts of the hull girder such as decks, bottoms, side shells, and longitudinal bulkheads are considered stiffened panels and modelled as stiffeners working in parallel. A curvature is applied to the longitudinal elements of the hull girder. The carrying load that corresponds to each stiffener is considered part of the stiffened panel and is obtained by considering a model that is elastic and perfectly plastic. Different failure modes are analysed for each stiffener, and at each step the strength corresponding to the weakest failure mode is kept to determine the stiffener force that corresponds to the prescribed strain resulting from the curvature χ . From these forces and the position of the stiffeners the resulting bending moment capacity is obtained.

Ship-shaped Offshore Structures

Quasi-static Loadings The requirements for quasi-static loading strength requirements are basically the same as for a ship (BV, 2010).

Protection from Explosion The scope of requirements for protection from explosion Pt D Ch 1 Sec 9 3 (BV, 2010) verify the strength of the structure against blasts due to leakages of explosive gas clouds. The principle is that the structural elements may suffer permanent deformation without any rupture, allowing the pressure waves and hot gases or liquids to be transmitted through the steel panel.

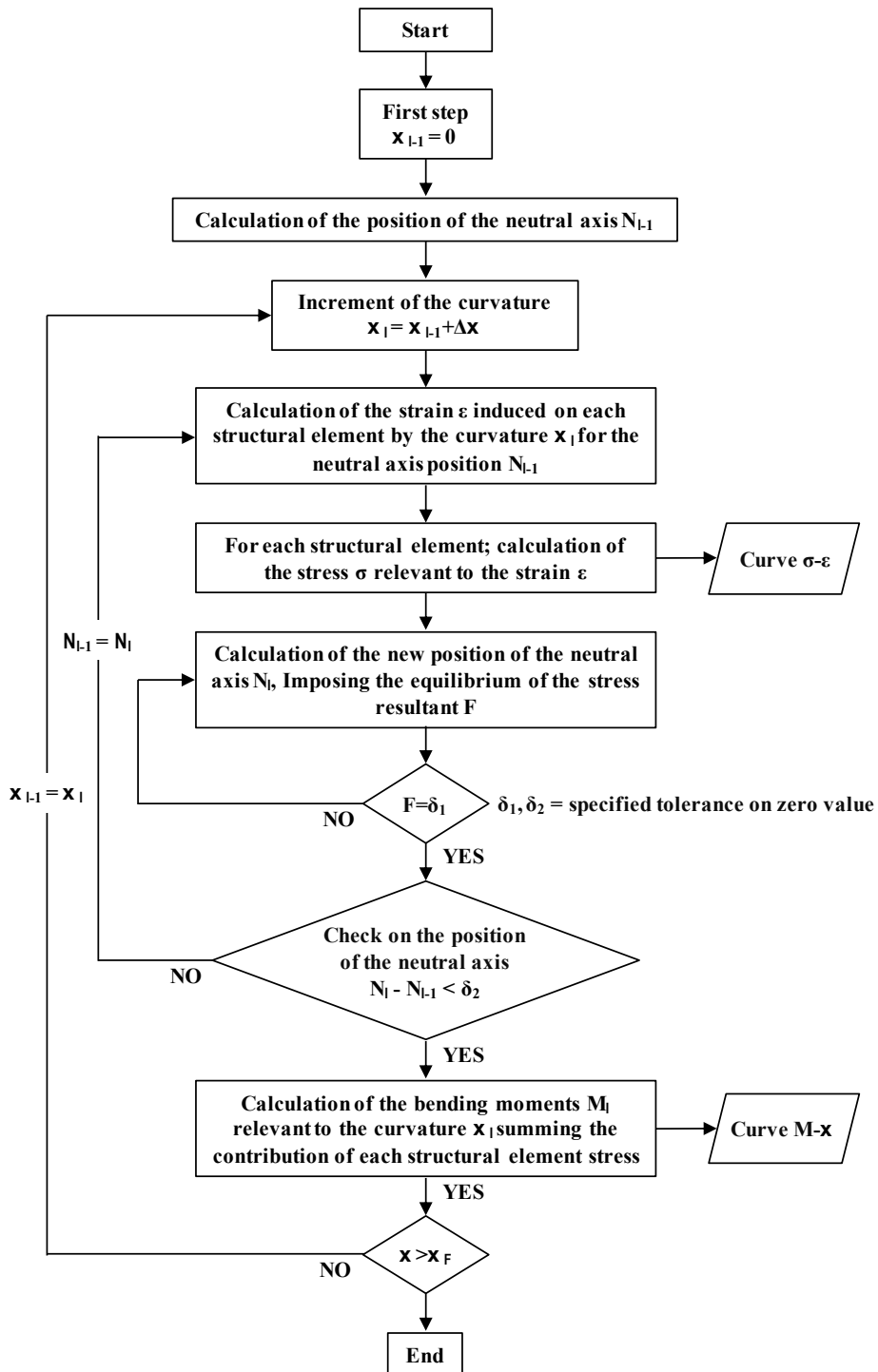


Figure 2: Flow chart of the procedure for the evaluation of the curve $M - \chi$.

The general areas of concern are the structural element close to the turret and turret moonpool, the main deck and the superstructure front. The calculation has to consider an equivalent exploded TNT mass the same distance from the explosion location. For external explosions an empirical pressure history is provided by the rules while an internal explosion test or numerical simulation is required to determine the loads. The maximum strain resulting from an elasto-plastic finite element response calculation should be lower than 0.8 times the ultimate strain.

Minor Collision The scope of the requirements Pt D Ch 1 Sec 9 4 (BV, 2010) is to check the strength of the structure against collision with shuttle tankers or supply vessels, the dimensions of which are supposed to be small compared to the unit. The energy of the colliding vessel is expected to be absorbed by the deformed side shell of the unit without any risk of flooding. The assessment versus a minor collision supposes that the shuttle tankers and supply vessels intended to be operating over the unit's life are listed and the colliding speed is to be justified. Then, a finite element analysis is carried out to justify that the colliding energy dissipates into the unit's structure, assuming that the bow of the colliding ship is nondeformable. Alternatively, when applicable, a simplified method such as the Rosenblatt method can be used. The criterion is the first rupture of a plate in the indented area.

Dropped Objects When specified Pt D Ch 1 Sec 9 5 (BV, 2010), the deck plate resistance to dropped objects is to be checked. The safety criterion is that the structural element may suffer permanent deformations without any rupture.

The assessment versus dropped object supposes that any equipment that is likely to fall on the deck is listed and the maximum dropped heights are to be justified. The procedure consists of a step by step static indentation of the deck up to the maximum allowed strain, generally 5% in the deformed area on the hull deck. For other decks the maximum strain corresponds to the ultimate strain. The energy of the dropping object at the moment of its contact with the deck should be lower than the absorbed indentation energy.

3.2.3 Det Norske Veritas (DNV)

Buckling strength analyses can be found in DNV-RP-C201 (DNV, 2010a, Buckling Strength of Plated Structures), DNV-RP-C202 (DNV, 2010b, Buckling Strength of Shells), and Classification Notes No.30.1 (DNV, 2010c, Buckling Strength of Bars and Frames, and Spherical Shells).

In DNV-RP-C201 (DNV, 2010a) two different but equally acceptable methods for the buckling and ultimate strength assessment of plated structures are described. This Recommended Practice is written in the load and resistance factor design format (LRFD format) to suit the DNV Offshore Standard DNV-OS-C101.

The first method, as given in Part 1, is a conventional buckling code for stiffened and unstiffened steel panels. It is an update on and development of the stiffened flat plate part of the previous DNV Classification Note No. 30.1 "Buckling Strength Analysis". Recommendations are given for individual plates (unstiffened plates), stiffened plates, and girders supporting stiffened plate panels.

For unstiffened plates, the buckling checks (in compression) shall be made according to the effective width method and the buckling resistance under various loading conditions, such as uniform uniaxial compression, shear, biaxial compression with shear, varying longitudinal, and transverse stress is listed. Different formulas for stiffeners

being continuous or simple supported are presented for stiffened plates. Local buckling should be avoided by limiting the stiffness and/or proportions.

The second method, as given in Part 2, is a computerized semi-analytical model called a PULS (Panel Ultimate Limit State). It is based on a recognized nonlinear plate theory, Rayleigh-Ritz discretizations of deflections, and a numerical procedure for solving the equilibrium equations. The method is essentially geometrically nonlinear, with stress control in critical positions along plate edges and plate stiffener junction lines for handling material plasticity. The procedure provides estimates of the ultimate buckling capacity to be used in extreme load design (ULS philosophy). The buckling limit is also assessed because it may be of interest in problems related to functional requirements (i.e., for load conditions and structural parts in which elastic buckling and thereby large elastic displacements are not acceptable (SLS philosophy)). The PULS code is supported by official, stand-alone DNV software programs. It is also implemented as a postprocessor in other DNV programs.

DNV-RP-C202 (DNV, 2010b) treats the buckling stability of shell structures based on the load and resistance factor design format (LRFD), as in DNV-RP-C201. The buckling modes for stiffened cylindrical shells are categorized as follows:

- Shell buckling: the buckling of shell plating between rings/longitudinal stiffeners.
- Panel stiffener buckling: the buckling of shell plating including longitudinal stiffeners. Rings are nodal lines.
- Panel ring buckling: the buckling of shell plating including rings. Longitudinal stiffeners act as nodal lines.
- General buckling: the buckling of shell plating including longitudinal stiffeners and rings.
- Column buckling: the buckling of the cylinder as a column. For long cylindrical shells it is possible that interaction between local buckling and overall column buckling may occur because the second order effects of axial compression alter the stress distribution calculated using linear theory. It is then necessary to take this effect into account in the column buckling analysis. This is done by basing the column buckling on reduced yield strength, as given for the relevant type of structure.
- Local buckling of longitudinal stiffeners and rings.

In contrast with the two Recommended Practices, the buckling stress analysis given in Classification Notes No.30.1 (DNV, 2010c) is based on the working stress design method (WSD).

Depending on the loading conditions, a bar may be referred to as a column (bar subject to pure compression), a beam (bar subject to pure bending), or a beam-column (bar subject to simultaneous bending and compression). Buckling modes for bars are categorized as follows:

- Flexural buckling of columns: bending about the axis of least resistance.
- Torsional buckling of columns: twisting without bending.
- Flexural-torsional buckling of columns: simultaneous twisting and bending.
- Lateral-torsional buckling of beams: simultaneous twisting and bending.
- Local buckling: the buckling of a thin-walled part of the cross-section (plate-buckling, shell-buckling).

The overall buckling of a built-up member – composed of two or more sections (chords) separated from one another by intermittent transverse connecting elements (bracings)

– corresponding to the flexural buckling of a homogenous member is also addressed, along with the buckling of unstiffened spherical shells and dished-end closures.

3.2.4 *Germanischer Lloyd SE (GL)*

GL rules on buckling and ultimate strength at the elementary plate panel level, and partial and total panel level (GL, 2011a) are in line with those in the CSR for Bulk Carriers (IACS, 2010b). In addition, an assessment of hull girder ultimate strength is required by the GL rules on longitudinal strength (GL, 2011b). The ultimate vertical bending moment has to be calculated by a procedure based on a simplified incremental-iterative approach.

3.2.5 *Registro Italiano Navale (RINA)*

Rules for the classification of ships (RINA, 2011) essentially include the same criteria as the BV requirements, except for the following minor differences:

- RINA requires the hull girder ultimate strength check for ships with $L > 150 m$ while BV requires it for ships with $L \geq 170 m$;
- Partial safety coefficients on wave bending moment and material are slightly different (1.15 vs. 1.10 for moment, and 1.05 vs. 1.03 for material) ;
- BV requires an ultimate strength check in both seagoing and harbour conditions while RINA requires such checks only in seagoing conditions;
- BV rules include a specific check for curved transversally stiffened plate panels that is not reported in RINA rules;
- Minor collision criteria are not included in RINA rules.

3.3 *Other Regulatory Agencies*

Other agencies and authorities have also published standards for addressing ultimate strength. ISO (2007) addresses the general requirements for the assessment of ship structures based on four types of limit states, namely the serviceability limit state (SLS), the ultimate limit state (ULS), the fatigue limit state (FLS) and the accidental limit state (ALS). The API Bulletin 2U (2004) provides stability criteria for determining the structural adequacy against buckling of large diameter circular cylindrical members when subjected to axial loads, bending, shear, and external pressure acting independently or in combination.

4 DEFINITION OF PARAMETERS AND THEIR UNCERTAINTIES

4.1 *Introduction*

The practical aspects related to the construction and operation of ship structures have an important influence on ultimate strength assessment. Uncertainties in these aspects must be considered in addition to those related to specific numerical idealizations of a particular structure. By practical aspects, we mean material properties, fabrication-related imperfections, and the in-service effects of the structure. Classifications for these are proposed in Table 1. Both hull girder and individual structural components (stiffened and un-stiffened panels) have been considered in the table's compilation.

All of the abovementioned aspects should be quantitatively defined by means of one or more appropriate parameters. It is clearly impossible to deal with all of them in a rigorous manner without making a number of simplifying assumptions. In fact, the studies available in the open literature focus on one or, at the very most, a few although no holistic perspective is achieved even when the trend is towards more and more complex models. For example, no interaction among the various aspects is generally

accounted for. Moreover, it is worth noting that large/full-scale experimental data focusing on such practical aspects are rather limited, especially on aspects concerning hull girder strength.

4.2 *Physical Aspects*

To list all of the physical aspects involved in the ultimate strength assessment and introduce uncertainties for the final results is a challenging task. Only a few examples from the literature have shown the impact of different and somewhat unusual aspects. The reader is referred to Paik and Thayamballi's (2003) book and to previous ISSC Technical Committee III.1 reports on Ultimate Strength, which summarize the state of the art up to 2009.

Garbatov *et al.* (2011) estimated the ultimate strength of stiffened panels by applying classical FEM models. However, the effect of different structural parameters on the uncertainty of results based on a Monte Carlo simulation and an ANOVA (Analysis of Variance) methodology were included in the study. A sensitivity analysis was used to determine the most relevant parameters among plate thickness, Young's modulus, the yield and ultimate tensile strain of material, the shape of initial geometry imperfection, and slenderness ratios. Moreover, the interactions between some of the considered parameters were also assessed.

The effect of intermittent welding was assessed by Khedmati *et al.* (2009a). They studied the ultimate strength of stiffened steel plates, selected from the deck structure of real ships and subjected to in-plane longitudinal or transverse compressive loads. Three different stiffener-to-plate welding procedures were considered: continuous, chain intermittent fillet, and staggered intermittent fillet welding. Detailed analyses were carried out using the commercial software ADINA and then validated by experiments. The full-range equilibrium path of the nonlinear elasto-plastic response of stiffened plates was traced.

Special attention was paid to the finite element modelling of the fillet welds as applied in practice to verify the reliability of the results by discussing the automatic-step incremental solution of a nonlinear finite element algorithm and the refinement of the mesh to appropriately represent the weld seam.

The sensitivity analysis involved several geometrical ratios, stiffener types, and boundary conditions in addition to the weld type. In comparison, the ultimate strength of continuously welded stiffened plates is more reduced in the case of chain intermittent fillet welds than it is in the case of staggered fillet welds.

Two interesting applications were recently proposed by Wang *et al.* (2009) and Suneel Kumar *et al.* (2007), both of whom considered the effect of plate openings on ultimate strength. A plate with an opening behaves in a very complex manner and is subject to yielding, buckling, stress concentration development, and fracturing.

Parametric FEM studies were carried out in both cases. Wang *et al.* (2009) considered typical manhole-shaped openings with different sizes while Suneel Kumar *et al.* (2007) assessed rectangular openings in plates under axial compression. Simplified formulae were proposed and strength reduction factors introduced that were useful for design guidance and to estimate the strength of plates on primary supporting members in way of openings. Compared to current classification societies, rules were reported showing how the rules account for the issue in cases of various structural behaviour and limit states.

Table 1: Practical aspects affecting ultimate strength behaviour

| | |
|---------------------|---|
| Physical aspects | <ul style="list-style-type: none"> • Material properties and behaviour (Young's modulus, Poisson's ratio, hardening, yield modelling, etc.) • Overall geometry (span, spacing, slenderness, etc.) • Strength properties of components (plate thickness, cross-section of stiffeners, etc.) • Local variations of geometry (e.g. openings on plates, scallops, cut-outs, manholes, etc.) • Fabrication/initial defects (misalignments, weld imperfections, residual stresses, etc.) |
| Model uncertainties | <ul style="list-style-type: none"> • Quantitative definition of limit state modes (buckling, collapse, etc.) • Approximations of analytical models (e.g., one dimensional or two dimensional idealization) or • Approximations of numerical models (both simplified numerical analyses like the ones proposed in the software of class societies or nonlinear FEM models), e.g.: <ul style="list-style-type: none"> – Element types/formulations – Assumed boundary conditions – Initial shapes (necessary in nonlinear numerical analyses) • Geometrical idealizations of structures (neglected physical aspects) • Solution algorithms (iterative, incremental, nonlinear, etc.) • Interaction among components (if considered, and how it is considered in the assessment) |
| Ageing effects | <ul style="list-style-type: none"> • Corrosion (uniform, pitting, microbial, crevice, etc.) • Fractures and fatigue cracks • Local buckling • Mechanical damages (permanent set due to loading, local dimples, distortions, etc.) • Coating protection/environmental effects (e.g., cargo effects) |

A similar analysis was carried out experimentally by Schleyer *et al.* (2011) in the frame of a project to study the blast loading of steel plates with penetrations as used for deck plating or bulkheads. Tests were studied by applying a simplified energy solution.

There has been increased interest in aluminium alloy structures in shipbuilding because of its lower stiffness in respect to steel, which makes the buckling behaviour of aluminium structures rather different. Khedmati *et al.* (2010a) carried out round robin FEM analyses based on previous work from the ISSC 2003 Technical Committee Report III.1 with the aim of assessing the influence of initial deflections and the heat-affected zones on the post-buckling behaviour and collapse of triple-span multi-stiffened panel, extruded or nonextruded angle-bar profiles made from AA6082-T6 aluminium alloy.

Defects and imperfections are very frequent in marine composite structures. Misirlis *et al.* (2010) performed a parametric study of initial geometric imperfections, specifically the ultimate compressive strength of square and long FRP plates. Gaiotti *et al.* (2011) presented a map of the reduction factor of the buckling strength of composite laminates containing delaminations in various positions. The two different FEM modeling strategies presented showed that results are not always the same depending on the element types.

The effect of distortion on the buckling strength of stiffened panels was considered by Chaithanya (2010) using both analytical and numerical analyses, but the effect of residual stress was not accounted for. The equivalent column model clearly showed

the effects of distortion and slenderness on the strength of the equivalent column, suggesting that the initial distortion affects the strength of the stiffened plate structures. FE analysis of the panels modified this conclusion because the strength decreased by less than the column model predicted for relatively stocky panels.

Few large-scale tests of hull girder collapse have been carried out for obvious reasons. Gordo and Guedes Soares (2008, 2009) carried out the collapse testing of mild steel-made, externally stiffened box girders, which was followed by similar tests using high strength steel specimens. Figure 3 shows the test structural models and test results.

The residual stress relief during loading and unloading paths was analysed and its effect was found to be significant. The residual stresses were removed by performing a series of loading cycles prior to the collapse of the structure. The approximate method based on the progressive collapse of the stiffened plate elements gave a good estimation of the ultimate load supported by the structure and allowed the effect of residual stresses on the box behaviour to be reproduced.

Deviations from the analytical results were attributed to the imperfections and defects always present in a large-scale welded specimen. A comparison of the results of a previous experiment on a similar specimen made from high strength steel highlighted a much higher development of plasticity in the mild steel specimen.

The efficiency of materials and geometry is a useful concept for identifying the governing parameters affecting the ultimate strength of 3-dimensional structures under a predominant bending moment. The sensitivity of the involved parameters such as span, spacing, and column slenderness was identified as was the global efficiency of the high strength steel (HTS 690), which was of the order of 2.5 taking the normal mild steel structure as its basis.

A comprehensive analysis of uncertainties in the ultimate longitudinal strength of a cross-section from a ship's hull girder based on nonlinear FEM was carried out by

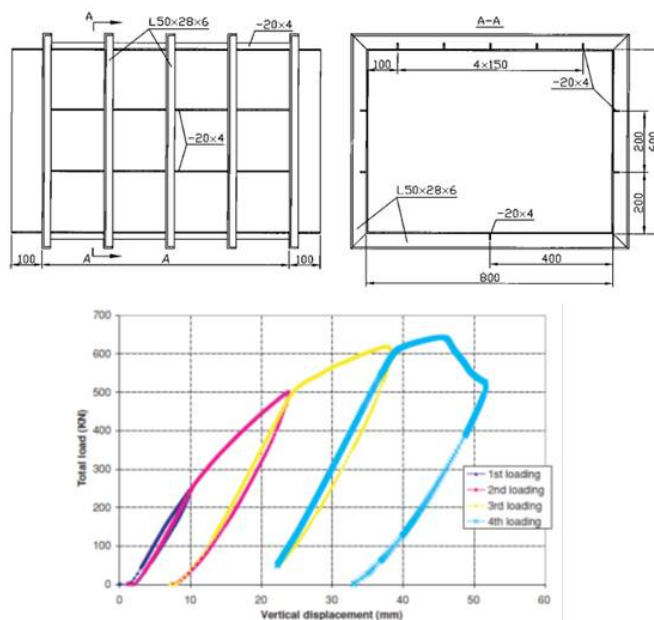


Figure 3: Structural models and measurements of the box girder tested by Gordo and Guedes Soares (2008)

Harada and Shigemi (2006) using a refined FEM model extending over one transverse frame spacing.

Initially, a systematic variation of thickness, material yielding stress, and Young's modulus were carried out to assess variations in hull girder ultimate strength. Next, variations in the shape and magnitude of initial deflections in the stiffened panels due to welding were examined. Finally, the influence of the mesh size in FE models was considered. Uncertainty coefficients were proposed for the rules, including model uncertainties, based on the obtained results.

The effects of randomness in yield strength and in the initial imperfections in ultimate hull girder strength were also determined by Vhanmane and Bhattacharya (2011). Different levels of statistical dependence between yield strength, the initial imperfection of stiffeners, and the plating between stiffeners were considered.

Two ship structures, a VLCC tanker and a cape-size bulk carrier, were analysed and the statistics of their ultimate hull girder moment capacities were obtained through Monte Carlo simulations. Correlation had no effect on the mean value of ultimate strength, but the uncertainty increased significantly with a higher correlation between yield strength and initial imperfections. Further, the variations in hull girder strength were lower when both sources of uncertainties, yield strength and initial imperfections, were considered compared to when uncertainties in yield or in initial imperfections alone were considered.

4.3 Modelling Uncertainties

Similar to the modelling uncertainties of physical aspects, those involved in ultimate strength assessments are rather varied.

Numerical models, mainly nonlinear FEM, are typically used even if analytical models can still provide sound information. Saeidifar *et al.* (2010) introduced a highly accurate numerical calculation of buckling loads for elastic rectangular plates with varying thickness, elasticity modulus, and density in one direction that considered various boundary conditions, including the beam one (i.e., elastic support at the edges due to the presence of a stiffener). The analytical solutions obtained regarding an infinite power series were compared to a finite element analysis and the differences were lower than 3%.

Piscopo (2010, 2011) recently improved classical analytical models for use in the analysis of rectangular plates under shear, uniaxial, and biaxial compressive loads and their combinations, considering different boundary conditions. Comparisons with FEM results highlighted that in several cases, analytical formulations – taking recent advancements into account – are as accurate as FEM analyses.

Özgülç and Barltrop (2008) analysed the hull girder strength of bulk carriers using a simplified incremental-iterative approach. Pure vertical bending moment was first examined using seven different methods. Next, the ultimate strength under coupled vertical and horizontal bending moment was considered and an interaction curve was obtained. The interaction design equations proposed by other researchers were also addressed.

The combined effect of the vertical and horizontal bending moments become important when a ship is damaged and simplified, but reliable methods are necessary to select the proper actions. The proposed simplified method is rather accurate, but it can be difficult to find a target for comparison in the case of hull girder ultimate strength.

Rizzo *et al.* (2002) compared the ultimate strength of hull girders obtained by applying different evaluation methods to a set of deep-V, high speed craft hulls ranging from 50 m to 125 m in length. Namely, the ultimate bending moment of the midship section was evaluated for seven ships with the same hull forms using five different methods. An analysis of the results made it possible to estimate uncertainties in the ultimate strength evaluation to be used in the reliability analysis or rules development derived from modelling assumptions and the size of the structure.

Okasha and Frangopol (2010) examined hull strength optimization from a probabilistic perspective. In addition to their probabilistic approach to material properties and fabrication details, hull section stresses were determined using constitutive models of stiffened panels that considered a variety of possible failure modes and initial imperfections. The ultimate strength was found by using an optimization search algorithm that claimed to be as accurate as the rigorous incremental curvature method, but with less computational time. This method was then applied to a sampling simulation and the output sample was tested against several potential distributions.

4.4 Ageing and In-service Damage Effects

The impact that ageing effects have on the ultimate strength of a hull girder and its components was recently considered by the ISSC Specialist Committees on the condition assessment of aged ships and offshore structures in 2006 and 2009. These reports are an ideal source of detailed, state-of-the-art information about ageing ship and offshore structures while the book *Condition Assessment of Aged Structures* (Paik and Melchers, 2008) provides a wider overview of the matter. A few advances can be cited in the material that follows regarding the main degradation modes of ship structures (i.e., corrosion, fracture, and mechanical damage as defined by the abovementioned ISSC Committees).

A statistical investigation of the time-variant hull girder strength of ageing ships and coating life was carried out by Wang *et al.* (2008) based on data from ships in service. In particular, they analyzed the measurement of section belts carried out during CAP surveys.

Difficulties in identifying plate renewals reportedly affected the analysis. However, uncertainties in the decrease of the hull girder section modulus for tankers were identified and such data were used to derive formulae that can be useful when applied to hull girder ultimate strength assessments.

Although Ivanov's study (2009) mainly focused on hull girder loads, it – like the abovementioned paper – also considered hull girder section modulus degradation due to corrosion. The hull girder geometric properties are presented in probabilistic format as annual distributions and distributions for any given lifespan. Probabilistic models of corrosion were also combined with as-built plate thickness variation models. Finally, a risk-based inspection planning framework was offered.

Moving from hull girder to hull structural components, the work of Silva *et al.* (2011) can be cited. They recognized that corrosion wastage is not uniform because it is commonly idealised. Steel plates are actually subject to random nonuniform corrosion, so the effect of nonlinear, randomly distributed, nonuniform corrosion on the ultimate strength of un-stiffened rectangular plates subjected to axial compressive loading was numerically analysed by means of nonlinear finite element analyses. A Monte Carlo simulation generated 570 plate surface geometries for different degrees of corrosion, location, and ages and their ultimate strength was assessed. Finally, a regression

analysis was proposed to derive empirical formulae for predicting strength reduction resulting from corrosion.

The strength and deformability of steel plates for marine use were studied by Rabiul Islam and Sumi (2011), focusing on the geometry of corrosion pits and the size effect of corroded plates. The effects of the two pit shapes (conical and ellipsoidal) was investigated through nonlinear, large deformation and three-dimensional finite element analyses for simulated corrosion surfaces, as generated by a probabilistic model of a corrosion process. Rizzuto *et al.* (2010) studied on reliability of a tanker in a damaged condition.

4.5 Conclusions on Practical Aspects in Ultimate Strength Assessment

In short, it has been briefly shown that several practical aspects have an effect on the ultimate strength assessment of hull girders and individual hull components. These are often implicitly accounted for in the assessments by safety factors, either because it is difficult to include them in the models or because their effects are simply not recognized. The following aspects can be summarized, recalling the information reported in Table 1.

As far as hull girder ultimate strength is concerned, simplified and analytical approaches can be applied in lieu of nonlinear FEM analyses. Both methods are valid in principle, depending on the aims of the calculation. Such analyses are generally carried out for comparative/optimization purposes rather than for limit state assessment.

The available experimental data that can be used as target values for the calibration of structural models is very limited, which makes it almost impossible to estimate the related uncertainties. Moreover, it should be acknowledged that it is difficult to properly include ageing effects and imperfections in the analyses. Similarly, the interactions between structural components are very difficult to simulate.

Individual structural components can be assessed using simplified and analytical approaches or FEM analyses. In this case several practical aspects can be accounted for, such as openings in plates, fabrication imperfections (dimples, distortions, residual stresses, etc.), the effect of adjacent plates (structural system strength), and ageing effects in addition to the consideration of complex situations like random corrosion.

Using survey automation and data management to build updated numerical models, structural monitoring, and other ways of measuring ships in service will possibly become the way to fill the gap between the practical aspects of ultimate strength assessment and the actual state of the art, especially considering the interactions between the various aspects that are too complex to be included in current assessment practices.

5 RECENT ADVANCES

5.1 Components

5.1.1 Plates

Paik and Seo (2009a) investigated the ultimate strength of unstiffened plate elements under combined biaxial thrust and lateral pressure using a nonlinear finite element approach. The one-bay plate model was supported along four edges with no rotational constraint and it was analysed along with the 1/2+1+1/2 bay continuous plate model with the lateral deflection restrained by supporting members. The latter was subjected to rotational restraint along the plate edges under the action of lateral pressure as

observed. They found that the ultimate strength of plate elements under biaxial thrust was significantly influenced by the rotational restraint under lateral pressure actions, and that ALPS/ULSAP program captured this influence in the ultimate strength prediction with reasonable accuracy. Most studies on the ultimate strength of plates under longitudinal compression are related to plates having unrestrained edges that remain straight and without a net transverse load applied.

Gordo (2011) studied the influence of the in-plane restraint of unloaded edges on the ultimate strength of long plates under axial compression using plate buckling modes to model the fabrication imperfections.

It is recognized that the current design practice for perforated plates, which uses a plasticity correction such as the Johnson-Ostenfeld formula, may not be relevant, particularly when the opening size is relatively large because the critical buckling strength is significantly greater than even the ultimate strength in such cases (Paik and Thayamballi, 2003). The primary reason for this is that the large opening enhances a yielding at the net section, but the elastic buckling strength is not similarly decreased by the local increase of stresses and is sometimes even increased by the presence of larger free edges and associated stress distribution in the plate (Harada and Fujikubo, 2002). To overcome the problem, Kim *et al.* (2009) performed a series of experimental and numerical studies on buckling and the ultimate strength of plates and stiffened panels with an opening that were subject to axial compression, and they derived design-formulae for measuring critical buckling strength. Extensive comparisons of numerical test results have shown that the developed critical buckling strength formula is useful for the design and strength assessment of steel plate panels with an opening. Wang *et al.* (2009) proposed simplified formulae for assessing the buckling and ultimate strength of plates with openings based on the FEM results that introduce strength reduction factors as ratios to the strength of plates without openings.

Cylindrically curved plates are extensively used in ship structures, such as deck plating with a camber, side shell plating at fore and aft parts, and bilge circle parts. The practical method for the ultimate strength assessment of curved plates, however, has not been clearly established. Park *et al.* (2009) studied the post-buckling behaviour of curved plates under longitudinal thrust with the effect of secondary buckling using nonlinear FE-analyses and proposed a simple formula for finding ultimate strength by introducing the curvature effect to the Faulkner's plate strength formula. Park *et al.* (2011) also derived a set of simple formulae to estimate the buckling/ultimate strength of curved plates under longitudinal/transverse thrust, combined biaxial thrust, and lateral pressure based on FE results. Amani *et al.* (2011) investigated the buckling and post-buckling behaviour of curved plates under uniform shear, including the elasto-plastic regime. Imperfection sensitivity was also studied for various geometrical parameters.

Benson *et al.* (2009) investigated the strength of aluminium plates with a range of geometric and material parameters and different imperfections using nonlinear finite element analyses. Their study showed that these parameters have a significant influence on the strength behaviour of aluminium plates. Daley and Bansal (2009) dealt with ice loading, wheel loads, collision, and the grounding loads of ship plating as patch loads. The recent IACS Polar Rule requirements and two other formulations were compared to nonlinear finite element results and revealed that there are still some significant differences. Finally, ideas for the development of an elasto-plastic response formulation were presented.

To efficiently analyse the progressive collapse analysis of plated structures, Pei *et al.* (2010a, 2010b) developed an ISUM plate element that considered the combined action of in-plane shear and thrust, and an isoparametric ISUM plate element for quadrilateral plate shape under thrust. The applicability of these models was confirmed by comparing them to FE analyses.

The edge condition of the plating in a continuous stiffened-plate structure is neither simply supported nor clamped because the torsional rigidity of the support members at the plate edges is neither zero nor infinite. In a robust ship structural design, it is necessary to accurately take into account the effect of the edge condition in analyses of plate behaviour in terms of buckling and post-buckling behaviour. Paik *et al.* (2012a) developed a new method for analyzing the geometric nonlinear behaviour (i.e., elastic large deflection or post-buckling behaviour) of plates with partially rotation-restrained edges in association with the torsional rigidity of the support members and under biaxial compression. It is also confirmed that the effect of plate edge condition is significant on the post-buckling behaviour.

The text book titled *Ship Structural Analysis and Design* (Hughes and Paik, 2010) presents the most recent theories for buckling and ultimate strength calculations of plates.

5.1.2 Stiffened Panels

With the recent trend toward the application of limit state design to the ultimate strength assessment of ships and offshore structures, continuous efforts have been devoted to the development of useful methodologies for predicting the ultimate strength of stiffened panels.

Paik and Seo (2009b), Paik *et al.* (2011b), and Frieze *et al.* (2011) performed a benchmark study on the ALPS/ULSAP method to determine the ultimate strength of stiffened panels under combined biaxial compression and lateral pressure. The plates' initial deflections with the shape of the elastic buckling mode and the column-type and sideways initial deflections of stiffeners with the shape of the buckling mode were assumed. The predicted ultimate strength correlated well with more refined ANSYS nonlinear finite element computations, assuming the same shape and magnitude of initial deflections.

Zhang and Khan (2009) carried out an extensive nonlinear finite element analysis of the plates and stiffened panels of ship structures under axial compression and developed some simple formulae for measuring their ultimate strength. A good agreement between their proposed formulae and the FE results was achieved with a mean value with the scatter of 3.2 %, based on the FE results. Wang *et al.* (2010) compared various buckling and ultimate strength assessment criteria of stiffened panels under combined longitudinal compression and lateral pressure. The ultimate strength predictions from these various methodologies were found to be generally close to the test data in most cases. They also found differences in the predicted ultimate strength's sensitivity with respect to lateral pressure in some of the rules.

Cho *et al.* (2011) derived formulae for stiffened panels that were subject to combined axial and transverse compression, shear forces, and lateral pressure. Residual stresses were included similar to those provided by the ISSC2000 committee VI.2 (ISSC, 2000) and shape imperfections were modeled using sinusoidal variations where a half wave was assumed for the axial direction to better represent reality – closer to the hungry-horse mode than the elastic buckling mode. The formulations were verified against FE-analyses using the DnV software PULS.

Gordo and Guedes Soares (2011) performed axial collapse tests for three-bay stiffened panels with associated plate made of very high tensile steel, namely S690. The use of this high strength steel led to the use of U stiffeners as an unconventional solution. Four different configurations were considered for the stiffeners, which were made of mild or high tensile steel for bar stiffeners and mild steel for 'L' and 'U' stiffeners. The results showed that the hybrid panels performed better than the fully S690 panels for similar squash loads due to their lower column slenderness relative to the fully S690 panels, which had large cross-section areas. The 'U' stiffeners were 2 mm thick and the large slenderness of the flange plating showed signs of early-stage buckling and unstable load shedding after ultimate strength had been reached. The buckling collapse behaviour of these stiffened panels was investigated numerically by Xu and Guedes Soares (2011c) using FEA, with special attention paid to the influence of the stiffener geometries and the appropriate boundary conditions for numerical models.

The stiffened plate structures in ships and ship-shaped offshore installations often display nonuniform plate thicknesses. Seo *et al.* (2011) checked the validity of the equivalent plate thickness method against the ultimate strength analysis of stiffened panels with nonuniform plate thicknesses using nonlinear finite element method computations. This method was based on the weighted average approach and showed that the equivalent plate thickness method can be successfully used with finite element models.

In addition to ultimate strength, the correct formulation of the post-buckling, stress-strain relationships between stiffened panel elements subject to various loads acting on their edges is another key aspect for evaluating the ultimate capacity of ship structures. Benson *et al.* (2010) presented a semi-analytical approach to predict the load shortening curves of stiffened panels under uniaxial compression. Their method considered local and overall failure modes, including gross panel collapse, interframe collapse, and local component buckling. The results revealed that their method predicted the effects of gross panel buckling on the pre- and post-collapse behaviour of the panels. Brubak *et al.* (2009) presented another semi-analytical method for the analysis of stiffened plates in the pre- and post-buckling range. Load-deflection curves were computed using this method in combination with a strength criterion that allowed the ultimate strength limit to be predicted. In particular, stiffened plates with a free edge or with an edge stiffener were considered. Taczala (2009) developed an approximate method for the evaluation of the stress-strain relationship of stiffened panels under tension, compression, and shear.

Amlashi *et al.* (2010) developed a probabilistic tool to assess the capacity distribution of stiffened panels. A Monte Carlo simulation scheme was applied using PROBAN (DNV), which interactively utilizes PULS method as an efficient ultimate strength prediction tool for plated panels. The suitability of the assumed distribution for the strength was demonstrated with relatively little computational time and the yield stress and imperfection sizes were treated as random variables.

There has been an increased interest in the buckling/plastic collapse behaviour of aluminium structures in recent years. Although a large number of ultimate strength prediction methods are available for steel stiffened panels, they cannot be directly applied to aluminium structures for various reasons, including softening effects in the heat-affected zones (HAZs) near fusion weld lines, a more rounded stress-strain relationship than steel, and more varieties of the cross-sectional geometries produced by extrusion.

The post-buckling behaviour and strength of multi-stiffened aluminium panels subjected to combined axial compression and lateral pressure were studied by Khedmati *et al.* (2010b), including the effect of HAZs at the longitudinal (axial) and/or transverse weld lines. The model without HAZs and model B (see Figure 1), which had longitudinal weld lines at the intersections of extruded elements, exhibited maximum ultimate strength in general, while model A+C, which had longitudinal weld lines at the junction lines between the plate and the stiffeners and the transverse weld lines exhibited minimum ultimate strength for any value of lateral pressure. This is partly due to the softening effect in HAZs and partly due to the location of the effective width of the plate after buckling. Chen and Moan (2010) investigated the effects of material softening and residual stresses on the ultimate strength of stiffened aluminium panels under axial and transverse compression. Their results were similar to those observed by Khedmati *et al.* (2010b). Chen and Moan also found that the softening effect of transverse welds on the axial strength of stiffened panels is greater for sturdy panels with smaller panel slenderness.

Khedmati *et al.* (2009b) investigated the elastic buckling and ultimate strength of continuous stiffened aluminium panels under combined axial compression and lateral pressure using a nonlinear finite element approach. The influence of initial deflections and the effect of the heat affected zone on the buckling/plastic collapse behaviour were investigated to discover the different lateral pressure values. Based on the results, Khedmati *et al.* (2010b) developed empirical formulae for predicting ultimate strength through a regression analysis that considered the effect of the weld on initial imperfections and heat affected zones.

Collette (2011) developed a series of rapid semi-analytical methods for predicting the compressive and tensile response of aluminium plates and stiffened panels. These models allowed Smith-type progressive collapse approaches to be implemented for aluminium vessels. Particular attention was paid to capturing aluminium-specific response features, such as round material stress-strain curves and the weakening effect of fusion welds. The methods were validated against finite element analysis and experimental results.

Paik *et al.* (2012b) carried out an experimental and nonlinear FEA-based numerical study on buckling collapse of a fusion-welded aluminium stiffened plate structure. A set of aluminium stiffened plate structures fabricated via gas metal arc welding in which the test structure is equivalent to a full scale deck of an 80 m long high speed vessel. The plate part of the test structure is made of 5383-H116 aluminium alloy and extruded stiffeners are made of 5083-H112 aluminium alloy. It is concluded that the nonlinear FEM computations significantly depend on the structural modelling technique applied. In particular, the welding-induced initial imperfections in terms of initial distortions, residual stresses, and softening in the heat-affected zone need to be modelled as appropriate for the nonlinear FEA of welded aluminium structures.

The text book titled *Ship Structural Analysis and Design* (Hughes and Paik, 2010) presents the most recent theories for buckling and ultimate strength calculations of stiffened panels.

5.1.3 Shells

Most offshore floating platform components are made as stiffened cylinders, and an improved model for the design process could affect their total construction costs and schedule to a great extent. A reliability-based design approach is considered advantageous over the deterministic type of structural designing process because the former

addresses uncertainties in the design variables, which leads to a more consistent level of safety. A reliability-based approach still needs a robust strength model to predict the capacity with respect to random design variables.

Das *et al.* (2011) proposed a strength model for ring, stringer, and orthogonally stiffened cylindrical shells that is a modified version of a previously proposed strength model. This model showed better agreement with the experimental results compared to the practicing DNV and API design codes. The model uncertainty factor and the strength model can be utilised in the reliability analysis of similar structures. It was also noted that the experimental data available for the radial pressure load cases for ring-stringer stiffened cylinders are very low and further investigation would be required to acquire more data.

An overview of current design practices for submarine pressure hulls was presented by MacKay *et al.* (2011), along with the results from a survey of the literature that was conducted to determine standard nonlinear numerical modeling practices for those structures. The accuracies of the conventional submarine design formulae (SDF) and nonlinear numerical analyses for predicting pressure hull collapse were estimated by comparing predicted and experimental collapse loads from the literature. The conventional SDF were found to be accurate within approximately 20 %, with 95 % confidence, for intact pressure hulls. The accuracy of a wide range of nonlinear numerical methods, including axisymmetric finite difference and general shell finite element models, was found to be within approximately 16 % with 95 % confidence. The accuracy was found to be within 9 % when only higher fidelity general shell FE models were considered.

A way for the incorporation of nonlinear numerical methods into the design procedure to move forward has also been discussed. Because real imperfections cannot be precisely anticipated, characteristic values must be used in partial safety factor approaches. The existing codes normally use the most pessimistic geometric imperfections that meet the specified design tolerances. One concept of an alternative approach that considers more realistic geometric imperfections for a given method of manufacture based on imperfection databanks was proposed. This would lead to less conservative design than the use of worst-case imperfection assumptions. Although a consensus with respect to the most appropriate modeling of imperfection is needed, this is an important topic that requires future research if it is to be successfully applied to any structural components.

Thick, truncated cones are primarily used in the offshore industries as transition elements between two cylinders of different diameters and as piles for holding jackets when driven into the sea bed. These conical shells undergo buckling within the elastic-plastic range. There are few results within this range compared to the thinner shells used in aeronautical applications where the load-carrying capacity is usually limited by elastic buckling. Blachut and Ifayefunmi (2010) conducted experimental and numerical examinations of the static stability of truncated metallic conical shells subjected to axial compression and/or external hydrostatic pressure. The FE predictions of the collapse pressures overestimated the experimental values by about 5 % and those of axial collapse loads by about 13 % to 30 %. Possible sources of discrepancy were discussed, including uncertainties in geometry, wall thickness, and welding residual stresses. Numerical studies were also performed by Ifayefunmi and Blachut (2011) on truncated cones under axial compression and/or external hydrostatic pressure to examine the sensitivity of their ultimate strength in relation to the following types of imperfections: (i) initial geometric imperfections, (i.e., deviations from perfect geometry), (ii) variations in wall thickness distribution, and (iii) imperfect boundary conditions.

Pan *et al.* (2010) performed nonlinear finite element analyses of a series of titanium alloy spherical pressure hulls that included structural imperfections. Based on their numerical results, the sensitivity of the ultimate strength to critical arch length, thickness to radius ratio, and structural imperfections were studied. The empirical formulae for the ultimate strength of titanium alloy spherical pressure hulls of deep manned submarines were proposed based on the numerical studies.

5.1.4 Composite and Sandwich Panels

Failure Theory of Composite Material

In order to increase confidence in the use of fibre-reinforced composites, an international activity called the World-Wide Failure Exercise (WWFE) has been organized. The aim of this exercise is primarily to benchmark and validate failure theories and design methodologies. The first WWFE-I originates from a meeting held at St Albans, UK in 1991. From that 19 failure theories were compared with experimental results for the failure of a unidirectional fibre reinforced lamina, initial and final failure of multi-directional laminates, and the large deformation of laminates under biaxial loads (Hinton *et al.*, 2004).

Some of the theories demonstrate good agreement with experimental results and others have limited capabilities. Some of the typical results are as follows.

- On a lamina level, Tsai was the highest scorer but Cuntze and Puck also did well and further experiments are required to confirm Tsai's predictions of increased lamina strength under biaxial compression.
- On final strength predictions for multi-directional laminates under biaxial loads; Puck, Cuntze, Tsai, and Zinoviev achieved the highest scores. The importance of a good post initial failure analysis method in the prediction of final failure was demonstrated.
- It has proven necessary to handle multiple nonlinearities arising from damage, nonlinear shear behaviour, and change in fibre orientation to accurately predict the stress-strain behaviour up to the failure of laminates under load conditions that result in matrix dominated behaviour.

There were many important outcomes from WWFE-I, and it also highlighted the significant shortfalls in predicting the strength and deformation response of polymer composite structures under biaxial stress states. To bridge some of the gaps that were identified, additional exercises were organized: (a) the Second World Wide Failure Exercise (WWFE-II) (Kaddour and Hinton, 2005), which considered triaxial failure and associated theories; and (b) the Third World Wide Failure Exercise (WWFE-III) (Kaddour *et al.*, 2007), which dealt with damage and associated modelling techniques.

There are many criteria that are used to predict the failure of composite materials. Several recently published methods are presented here. Daniel (2007) gave a concise overview of theories and procedures for predicting and analysing failure in composite materials. The validity and applicability of the various theories were evaluated based on convenience of application and agreement with experimental results. In the case of ultimate laminate failure, a progressive damage scheme coupled with a failure mode-discriminating criterion was discussed with special attention paid to textile composites.

Las *et al.* (2008) focused on the prediction of composite material failure using modern failure criteria for composites, namely LaRC04 and Puck. Three types of specimens were analysed and the the process of failure propagation was monitored using a method known as progressive failure analysis, which uses a material degradation approach.

Liu *et al.* (2010) focused on developing a model to predict the failure of notched cross-ply laminates with the influence of matrix failure. To estimate the local stress concentration in the critical damage zones, a method was developed to decompose the local stress concentration into several parts: the geometrical contribution of the notch, the damage contribution, and the stacking-ratio contribution. The damage-dependent stress concentration of the laminate was established for different notches and it was then utilised to predict the ultimate strength of the notched laminates.

WWFE-I indicated that the bridging micromechanics model exhibited a unique feature for calculating internal thermal stresses in the constituent fibre and resin materials of a laminated composite. Once applied to laminate strength prediction, however, the model only produced a moderate correlation with the experiments. Zhou and Huang (2008) incorporated a material degradation scheme and a modified ultimate failure criterion for laminates into the bridging model to improve its predictive capacity. Pure resin inter-layers were also introduced to simulate the effect of interfaces between the lamina plies. With these modifications, much more accurate predictions were obtained for the majority of the exercise problems, especially for the ultimate strengths and deformations of the multi-directional laminates.

Many different kinds of degradation schemes have been proposed in the literature, and none of them have proven accurate enough to describe the degradation behaviour of various materials.

Zhou and Huang (2008) multiplied the modulus of the resin by a factor of 0.01 to deteriorate the stiffness of the failed lamina. This deterioration scheme was motivated to be reasonable because the resin had undergone a significant plastic deformation before failure and the hardening modulus, which was defined as a tangent to the resin stress-strain curve, of the resin at failure had to be significantly smaller than its elastic modulus.

In the original problem (Huang, 2004), an ultimate failure of the laminate was considered to occur when all of the laminate had failed regardless of whether the failures were caused by the failure of the fibres or the resin, which gave poor ultimate strength predictions for the laminates subjected to some of the loading conditions. Thus, the ultimate failure of the laminate was considered to occur if and only if any single ply failure was due to that of the fibres or due to the compressive failure of the resin. In other words, even if all of the lamina plies failed due to the tensile failure of the resin, it could not be stated that the laminate had attained an ultimate failure.

Sandwich Panels

Sandwich constructions are commonly used in automotive, aerospace, wind energy, and marine applications due to their high strength-to-weight and stiffness-to-weight ratios. Sandwich elements consist of two strong, stiff face skins that are separated by a thick, flexible core. The skins provide flexural stiffness while the core provides shear resistance and composite interaction between the skins. Common skin materials include thin metal sheets or fibre reinforced polymer (FRP) composites. Core materials include balsa wood, polymeric foams, FRP reinforced foam cores, metallic foams, honeycomb constructions, and lattice structures.

Reany and Grenestedt (2009) presented a technique for analysing sandwich panels with one flat and one corrugated skin. Corrugated skins can significantly increase the wrinkling strength of uniaxially compression loaded lightweight sandwich structures. The corrugations can also be used to carry some of the shear load of a sandwich

panel. Such panels could, for example, be used as bottom panels in ship hulls. The structural improvements that result from skin corrugation were studied numerically for the buckling of simply supported panels subjected to uniaxial compression or shear loading. The numerical analysis predicted the corrugated panel to be 25 % stronger than its flat counterpart despite being 15 % lighter.

Dawood *et al.* (2010) conducted research that evaluated the two-way bending behaviour of 3D glass fibre reinforced polymer (GFRP) sandwich panels. The panels consisted of GFRP skins with a foam core and through-thickness fibre insertions. The experimental results were compared to those from a nonlinear, finite element model. The measured and predicted responses indicated that at lower deflections the panel behaviour was dominated by plate bending action while membrane action dominates at higher deflections. Yoon and Lee (2011) discussed sandwich panels composed of glass fibre epoxy composite faces and foam cores. The flexural bending strength and deformation of these panels were evaluated using FE analysis and compared to the experimental test results. It was found that the weight efficiency of the asymmetric sandwich panel was higher than that of the symmetric sandwich panel.

Polymer foam-cored sandwich composites are widely used in the load-bearing components of naval structures. One of the prominent characteristics of polymers is their viscoelasticity. Temperature changes and humid environmental conditions can significantly degrade the stiffness and strength of the polymer foam core, which in turn affects the performance of the entire sandwich structure. Joshi and Muliana (2010) analysed the effect of moisture diffusion on the deformation of viscoelastic sandwich composites. The time-dependent responses of the sandwich composites subject to moisture diffusion were analysed using a finite element method. FE analyses of the delamination between skins and core under combined moisture diffusion and mechanical loading were also performed.

Frank *et al.* (2011) discussed the structural design of a laser-welded, steel-sandwich structure. They introduced a design system to design the steel sandwich panel structure with a minimum weight that still satisfied yield and buckling criteria. To decrease the calculation time, a homogenization of the panel was carried out based on the Reissner-Mindlin plate theory. To validate and illustrate the optimization system, two case studies were presented featuring corrugated core sandwich panels.

Web-core sandwich panels have a uni-directional core that causes their high orthotropic to shear stiffness. Romanoff *et al.* (2009) investigated the influence of filling material on the shear characteristics of web-core sandwich structures. Beams with spans that are opposite the web plate direction, were tested and simulated under four point bending. The results showed that the decrease in shear deflection and shear-induced normal stress in the face plates was 3 and 7 times, respectively, in the linear elastic regime with an increase in weight of only 6 % and 15 %, respectively. The increase in ultimate strength was not as large as the increase in stiffness or the decrease in stresses. The beams failed by the shear failure of the filling material, followed by the formation of plastic hinges at the laser-welds.

Romanoff *et al.* (2011) studied the interaction between the web-core sandwich deck, including the joints, and the hull girder of a modern passenger ship. The investigation was carried out using FEM. In the analysis the sandwich decks were modelled as equivalent orthotropic shell elements that included the influence of out-of plane bending and shear deformations. A case study of a post-Panamax passenger ship was presented where the ship was subjected to vertical bending loading. In that case, the

traditional deck, made from stiffened plates, was replaced by sandwich decks that had equal cross-sectional areas and symmetrical or nonsymmetrical joints. Both deflection and normal stresses were considered as the response.

Sandwich panels constructed from metallic face sheets with cores composed of an energy-absorbing material have shown potential as effective blast resistant structures. The energy-absorbing crushed cellular material can form a stable configuration post-collapse that further contributes to blast resistance. Two commonly studied cellular materials are aluminium foams and honeycomb. Theobald *et al.* (2010) conducted air-blast tests on sandwich panels composed of steel face sheets with unbonded aluminium foam or hexagonal honeycomb cores. The test results showed that face sheet thickness has a significant effect on the performance of the panels relative to an equivalent monolithic plate. Ruan *et al.* (2010) experimentally investigated the mechanical response and energy absorption of aluminium foam sandwich panels subjected to quasi-static indentation loads. Quasi-static indentation tests were conducted with sandwich panels either simply supported, or fully fixed. Force-displacement curves were recorded and the total energy absorbed by the sandwich panels was calculated accordingly. The effects of face-sheet thickness, core thickness, boundary conditions, and the adhesive and surface conditions of face-sheets on the mechanical response and energy absorption of sandwich panels were discussed.

The stability of a sandwich structure is characterized by its buckling failure. This behaviour can be explained by several mechanisms such as fibre breaking, the debonding of the face-skin from the core, and delamination in the faces. These mechanisms reduce the structure's capacity to bear loads, leading to premature failure. Henao *et al.* (2010) presented a study about the influence of through-thickness tufted fibres on the compression and bending properties of sandwich structures.

5.1.5 Tubular Members and Joints

Pipelines operating in arctic and seismically active regions may be subjected to large ground movement that can lead to large plastic deformation in the pipelines. Deepwater flowline can also experience large lateral displacement in start-up and shut-down operations. The traditional allowable stress design methods may not be sufficient for design of pipelines that may experience large strains, and there is a need for developing the design method for pipelines beyond yield, commonly termed strain-based design. Extensive works on the strain-based design have been performed from several aspects, such as material, strain capacity both in tension and compression, testing, macro and microscopic FE modelling and pipeline system modelling (e.g., Newbury, 2010). Gresnigt and Karamanos (2009) gave an overview of the available test results and differences in various design standards concerning the local buckling strength and deformation capacity of pipes in bending. Tsuru *et al.* (2010) investigated the effect of the possible variation of the pipe geometries and the material strengths on the strain limit of girth-welded line pipes in bending through full-scale tests and FE analyses.

Offshore pipelines often carry hot hydrocarbons at a certain internal pressure. When such a line is trenched, buried or anchored, it is simultaneously subjected to axial compression due to the axial constraint. When these load effects are high enough to produce plasticity, the line buckles into an axisymmetric wrinkling mode. The subsequent cyclic load actions during lifetime may cause a gradual increase of plastic strain, called ratcheting, which may eventually leads to the collapse by localization of the wrinkling. Jiao and Kyriakides (2009, 2011a, 2011b) made detailed investigation of the ratcheting and wrinkling behaviour of tubes subjected to axial cycling with and

without internal pressure, both experimentally and numerically. One of the major findings is that the collapse under cyclic loading occurs when the net shortening of, or average strain in, the tube reached a level that corresponds to the average strain at the load maximum under monotonic loading. This provides a practical way of estimating the life expectancy of a wrinkled tube that is experiencing cyclic loading.

Limam *et al.* (2010) investigated the bending capacity of long cylinders under different values of internal pressure and the factors that affect it using both experiments and analyses. It was shown that internal pressure can significantly stabilize the structure by delaying localization and collapse, provided that the material exhibits sufficient ductility and the tube is relatively free of imperfections. The onset of wrinkling and the associated wrinkle wave length were well simulated by the bifurcation buckling formulation, and also the evolution of wrinkling and its eventual localization by the FE shell model in which the inelastic material response including yield anisotropies and the initial geometric imperfections are accurately considered.

Current design practice to assess the collapse resistance of corroded pipelines is based on the conservative approaches such as those in which thickness losses at corrosion defects are extended to the entire circumference. The typical corrosion defects, however, have more localized features, such as corrosion pits, small patches, axial or circumferential grooves. Chen *et al.* (2011) investigated the effect of corrosion defects on the collapse capacity of corroded pipelines under external pressure using finite element method. The numerical results were validated with the full-scale collapse tests. A reliability-based practical assessment method to determine the remaining collapse capacity was developed through extensive sensitivity and probabilistic studies. The selected example showed that when the proposed criteria were applied, the remaining capacity was considerably higher than assumed in current practice.

Li *et al.* (2011) investigated the burst capacity of steel pipeline with a colony of corrosion defects under internal pressure, i.e. longitudinal and circumferential aligned double corrosion defects. A basic combination of a pair of defects called as compound aligned defects was proposed with the concepts of effective corrosion width and effective corrosion length. Considering the interacting between adjacent defects and all possible combinations of defects, an assessment method of the burst capacity were presented. The predicted failure pressure was compared with the measured failure pressure from burst tests and the improved agreement with experimental results was obtained compared to the prediction by the existing methods.

A promising possibility to reduce costs in pipelines that require corrosion resistant alloys (CRA) is the use of lined pipe, consisting of a carbon steel load-bearing outer pipe that provides the structural capacity and a corrosion-resistant alloy (CRA) liner, protecting the carbon steel outer pipe from the transported corrosive product. Hilberink *et al.* (2010, 2011) performed a series of numerical and experimental studies on the mechanical behaviour, including a liner wrinkling, of Tight Fit Pipe (TFP) under axial compression and also that under bending. TFP is a type of lined pipe, where the CRA liner is fitted inside the carbon steel outer pipe through a thermo-hydraulic manufacturing process. The effect of mechanical parameters, such as the friction between liner and outer pipe, initial hoop and axial stresses, initial imperfections on the deformation and load carrying capacity was investigated. Vasilikis and Karamanos (2011) investigated the buckling of clad pipes under bending and external pressure including the difference in the mechanical behaviours between TFP and Snug Fit Pipes (i.e., stress free liner initially in contact with the outer pipe).

Some other concepts for submarine pipelines have been studied. Recent advances have been made for the better understanding of the strength of pipe-in-pipe and sandwich pipe systems. Goplen *et al.* (2011) made an analytical estimate of the global buckling of pipe-in-pipe systems under axial loads generated by differential pressure and thermal change. They concluded that the recommendations of DNV OS F101 and DNV RP F110 can be used to design and estimate the global buckling of such structures.

In view of the large application of flexible pipes and hoses on offshore industry, many researchers have dedicated their studies to the comprehension of such structures. The layers strength of flexible pipes was studied individually by several authors. Neto *et al.* (2010) has obtained the burst pressure of the pressure armor layer comparing the results of three different FE models and an analytical approach. Pesce *et al.* (2010) proposed a numerical-analytical-experimental study to get the crushing capacity of the interlocked carcass layer. Nogueira and Netto (2010) developed a simple FE model of the same layer to obtain its collapse pressure. Although these recent works are relevant for the complete understanding of the ultimate strength of such structures, much more must be done to have conclusive results.

The behavior of a flexible pipe under axial compression was studied by Sousa *et al.* (2010) through a numerical-experimental approach. The nonlinear FE model representing all the structural layers of the flexible pipe is theoretically coherent and seems to represent the axial stiffness of the structure, but the onset of the collapse cannot be detected precisely, when compared with the experimental results. The same FE model was employed by Merino *et al.* (2010) to conduct the strength study of a flexible pipe under torsion. The results showed that the correct characterization of friction between layers plays an important role in this case.

The ultimate limit state of composite hoses for fluid transferring operation (offloading) was obtained by Lassen *et al.* (2010) from experimental tests of combined bending and tension loads. Therefore, in view of the reduced number of samples employed (two) it is difficult to have conclusive results. The complex structure of a cryogenic flexible hose to LNG transferring operations was studied by Bardi *et al.* (2011). The ultimate strength of the corrugated layers was determined with the aid of a FE model under loadings of tension, compression, bending, torsion and internal pressure.

Concerning the ultimate strength of tubular joints, Lie and Yan (2011) developed a method of plastic collapse loads of cracked square hollow sections (SHSs) T-, Y- and K-joints. The concept of a reduction factor F_{AR} , which has been adopted in BS7910 but validated only for cracked circular hollow sections (CHSs) T-, K- and DK-joints, was applied to SHS T-, Y- and K-joints. The numerical plastic collapse strength was also calculated by the nonlinear finite element method using the twice elastic compliance method. It was found that the plastic collapse loads predicted by the reduction factor were on the 10–15% conservative side compared to the numerical results, and that the numerical plastic collapse loads were in good agreement with the full-scale experimental tests results.

Advanced methods of well completion and enhance oil recovery are increasingly implemented in many existing offshore oil & gas fields to continue production. Structural Integrity Management (SIM), or Platform Re-assessment and Rehabilitation (RRR), is a key to extending the useful life of offshore platforms that support the infrastructure. Puskar *et al.* (2006) summarised background details on the development of the API Recommended Practice (RP) 2SIM to offer in-depth guidance on risk-based inspection, assessment, upgrades and repairs, and platform decommissioning. Marshall

and Choo (2009) provided an overview of the SIM research at National University of Singapore and re-assessments conducted to support the case for renewed drilling offshore California.

The International Institute of Welding (IIW) sub-commission XV-E members have conducted extensive research in recent years on tubular (also referred as circular hollow section, CHS) connections or joints. Zhao *et al.* (2010) summarised the IIW static design recommendations for welded tubular joints. These recommendations refer to the key technical contributions that included the investigations on effects of chord length and boundary conditions on CHS T- and X-joints (van der Vegte and Makino, 2010), strength of thick-walled joints (Qian *et al.*, 2009), moment capacity of CHS joints (van der Vegte *et al.*, 2010), and evaluation of the CHS strength formulae to design strengths (van der Vegte *et al.*, 2009). Detailed comparisons of the new IIW strength formulae to those of API RP2A were provided by Wardenier *et al.* (2009).

5.1.6 Influence of Fabrication-related Initial Imperfections

The primary load for which ship hull girders are designed is wave-induced longitudinal bending. The bending stresses are resisted by longitudinally stiffened plates that can also contain residual stresses caused by the fabrication of the structure. The welding process has a significant influence on the fabrication factors associated with distortion and the residual stress of the steel stiffened panels that are representative of ship and offshore structures. The shape of the residual stress field can often be approximated for a butt welded panel or a panel's fillet welded stiffener if a single pass weld is performed. In the longitudinal direction, a high tensile value in the weld region (often close to the yield stress value) is balanced by a lower compressive value away from the weld region. However, the shape of the weld residual stress field may be more complicated if more weld passes are needed to complete a weld joint, or if the panel or structure to be welded is restrained during the welding process, as is the case when fabricating larger structures. Moreover, depending on the location of the panels in the ship's structure, the residual stresses in welds may be partly or fully redistributed or relaxed during the elastic shakedown caused by overloads during the operation of the ship's hull structure. In addition to residual stresses, the welding process also forms residual deformations in the panel, particularly out-of-plane deformations or so called fabrication imperfections which in most cases are detrimental to the ultimate strength.

Focusing on welded stiffened panels that are mainly subject to axial compression, the welding deformations are normally difficult to obtain from numerical FE-analyses because the complete assembly and fabrication process and possibly the change in shape during overload under operation must be simulated. One option is to measure out-of plane deformations during the fabrication and during service. When measured distortions are not available, there are three possible methods to account for the initial imperfection in FE-analyses (Amlashi and Moan, 2008):

1. Use the lowest buckling modes obtained from an eigen mode analysis.
2. Use Fourier displacement function (sinusoidal variation in the plane of the panel) for the deformation modes of interest. The generated coordinates are given directly to the nodes.
3. Use the initial imperfections resulting from a pseudo-static analysis.

A disadvantage of method (1) is that it may be difficult to extract the buckling modes of interest from the eigenvalue analysis for large-scale or complicated structures. An enhanced technique changes the geometry properties, such as plate and stiffener thickness, to decouple the local deformations of interest from the lower eigen modes, fol-

lowing Amlashi and Moan (2008) and Xu and Guedes Soares (2011a, 2011b). The modes of interest are the local plate panel deflection, the column-type initial deflection of stiffeners, the pure torsional deflection of stiffeners, and the sideways initial deflection of stiffeners. Method (2) contains there two typical approaches for the initial deflection of a local plate panel. The first is to consider the lowest elastic buckling mode, and the second is to consider the more realistic shape of initial deflection from the thin-horse mode expressed by the sum of several sinusoidal deflection components. When the same maximum amplitude is assumed, the ultimate strength obtained by the former approach normally falls on the conservative side. Method (3) has a less rational background.

The imperfection amplitudes to be used are often determined according to design codes and based on statistical data from actual panels, however, in practice the amplitude may vary from case to case. The common proposal for steels is that the amplitude $w \sim \beta$ or β^2 , where β is the plate slenderness ratio, $\beta = (b/t) \sqrt{\sigma_Y/E}$, where b = breadth of panel, t = thickness of panel, σ_Y = yield stress, and E = Young's modulus for the plate material. The value of the proportionality factor depends on the severity of the fabrication imperfection. One may also put $w \sim a, b$ (length or breadth of the panel, respectively).

Gannon *et al.* (2009) developed a finite element model capable of simulating thermo-mechanical welding process and examined the distortion and residual stresses generated during welding for different welding sequences. The distribution pattern of the longitudinal residual stress was not significantly influenced by the welding sequence; however, it did affect the peak values. The welding-induced distortions were influenced by the welding sequences and the predicted magnitude of the distortions was of a lower magnitude than the typical values suggested in the literature.

Gannon *et al.* (2011) studied the influence of welding residual stresses and deformation on the strength of tee-stiffened panels under axial compression. Residual stresses were obtained from a full thermo-mechanic simulation. Prior to the strength analysis, the panel was subject to axial shakedown loads that reduced both the tensile welding stress peaks and the amplitudes of the welding deformations. A partial relief of welding stresses was found to increase the ultimate strength somewhat, neglecting residual stresses and only considering fabrication imperfections to produce what was seen as an overly optimistic hull girder strength.

Paik and Sohn (2012) investigated the effect of welding residual stresses in a butt welded plate subject to axial compression. The welding stresses were introduced as a simplified, uniaxial initial stress field. Welding deformations were modeled as a sinusoidal field in two directions and the results revealed that longitudinal residual stresses influenced the maximum load level for thicker plates. Transverse residual stresses were also less important before buckling for the axial load situation.

Loose (2008) analyzed the stability of cylindrical shells and the influence of residual stresses and deformations introduced by a single pass circumferential weld using FEA. The influence of the different weld sequences on the radial deformation and shell stability was quantified.

Several papers investigate the influence of fabrication-induced imperfections on the ultimate strength of stiffened plates (panels) under axial compression or combined axial and transverse compression and lateral pressure. In these cases the fabrication residual stress field was not considered. Chaithanya *et al.* (2010) compared two different shapes, namely a sinusoidal variation and a cusp-shaped variation, for plate, stiffener

bowing, and stiffener warping imperfections. Khedmati *et al.* (2009a, 2009b) studied the influence of three different fillet welding procedures for stiffener to plate junction lines in stiffened plates subject to axial and transverse compression. The methods were continuous welding, chained intermittent welding, and staggered intermittent welding – all of which were considered through the modeling of the weld stiffness. Intermittent welding was found to reduce the ultimate strength.

Different methodologies for determining the ultimate strength of stiffened panels have been compared by Zhang and Khan (2009), Paik and Seo (2009b), Paik *et al.* (2011b), Frieze *et al.* (2011), and Wang *et al.* (2010) using sinusoidal variations or linearized buckling modes as fabrication imperfections and with imperfection amplitudes taken from recommendations based on experience. While typical shapes of initial deflection found in actual ship plates are summarized in textbooks (e.g., Paik and Thayamballi, 2003), some studies such as Ueda and Yao (1985), Paik and Pedersen (1996), Fujikubo *et al.* (2005), and Cho *et al.* (2011) used the initial deflection that resembles the thin-horse mode. The influence of the shape of initial plate deflection on the ultimate strength of stiffened panels has also been studied by this committee.

For welded aluminium panels, there is a special complication caused by the softening of HAZs during fusion welding, presumably caused by the annealing of the HAZs during the temperature cycle experienced during welding. This results in a lower yield strength in the HAZs, which normally reduces the ultimate strength.

Yoon *et al.* (2009) studied the buckling of a stiffened square Aluminium panel where Friction Stir Welding was used for the fabrication. Two or three stiffener cases were studied. Welding residual stresses were not included and fabrication imperfections were introduced using a buckling mode. The presence of the FSW (with a resulting lower yield strength) reduced the ultimate strength for the panel by 3%–10%.

Benson *et al.* (2011) studied the ultimate strength of aluminium plates subject to axial and compressive loading. Welding residual stresses were modelled using a simplified, uniaxial stress field (initial stress) and fabrication imperfections using sinusoidal variations. The softening of the HAZ is seen to have a significant influence on the ultimate strength, whereas the residual stress field has a moderate effect except for the most stocky plates analyzed.

5.1.7 Influence of In-service Damage

Significant research has been conducted on the ultimate strength of plates and stiffened panels with in-service damage such as corrosion wastage, fatigue cracking, and mechanical damage.

Ahmmad and Sumi (2010) investigated the strength, deformability, and energy absorption capacity of steel plate specimens with pitting corrosion or general corrosion and subject to uniaxial tension, both experimentally and numerically. The pitted surface of the specimens was generated using a CAD/CAM technique and the same model was employed for nonlinear 3D-solid FE analysis. The strength reduction factor given by Paik *et al.* (2003) for the compressive strength of pitted plates was also applicable to the tensile strength reduction factor. The empirical formulae to estimate the reduction in deformability and energy absorption capacity due to pitting corrosion and general corrosion were proposed. Islam and Sumi (2011) studied the effects of pit shape (i.e., conical or ellipsoidal) and plate size on the strength and deformability of corroded steel plates. Strength and deformability increased along with the plate width and decreased along with an increasing length. In addition, while the size effect was

not so significant for a plate wider than 500 mm, deformability was affected in a much wider range.

Silva *et al.* (2011) investigated the effect of randomly distributed nonuniform corrosion on the ultimate strength of rectangular plates under axial compression using shell FE models. Based on analyses of the surface geometry of 570 plates as generated by Monte Carlo simulation, empirical formulae for predicting strength reduction due to corrosion was developed. Jiang and Guedes Soares (2011) studied the ultimate strength of pitted mild steel plates under biaxial compression.

As for the effects of cracking damage, Paik (2009) analysed the residual ultimate strength of steel plates with longitudinal cracks under axial compression, by ANSYS nonlinear FEM. The effects of crack orientation, crack location, crack size, plate thickness and plate aspect ratio on the residual ultimate strength were discussed. It was found that either longitudinal-inside cracks or longitudinal-end cracks more significantly reduced a plate's ultimate strength under axial compression because the location of these cracks approached the plate's edge. The results were deemed to be a starting point for designing cracking damage-tolerant steel-plated structures and to assess and monitor the condition of aging steel-plated structures with cracking damage. A numerical study on the influence of crack location and crack length on the ultimate strength of a steel plate under longitudinal compression was also conducted by Bayatfar *et al.* (2011). The most critical type of cracks were transversally located in the longitudinal (unloaded) edges of an imperfect plate component.

Wang *et al.* (2009) discussed the residual ultimate strength of structural members with multiple crack damage in tension by employing nonlinear FE methods. The existence of small, disturbing cracks reduced the ultimate strength relative to a single-cracked plate, although such cracks in low-stress regions can be ignored in residual ultimate strength assessment. The obtained results provided an initial basis for considering the multi-crack problem, but further studies are needed, including crack propagation under combined loads.

Witkowska and Guedes Soares (2009) showed, numerically, that local damage to the stiffener could change the collapse mode of the plate and decrease its ultimate strength. The reduction of strength depended on the location of the dent and the initial global deflection. According to cases with more than one type of existing damage, the behaviour of a plate depends mostly on whichever type of damage is more dominant. Liu and Amdahl (2009) conducted a numerical simulation of the residual strength of a damaged double bottom. The initial damage was caused by a variety of indenters. A single stiffener model was proposed to predict the residual strength of the double bottom and an analytical equation was derived.

Amante and Estefen (2011) carried out the collapse test of six small-scale stiffened panels fabricated by special techniques to keep them in accordance with the usual full-scale tolerances related to initial geometric imperfections (Estefen *et al.*, 2007). The longitudinal length of the models was 178 mm, the transverse length was 268 mm, the plate thickness was 1.03 mm, and the stiffener space was 53.6 mm. tee-bar stiffeners ($21.6 \times 0.77 + 21.6 \times 1.03$ mm) were TIG welded to the plate. The nonlinear finite element analysis considering the initial shape imperfections obtained by measurements showed good numerical experimental correlations in the collapse behaviour of both intact and damaged stiffened panels. The results indicated that damage located at the stiffener was potentially worse for the panel's overall ultimate strength than the damage to the plate.

5.2 Systems

5.2.1 Ship-shaped Structures

An essential step of the safety check performed on ship-shaped structures is the assessment of the progressive collapse behaviour and ultimate strength of the hull girder. Simplified methods, such as the Smith method, ISUM (idealised structural unit method), ISFEM (intelligent supersize finite element method, Hughes and Paik, 2010), and empirical methods are usually employed in the ultimate strength analysis of hull girders. However, the continued growth of computer capabilities and an advance in robust nonlinear finite element methodologies have made it possible to carry out the nonlinear finite element analysis of ultimate hull girder strength with reasonable computational effort and proper modelling.

Amlashi and Moan (2008, 2009) developed a methodology for the nonlinear finite element modelling of holding tanks in a bulk carrier under different alternate hold loading conditions (i.e., fully loaded cargo and (partially) heavy cargo) that used the Abaqus program. A critical review of the external and internal design pressures for different alternate hold loading conditions was accomplished using both CSR-BC rules and DNV rules. The implications of using different design pressures on the hull girder strength were assessed. The FE results were then used to contribute to the development of simplified methods that are applicable to the practical design of ship hulls under combined global and local loads. Factors in the influence of double bottom bending such as initial imperfections, local loads, stress distribution, and failure modes on the hull girder strength were discussed. Simplified procedures for determining the hull girder strength of bulk carriers under alternate hold loading conditions were also discussed in light of the FE analyses.

Progress has been made in the reliability assessment of bulk carriers under alternate hold loading conditions based on the achievements of nonlinear finite element analyses. Amlashi and Moan (2011) proposed a reliability-based approach that fulfilled the semi-probabilistic design criteria for the ultimate hull girder strength of bulk carriers under alternate hold loading conditions with an emphasis on combined global and local loads. They found that the interaction formula proposed for bulk carriers under local pressures resulted in a consistent safety level. However, the model uncertainty in the prediction of the ultimate pressure should be more thoroughly assessed. The effect of correlations between global and local loads for both still-water and wave loads was found to be relatively important. Shu and Moan (2011) adopted an interaction equation based on the ultimate hull girder strength assessment obtained by nonlinear finite element analyses to consider the relationship between ultimate longitudinal bending capacity and average external sea pressure over the bottom. They showed that the local lateral pressure had a significant influence on the annual probability of bulk carrier failure in hogging and alternate hold loading conditions.

Okasha and Frangopol (2010) proposed a probabilistic approach to determine the strength of the ship hull where the ultimate strength of the hull girder was found using an optimization search algorithm modelling stiffened panels deterministically according to an IACS methodology. The best-fit probability distribution of the ultimate strength of the ship hull was provided. Vhanmane and Bhattacharya (2011) discussed the effect of randomness in yield strength and initial imperfections on ultimate hull girder strength. Different levels of statistical dependence between yield strength and the initial imperfection of stiffeners and the plating between stiffeners

have been considered. The methodology was applied to a bulk carrier and a VLCC tanker.

Significant progress has also been noted in both empirical and simplified approaches for predicting ultimate hull girder strength. Paik *et al.* (2011a) extended the Paik-Mansour formula for the ultimate strength calculations of ship hulls subject to vertical bending moments. The original method did not allow for the expansion of the yielded part in the vertical members, but rather limited this part to the tension flange (i.e., the deck panel in hogging conditions and the outer bottom panel in sagging conditions). The modified method permitted the expansion of the yielded part, thereby allowing the pure vertical bending moment condition to be achieved regardless of the geometrical properties of the hull cross-sections or the vertical bending loading direction. The modified Paik-Mansour formula gave an improved estimate of the ultimate strength that was in good agreement with the ANSYS and ALPS/HULL method predictions.

Yao *et al.* (2009) developed a total system that included a capacity calculation and applied the most recent version of ISUM method developed by Fujikubo and Kaeding (2002), in addition to the load calculation for the progressive collapse analysis of a ship's hull girder under longitudinal bending. Pei *et al.* (2011) applied this ISUM system to the collapse analysis of a container ship model under combined bending and torsion, considering the initial deflection and welding residual stresses. Good agreement was reached with the results of the collapse test carried out by Tanaka *et al.* (2009). The ultimate strength of the hull girder under combined global and local loads depended on the accuracy of the collapse analysis of double hull structures. The ISUM code for the double hull structure, considering shear and lateral pressure along with thrust and welding residual stresses, was developed by Gao *et al.* (2011) and applied to the double bottom structures.

Wang *et al.* (2011) applied three different methodologies of hull girder ultimate strength assessment to the hull girder ultimate strength calculations of six different FPSO designs. The three methodologies were the incremental-iterative approach by Sun and Wang (2005b), the HULLST method developed by Yao and Nikolov (1991) based on Smith's method, and the ISUM of Fujikubo and Kaeding (2002). All three methods showed good agreement in terms of the hull girder ultimate strength calculation of selected FPSOs. In general, the prediction of HULLST and ISUM are almost identical for most cases, although Sun and Wang's method produced slightly conservative results.

An issue was raised by Lehman (2006) in his official discussion of the report from Committee III.1, ISSC2006; i.e., the calculation of the moment versus curvature curves beyond the maximum sustainable bending moment is far from realistic. The natural world is, however, not controlled by pathways, but by forces. The input of a curvature does not adequately represent the failure process. To determine the realistic failure process of a hull girder when it is subjected to external loads that exceed its ultimate capacity, the progressive collapse analysis – including the effects of inertia forces and the interaction between fluid forces and structural deformations – is needed. The consequence or the severity of the failure calculated by such advanced analyses may be utilised in the risk assessment of the hull girder collapse of ships.

Xu *et al.* (2011a) investigated the dynamic collapse behaviour of a ship's hull girder in waves. The ship's entire hull was modelled as a two-rigid-bodies system connected by a rotational spring, which represented the nonlinear relation between the displacement and the moment. Nonlinear strip theory was used to solve the force equilibrium

of the two bodies. The approach was validated against tank tests, which showed that the collapse increased rapidly after the ultimate strength was reached, and the plastic deformation grew until unloading started and the bending rigidity recovered. Xu *et al.* (2011b) proposed a numerical analysis system to predict the collapse behaviour in waves, including the post-ultimate strength behaviour of ship hulls. An analytical solution to describe the post-ultimate strength behaviour was proposed. They found that the plastic deformation could be characterised by the magnitude of the load and the post-ultimate strength of the hull girder in addition to the load frequency. They also found that the plastic collapse under whipping loads after slamming is less significant.

Yang *et al.* (2011) investigated the structural dynamic buckling strength of container-ship bow structures subjected to impact force using a finite element method. A transient dynamic program was used in which the wave impact pressures were obtained by applying the semi-empirical formula established by Lloyd's Register. The results revealed that the impact force integration was the dominant factor in the structure buckling strength assessment.

The text book titled *Ship Structural Analysis and Design* (Hughes and Paik, 2010) presents the fundamental theories for ultimate strength of ship hulls.

5.2.2 Other Marine Structures

A variety of types of structures are used for offshore applications depending on the required functions and working conditions. Ye *et al.* (2011) investigated the ultimate strength of a typical drilling semisubmersible platform subjected to typical hydrodynamic loads using nonlinear finite element method. The final collapse mode of each case was found to have a close relationship to the corresponding wave load case. The initial yielding point due to split force is generally on the horizontal brace and that due to bending moment is at the regions of pontoon longitudinal centreline bulkhead around column. Pontoon and column connections are vulnerable regions to shear force and torsional moment.

Despite the efforts to reduce ship accidents, the collision between supply vessels and offshore platforms continues to happen. Amante *et al.* (2010) investigated the residual strength of a semisubmersible platform column damaged by a supply vessel collision. Finite element method simulations were performed considering material and geometric nonlinearities, initial fabrication imperfections, friction and contact formulations. The column damages due to the sideway and bow collisions of the conventional and bourbon types supply vessels with different collision energies were calculated and then the residual strength of the damaged columns under axial loading was studied to estimate the safety margin associated with the column structural capability after the collisions.

5.2.3 Influence of Fabrication-related Initial Imperfections

Kippenes *et al.* (2010) performed a nonlinear finite element (FE) analysis of a 170.000 DWT capsized bulk carrier. A three cargo hold FE model with a detailed representation of the geometry was developed. Different combinations of vertical bending moment, sea pressure, and cargo load were considered. Transverse stresses giving the long-waved buckling of the hopper plating were induced during the progressive collapse for an analysis of the initially perfect model in alternate hold loading. Two kinds of FE models with and without initial geometrical imperfections in the hopper, bilge, and side shell were analysed. Initial geometrical imperfections were seen to reduce the hull girder's ultimate strength in alternate hold loading by 5%. The effect of geometrical imperfections for real welded structures is expected to be even less.

Estefen *et al.* (2010) determined the ultimate strength of the middle section of a bulk carrier due to longitudinal bending moments using FEA. The influence of a repair weld in the upper wing tank was studied. The ship section was assumed to have sinusoidal variations of the fabrication-induced imperfections. For the plates in the upper wing area, imperfections after repair welding were measured in-locus using laser technology. The repair weld was also modelled using activating elements, hence the weld stiffness was included but the residual stresses were not. The analysis was able to identify panels and stiffeners that should be reworked to avoid damage during operation.

5.2.4 Influence of In-service Damage

The effect of corrosion on the ultimate strength of hull girders has been investigated by several research groups. Wang *et al.* (2008) performed a statistical study of the time-variant hull girders of tankers using a database of as-gauged hull structures. The expanded data set was collected from 2195 as-gauged girth belts (transverse sections) of 211 single-hull tankers that were 12–32 years old. The data set demonstrated a high variation of hull girder section moduli that changed over time. They showed that almost all previous studies estimated a much greater HG loss than what this database revealed.

Saad-Eldeen *et al.* (2011) performed an experimental assessment of the ultimate strength of a severely corroded box girder subjected to a uniform bending moment resulting from four-point loading. Three box girders capable of simulating the behaviour of midship sections were deteriorated in a corrosive seawater environment to simulate different levels of corrosion degradation in ageing ship structures. It was concluded that the load-carrying capacity and ultimate bending were highly affected by the corrosion deterioration of plating and material property changes. An interpretation of the latter should confirm that the effective elastic modulus and yield strength were reduced due to the local undulating material surface resulting from corrosion.

Notaro *et al.* (2010) performed comprehensive nonlinear analyses of a Bulk Carrier, a FPSO vessel, and a container vessel that were documented under different damage conditions. The damage size and shape were varied systematically, considering likely collision and grounding scenarios. Full ship width models were used to account for asymmetric damages. Other issues considered included FE model extension, the extension of the damages, boundary/transverse frame supports, and the model imperfection shape of the intact areas. It was found that the effect of the damage extent in the vertical and transversal directions was more critical than it was in the longitudinal direction, and the damage modified the location of the neutral axes, inducing higher stresses in proximity to the damaged areas.

6 BENCHMARK STUDIES

To validate some of the selected methods that are applicable in the ultimate strength calculations of ship and offshore structures, and also to investigate the ultimate strength characteristics, benchmark studies were undertaken on unstiffened plates, stiffened panels, and hull girders. Because of page limits, the benchmark study results are briefly summarized in this report, while details of the benchmark studies will be published in a separate article.

6.1 Candidate Methods

Table 2 – 4 indicates the candidate methods selected for the present benchmark studies.

Table 2: Candidate methods for unstiffened plates

| Method/Tool | Symbol | Working Organization |
|-------------|----------------------------|--|
| ALPS/ULSAP | ALPS/ULSAP (PNU) | Pusan National University |
| DNV/PULS | DNV/PULS (DNV) | Det Norske Veritas |
| ANSYS | ANSYS (ULG) ANSYS (IRS) | University of Liege Indian Register of Shipping |
| MSC/MARC | MSC/MARC (OU) | Osaka University |

Table 3: Candidate methods for stiffened panels

| Method/Tool | Symbol | Working Organization |
|----------------------|---|---|
| ALPS/ULSAP | ALPS/ULSAP (PNU) | Pusan National University |
| BV Advanced Buckling | BV Advanced Buckling (BV) | Bureau Veritas |
| DNV/PULS | DNV/PULS (DNV) | Det Norske Veritas |
| Abaqus | ABAQUS (NTUA) ABAQUS (DNV) | National Technical University of Athens Det Norske Veritas |
| ANSYS | ANSYS (ULG) ANSYS (IRS) ANSYS (PNU) | University of Liege Indian Register of Shipping Pusan National University |
| MSC/MARC | MSC/MARC (OU) | Osaka University |

Table 4: Candidate methods for hull girders

| Method/Tool | Symbol | Working Organization/Reference |
|--------------------------------|-----------------------------------|---|
| Test (1/3-scale frigate model) | Test result | Dow (1991) |
| Modified Paik-Mansour method | Modified P-M at ULS (PNU) | Pusan National University (Paik <i>et al.</i> , 2011a) |
| RINA Rules | RINA Rules (UoG) | University of Genova |
| Common Structural Rules | CSR (BV) CSR (CR) CSR (PNU) | Bureau Veritas China Corporation Register of Shipping Pusan National University |
| ALPS/HULL ISFEM | ALPS/HULL (PNU) | Pusan National University |
| Abaqus | ABAQUS (CR) | China Corporation Register of Shipping |
| ANSYS | ANSYS (IRS) ANSYS (PNU) | Indian Register of Shipping Pusan National University |
| ISSC 2000 | ISSC 2000 | ISSC (2000) |

Table 5: Geometric and material properties of target plates

| Geometric and material properties | Nomenclature |
|---|--------------|
| <ul style="list-style-type: none"> • Yield stress of plate, $\sigma_{Yp} = 313.6 \text{ N/mm}^2$ • Elastic modulus, $E = 205800 \text{ N/mm}^2$ • Poisson's ratio, $\nu = 0.3$ • Plate length, $a = 2550 \text{ mm}$ • Plate breadth, $b = 850 \text{ mm}$ • Plate thickness, $t_p = 9.5, 11, 13, 16, 22, 33 \text{ mm}$ • Under biaxial compressive loads | |

6.2 Target Structures

6.2.1 Plates

Plates surrounded by longitudinal stiffeners and transverse frames are selected as the target structure of the benchmark studies. The geometric and material properties of target plates are defined as shown in Table 5.

Table 6: Panel A and Panel C

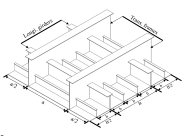
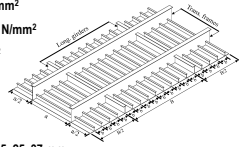
| Panel A: Bottom of a bulk carrier | Panel C: Deck of a double hull tanker |
|---|--|
| <ul style="list-style-type: none"> • Yield stress of plate, $\sigma_{yp} = 313.6 \text{ N/mm}^2$ • Yield stress of stiffener, $\sigma_{ys} = 313.6 \text{ N/mm}^2$ • Elastic modulus, $E = 205800 \text{ N/mm}^2$ • Poisson's ratio, $\nu = 0.3$ • Plate length, $a = 2550 \text{ mm}$ • Plate breadth, $b = 850 \text{ mm}$ • Plate thickness, $t_p = 9.5, 11, 13, 16, 22, 33 \text{ mm}$ • Number of stiffeners: 2 stiffeners in a panel  | <ul style="list-style-type: none"> • Yield stress of plate, $\sigma_{yp} = 313.6 \text{ N/mm}^2$ • Yield stress of stiffener, $\sigma_{ys} = 313.6 \text{ N/mm}^2$ • Elastic modulus, $E = 205800 \text{ N/mm}^2$ • Poisson's ratio, $\nu = 0.3$ • Plate length, $a = 4750 \text{ mm}$ • Plate breadth, $b = 950 \text{ mm}$ • Plate thickness, $t_p = 11, 12.5, 15, 18.5, 25, 37 \text{ mm}$ • Number of stiffeners: 8 stiffeners in a panel  |

Table 7: Geometry of stiffeners considered

| Dimensions [mm] | Nomenclature | | |
|-----------------|-------------------------------|---|---|
| | Flat bar ($h_w \times t_w$) | Angle bar ($h_w \times b \times t_w / t_f$) | Tee bar ($h_w \times b \times t_w / t_f$) |
| Size 1 | 150x17 | 138x90x9/12 | 138x90x9/12 |
| Size 2 | 250x25 | 235x90x10/15 | 235x90x10/15 |
| Size 3 | 350x35 | 383x100x12/17 | 383x100x12/17 |
| Size 4 | 550x35 | 580x150x15/20 | 580x150x15/20 |

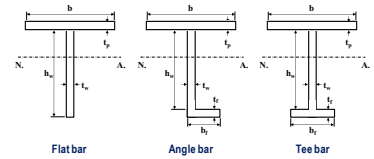


Table 8: Coefficients of the initial distortion equations

| Methods | A_0 | B_0 | C_0 |
|--|------------------|------------|------------|
| ALPS/ULSAP, ALPS/HULL, Abaqus, ANSYS, MSC/MARC | $0.1\beta^2 t_p$ | $0.0015 a$ | $0.0015 a$ |
| DNV/PULS | $b/200$ | $0.001 a$ | $0.001 a$ |

6.2.2 Stiffened Panels

Stiffened panels surrounded by longitudinal girders and transverse frames are selected as the target structure of the benchmark studies. Two types of stiffened panels are considered, namely Panel A and Panel C (see Table 6), which were taken from the bottom panels of a bulk carrier and the deck panels of a very large, double hull crude oil tanker, respectively.

Three types of stiffeners, namely flat bar, angle bar, and tee bar, were considered with varied dimensions as shown in Table 7.

Three types of initial distortions are considered, namely plate initial deflection, the column type initial distortion of the stiffener, and the sideways initial distortion of the stiffener, which can be expressed as follows (Hughes and Paik, 2010).

- Buckling mode initial deflection of plating: $w_{opt} = A_0 \sin \frac{m\pi x}{a} \sin \frac{\pi y}{b}$
- Column type distortion of stiffener: $w_{oc} = B_0 \sin \frac{\pi x}{a} \sin \frac{\pi y}{B}$
- Sideways initial distortion of stiffener: $w_{os} = C_0 \frac{z}{h_w} \sin \frac{\pi x}{a}$

where m = buckling mode of the plate which is defined as a minimum integer satisfying $a/b \leq \sqrt{m(m+1)}$. In the present benchmark studies, the coefficients of the abovementioned initial distortion equations are presumed for each of the following candidate methods as shown in Table 8.

6.2.3 Hull Girders

The six kinds of hull structures considered in the present benchmark studies are shown in Figure 4, 5, 6, 7, 8 and 9.

| Stif. No. | Dimensions | Type | σ_y (MPa) | Stif. No. | Dimensions | Type | σ_y (MPa) |
|--------------------------------|----------------|---------|------------------|----------------|----------------|---------|------------------|
| All deck & shell Longitudinals | 38.1+78.14+3.3 | Tee-bar | 245 | No. 3 | 162.2+51.2 | Tee-bar | 245 |
| No. 2 Deck | 292.6+120.10 | Tee-bar | 245 | No. 7 | 117.5+2+51.2 | Tee-bar | 245 |
| No. 2 Deck bar | 60+6 | At-bar | 245 | No. 11 | 111.2+51.2 | Tee-bar | 245 |
| Vertical Keel | 228.6+3+51.2 | tee-bar | 245 | No. 3 & 4 Deck | 114.5+44.5+9.5 | Tee-bar | 245 |

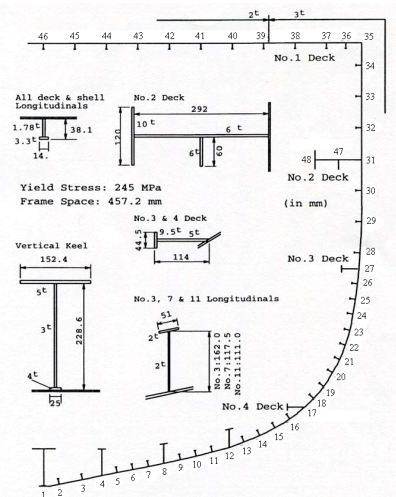


Figure 4: Dow's test hull – 1/3-scale frigate

| Stif. No. | dimensions | type | σ_y (MPa) | Stif. No. | dimensions | type | σ_y (MPa) |
|-----------|------------------------|-----------|------------------|-----------|---------------------|-----------|------------------|
| 1 | 300 x 38 | at-bar | 352.8 | 9 | 230 x 10 | at-bar | 313.6 |
| 2 | 300 x 28 | at-bar | 313.6 | 10 | 300 x 90 x 13/17 IA | angle-bar | 313.6 |
| 3 | 250 x 90 x 10/15 IA | angle-bar | 313.6 | 11 | 150 x 90 x 12/12 IA | angle-bar | 313.6 |
| 4 | 250 x 90 x 12/16 IA | angle-bar | 313.6 | 12 | 250 x 90 x 12/18 IA | angle-bar | 313.6 |
| 5 | 300 x 90 x 11/16 IA | angle-bar | 313.6 | 13 | 150 x 12 | at-bar | 313.6 |
| 6 | 300 x 90 x 13/17 IA | angle-bar | 313.6 | 14 | 150 x 90 x 9/9 IA | angle-bar | 313.6 |
| 7 | 350 x 100 x 12/17 IA | angle-bar | 313.6 | 15 | 150 x 10 | at-bar | 313.6 |
| 8 | 400 x 100 x 11.5/16 IA | angle-bar | 313.6 | 16 | 300 x 90 x 11/11 IA | angle-bar | 313.6 |

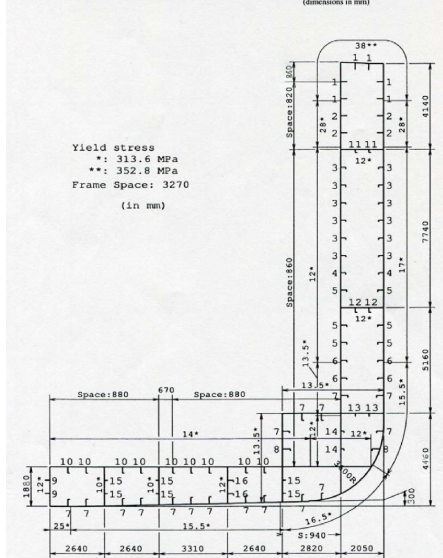


Figure 5: Container ship hull

| Stif. No. | dimensions | type | σ_y (MPa) | Stif. No. | dimensions | type | σ_y (MPa) |
|-----------|------------------|----------|------------------|-----------|-----------------------|---------|------------------|
| 1 | 393.2 | at-bar | 392.0 | 8 | 383.9 x 9 + 100 x 17 | tee-bar | 352.8 |
| 2 | 333.9 x 100 x 10 | tee-bar | 352.8 | 9 | 333.9 x 9 + 100 x 18 | tee-bar | 352.8 |
| 3 | 283.9 x 100 x 14 | tee-bar | 352.8 | 10 | 333.9 x 9 + 100 x 19 | tee-bar | 352.8 |
| 4 | 383.9 x 100 x 18 | tee-bar | 352.8 | 11 | 382.9 x 9 + 100 x 17 | tee-bar | 352.8 |
| 5 | 333.9 x 100 x 17 | tee-bar | 352.8 | 12 | 383.9 x 10 + 100 x 18 | tee-bar | 352.8 |
| 6 | 283.9 x 100 x 16 | tee-bar | 352.8 | 13 | 383.9 x 10 + 100 x 21 | tee-bar | 352.8 |
| 7 | 180 x 32.5 x 9.5 | hull-bar | 235.2 | 14 | 300 x 27 | at-bar | 392.6 |

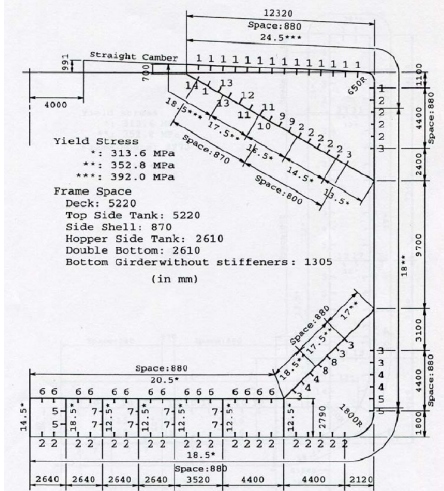


Figure 6: Bulk carrier hull

| Stif. No. | Dimension | Type | σ_y (MPa) | Stif. No. | Dimension | Type | σ_y (MPa) |
|-----------|---------------------|---------|------------------|-----------|--------------------|-----------|------------------|
| 1 | 400-10+150-13 | Tee-bar | 315.0 | 20 | 750-14+200-13 | Tee-bar | 315.0 |
| 2 | 400-10+150-13 | Tee-bar | 315.0 | 21 | 385-10+125-13 | Tee-bar | 315.0 |
| 3 | 500-10+150-22.5 | Tee-bar | 355.0 | 22 | 480-10.2+150-24.75 | Tee-bar | 315.0 |
| 4 | 500-10+150-18.5 | Tee-bar | 355.0 | 23 | 440-10.2+150-0.75 | Tee-bar | 315.0 |
| 5 | 520-10+150-18.5 | Tee-bar | 315.0 | 24 | 400-10.2+150-16.75 | Tee-bar | 315.0 |
| 6 | 480-10+150-16.5 | Tee-bar | 315.0 | 25 | 400-10.2+150-14.75 | Tee-bar | 315.0 |
| 7 | 440-10+150-16.5 | Tee-bar | 315.0 | 26 | 385-10.2+125-13.75 | Tee-bar | 315.0 |
| 8 | 420-10+150-14.5 | Tee-bar | 315.0 | 27 | 340-10.2+125-13.75 | Tee-bar | 315.0 |
| 9 | 400-10+150-14.5 | Tee-bar | 315.0 | 28 | 750-14+200-13 | Tee-bar | 315.0 |
| 10 | 385-10+150-13.5 | Tee-bar | 315.0 | 29 | 385-10+150-13 | Tee-bar | 315.0 |
| 11 | 500-9.75+150-22.5 | Tee-bar | 355.0 | 30 | 350-100-10.515.5 | Angle-bar | 315.0 |
| 12 | 500-11.5+150-20 | Tee-bar | 355.0 | 31 | 250-13.5 | At-bar | 315.0 |
| 13 | 480-9.75+150-20.25 | Tee-bar | 315.0 | 32 | 150-13.5 | At-bar | 315.0 |
| 14 | 440-9.75+150-22.25 | Tee-bar | 315.0 | 33 | 150-10.75 | At-bar | 315.0 |
| 15 | 400-9.75+150-20.25 | Tee-bar | 315.0 | 34 | 400-100-11.516.5 | Angle-bar | 315.0 |
| 16 | 400-9.75+150-16.25 | Tee-bar | 315.0 | 35 | 385-9.5+150-13 | Tee-bar | 315.0 |
| 17 | 385-9.75+150-13.25 | Tee-bar | 315.0 | 36 | 385-10+125-13 | Tee-bar | 315.0 |
| 18 | 385-9.75+125-13.25 | Tee-bar | 315.0 | 37 | 340-9.5+125-13 | Tee-bar | 315.0 |
| 19 | 385-10.25+125-13.25 | Tee-bar | 315.0 | | | | |

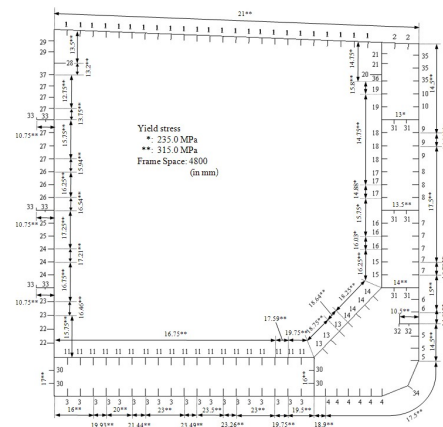


Figure 7: Suezmax class double hull oil tanker hull

| Stif. No. | dimensions | type | σ_y (MPa) | Stif. No. | dimensions | type | σ_y (MPa) |
|-----------|-----------------------|------------|------------------|-----------|-----------------------|------------|------------------|
| 1 | 797 × 15 × 200 × 33 | tee-bar* | 313.6 | 17 | 747 × 12.7 × 180 × 25 | angle-bar* | 235.2 |
| 2 | 300 × 100 × 11.5/16 | angle-bar | 313.6 | 18 | 792 × 14 × 180 × 25 | tee-bar* | 235.2 |
| 3 | 370 × 16 | at-bar | 313.6 | 19 | 847 × 14 × 180 × 25 | angle-bar* | 313.6 |
| 4 | 425 × 25 | at-bar | 313.6 | 20 | 847 × 14 × 180 × 32 | tee-bar* | 235.2 |
| 5 | 480 × 32 | at-bar | 313.6 | 21 | 847 × 15 × 180 × 25 | angle-bar* | 313.6 |
| 6 | 300 × 100 × 11.5/16 | angle-bar | 313.6 | 22 | 847 × 15 × 180 × 32 | angle-bar* | 313.6 |
| 7 | 330 × 16 | at-bar | 313.6 | 23 | 897 × 15 × 200 × 25 | angle-bar* | 235.2 |
| 8 | 447 × 11.5 × 125 × 22 | tee-bar* | 313.6 | 24 | 945 × 16 × 200 × 25 | angle-bar* | 235.2 |
| 9 | 549 × 11.5 × 125 × 22 | angle-bar* | 235.2 | 25 | 897 × 15 × 200 × 25 | angle-bar* | 313.6 |
| 10 | 597 × 11.5 × 125 × 22 | angle-bar* | 235.2 | 26 | 792 × 15 × 180 × 25 | angle-bar* | 313.6 |
| 11 | 597 × 11.5 × 125 × 22 | angle-bar* | 235.2 | 27 | 347 × 11.5 × 125 × 22 | angle-bar* | 313.6 |
| 12 | 647 × 11.5 × 125 × 22 | angle-bar* | 235.2 | 28 | 397 × 25 | at-bar | 313.6 |
| 13 | 330 × 24 | at-bar | 235.2 | 29 | 300 × 25 | at-bar | 235.2 |
| 14 | 646 × 12.7 × 150 × 25 | angle-bar* | 235.2 | 30 | 230 × 12.7 | at-bar | 235.2 |
| 15 | 697 × 12.7 × 150 × 25 | angle-bar* | 235.2 | 31 | 230 × 12.7 | at-bar | 235.2 |
| 16 | 747 × 12.7 × 150 × 25 | angle-bar* | 313.6 | 32 | 397 × 11.5 × 100 × 25 | tee-bar* | 313.6 |

(* fabricated by welding; dimensions in mm)

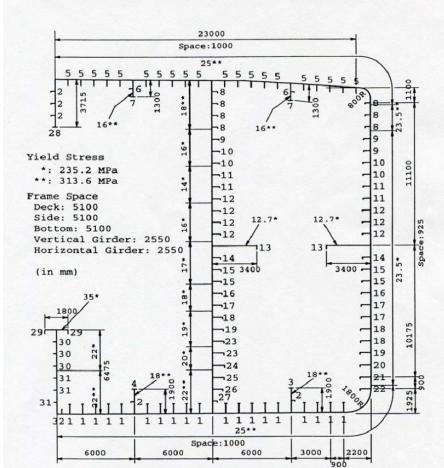


Figure 8: Single hull VLCC hull

| Stif. No. | dimensions | type | σ_y (MPa) | Stif. No. | dimension | type | σ_y (MPa) |
|-----------|-----------------------|------------|------------------|-----------|----------------------|-----------|------------------|
| 1 | 300 × 90 × 12/17 IA | angle-bar | 313.6 | 25 | 350 × 90 × 12/16 IA | angle-bar | 313.6 |
| 2 | 350 × 100 × 12/17 IA | angle-bar | 313.6 | 26 | 450 × 11 × 150 × 23 | tee-bar* | 352.8 |
| 3 | 400 × 100 × 12/17 IA | angle-bar | 313.6 | 27 | 450 × 11 × 150 × 19 | tee-bar* | 352.8 |
| 4 | 400 × 11 × 150 × 12 | tee-bar* | 313.6 | 28 | 450 × 11 × 150 × 16 | tee-bar* | 352.8 |
| 5 | 400 × 11 × 150 × 14 | tee-bar* | 313.6 | 29 | 450 × 11 × 150 × 14 | tee-bar* | 352.8 |
| 6 | 450 × 11 × 150 × 12 | tee-bar* | 313.6 | 30 | 450 × 11 × 150 × 12 | tee-bar* | 352.8 |
| 7 | 450 × 11 × 150 × 14 | tee-bar* | 313.6 | 31 | 450 × 11 × 150 × 14 | tee-bar* | 352.8 |
| 8 | 450 × 11 × 150 × 16 | tee-bar* | 313.6 | 32 | 400 × 100 × 12/16 IA | angle-bar | 352.8 |
| 9 | 450 × 11 × 150 × 19 | tee-bar* | 313.6 | 33 | 350 × 100 × 12/17 IA | angle-bar | 352.8 |
| 10 | 450 × 11 × 150 × 22 | tee-bar* | 313.6 | 34 | 300 × 90 × 12/17 IA | angle-bar | 352.8 |
| 11 | 450 × 11 × 150 × 25 | tee-bar* | 313.6 | 35 | 450 × 11 × 150 × 19 | tee-bar* | 352.8 |
| 12 | 500 × 11 × 150 × 28 | tee-bar* | 313.6 | 36 | 250 × 90 × 12/16 IA | angle-bar | 352.8 |
| 13 | 500 × 11 × 150 × 30 | tee-bar* | 313.6 | 37 | 300 × 90 × 12/16 IA | angle-bar | 352.8 |
| 14 | 500 × 11 × 150 × 32 | tee-bar* | 313.6 | 38 | 400 × 11 × 150 × 14 | tee-bar* | 352.8 |
| 15 | 500 × 11 × 150 × 34 | tee-bar* | 313.6 | 39 | 450 × 11 × 150 × 12 | tee-bar* | 352.8 |
| 16 | 550 × 12 × 150 × 30 | tee-bar* | 313.6 | 40 | 450 × 11 × 150 × 14 | tee-bar* | 352.8 |
| 17 | 550 × 12 × 150 × 25 | tee-bar* | 313.6 | 41 | 450 × 11 × 150 × 16 | tee-bar* | 352.8 |
| 18 | 350 × 100 × 12/17 IA | angle-bar* | 313.6 | 42 | 450 × 11 × 150 × 19 | tee-bar* | 352.8 |
| 19 | 350 × 12.5 × 150 × 32 | tee-bar* | 352.8 | 43 | 450 × 11 × 150 × 23 | tee-bar* | 352.8 |
| 20 | 500 × 11.5 × 150 × 20 | tee-bar* | 252.8 | 44 | 450 × 11 × 150 × 25 | tee-bar* | 352.8 |
| 21 | 500 × 11.5 × 150 × 28 | tee-bar* | 252.8 | 45 | 450 × 11 × 150 × 28 | tee-bar* | 352.8 |
| 22 | 500 × 11 × 150 × 25 | tee-bar* | 352.8 | 46 | 500 × 11 × 150 × 25 | tee-bar* | 352.8 |
| 23 | 450 × 11 × 150 × 28 | tee-bar* | 352.8 | 47 | 500 × 11 × 150 × 28 | tee-bar* | 352.8 |
| 24 | 250 × 12.5 | at-bar | 313.6 | 48 | 230 × 12.5 | at-bar | 313.6 |

(* fabricated by welding; dimensions in mm)

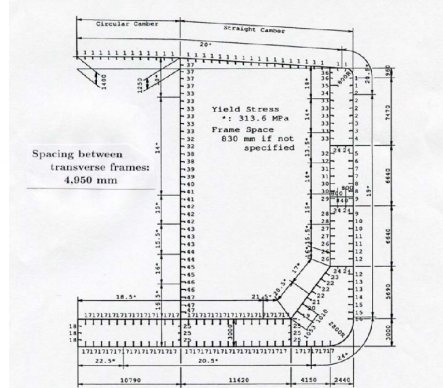


Figure 9: Double hull VLCC hull

6.3 Modelling Techniques

6.3.1 Plates

It is assumed that the four plate edges are simply supported for theoretical computations of ultimate strength. However, the nonlinear finite element methods take into account the effect of rotational restraints along the plate edges. The effects of fabrication-related initial imperfections on plate ultimate strength are also studied.

6.3.2 Stiffened Panels

It is assumed that the four panel edges are simply supported in theoretical methods, while the nonlinear finite element methods more realistically consider the effect of rotational restraints along the panel edges. Three types of finite element method modelling techniques are considered and the effect of initial distortions is also studied.

Figure 12 compares the ultimate strength behaviour of Panel C under longitudinal compressive loads between the one bay/one span model, Figure 10, and the two

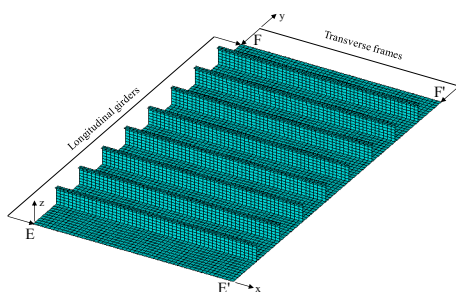


Figure 10: One bay/one span model

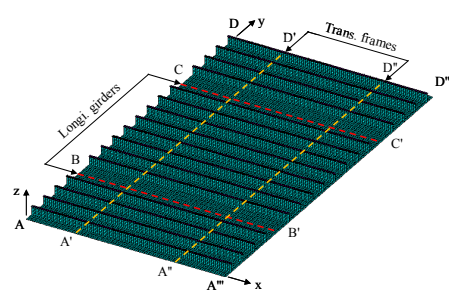


Figure 11: Two bay/two span model

Table 9: Boundary condition for one bay/one span model

| Boundary | Description |
|-----------------------|--|
| $E - E'$ and $F - F'$ | Simply supported condition with $R_y = R_z = 0$ and $U_z = 0$, uniform displacement in the y direction ($U_y = \text{uniform}$), coupled with the plate part |
| $E - F$ and $E' - F'$ | Simply supported condition with $R_x = R_z = 0$ and $U_z = 0$, uniform displacement in the x direction ($U_x = \text{uniform}$), coupled with the longitudinal stiffeners |

Table 10: Boundary condition for two bay/two span model

| Boundary | Description |
|--|--|
| $A - A'''$ and $D - D'''$ | Symmetric condition with $R_x = R_z = 0$ and uniform displacement in the y direction ($U_y = \text{uniform}$), coupled with the plate part |
| $A - D$ and $A''' - D'''$ | Symmetric condition with $R_y = R_z = 0$ and uniform displacement in the x direction ($U_x = \text{uniform}$), coupled with the longitudinal stiffener |
| $A' - D'$, $A'' - D''$, $B - B'$ and $C - C'$ | $U_z = 0$ |

bay/two span model, Figure 11. The results of the one bay/one span model are usually in good agreement with those of the two bay/two span model, but it is cautioned that the former are significantly larger than the latter in the other case. This is due to the fact that in the former case, the sideways deformations of stiffeners located at the transverse frames are not allowed. It is desirable to apply the two bay/two span model in this regard when the transverse frames may distort before the panel reaches the ultimate strength.

An MSC/MARC nonlinear finite element method analysis was undertaken by Osaka University using two bay/two span models. The boundary condition of the models

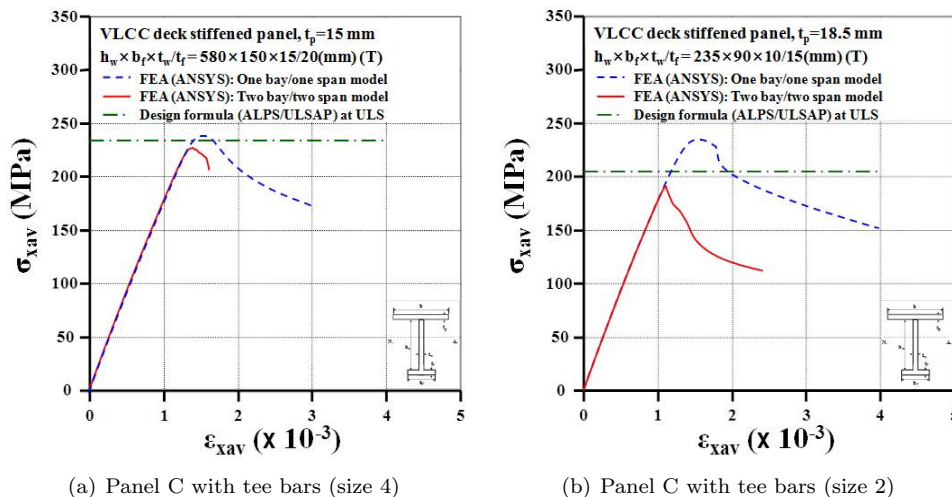


Figure 12: Ultimate strength behaviour of Panel C under longitudinal compressive loads

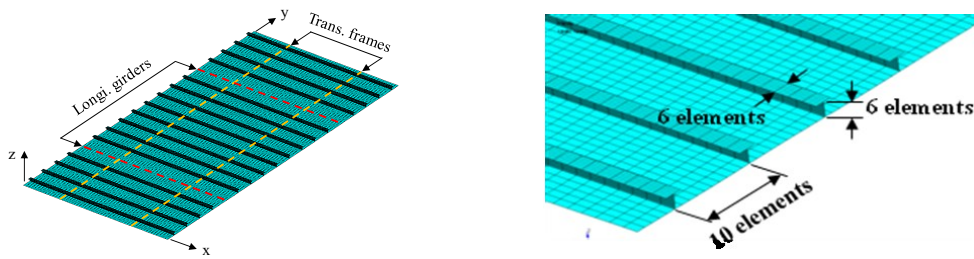


Figure 13: 6,480 elements for Panel A and 37,200 elements for Panel C

for in-plane displacements are as indicated in Table 10, while that for out-of-plane displacements is the periodically symmetric boundary condition. The same mesh sizes were applied regardless of the different sized stiffeners in the stiffened panels, as shown in Figure 13.

An Abaqus nonlinear finite element method analysis was carried out by DNV using a three bay (1/2+1+1+1/2)/one span model, in which only a longitudinal compressive load case was studied (i.e., without transverse compressive loads). The same mesh sizes were applied regardless of the different sized stiffeners in the stiffened panels, see Figure 14. Table 11 indicates the mesh sizes applied for the Abaqus nonlinear FEA by DNV.

The Abaqus nonlinear finite element method analysis was also undertaken by NTUA

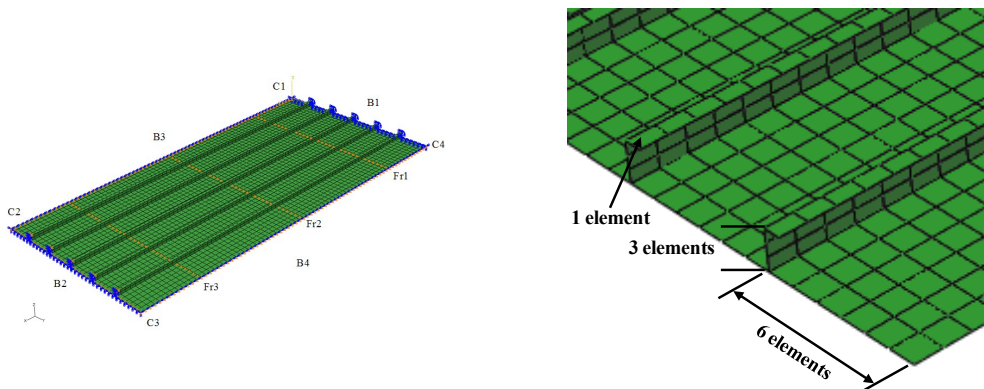


Figure 14: 7,740 elements for Panel C

Table 11: Boundary condition for three bay/one span model applied for Abaqus nonlinear FEA

| Boundary | Description |
|------------------|---|
| B1 and B2 | All fixed condition with $R_x = R_y = R_z = U_y = U_z = 0$, uniform displacement in the x direction ($U_x = \text{uniform}$), coupled with the longitudinal stiffeners |
| B3 and B4 | Simply supported condition with $R_y = R_z = 0$ and $U_z = 0$, uniform displacement in the y direction ($U_y = \text{uniform}$), coupled with the plate part |
| Fr1, Fr2 and Fr3 | $U_z = 0$ |

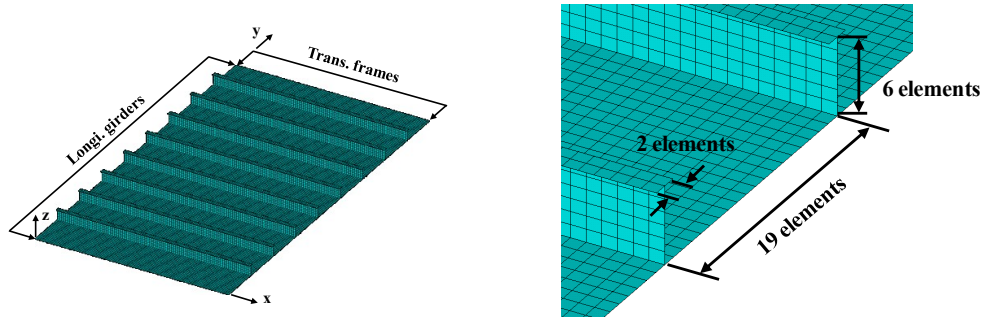


Figure 15: 22,325 elements for Panel C

using a one bay/one span model. The same mesh sizes were applied regardless of the different sized stiffeners in the stiffened panels, as shown in Figure 15.

6.3.3 Hull Girders

The hull structures between two adjacent transverse frames at midship are taken as the extent of the analysis.

6.4 Results and Observations

6.4.1 Plates

Under Biaxial Compression

Figure 16 represents the results of the benchmark studies on unstiffened plates under biaxial compressive loads.

Effect of Initial Deflection

The effects of plate initial deflection in terms of magnitude and shape are studied considering two types of initial deflection shapes, namely buckling mode shape and hungry-horse mode shape, as shown in Figure 17. It is found that the ultimate strength of plates with the hungry-horse initial deflection shape is greater than that of plates

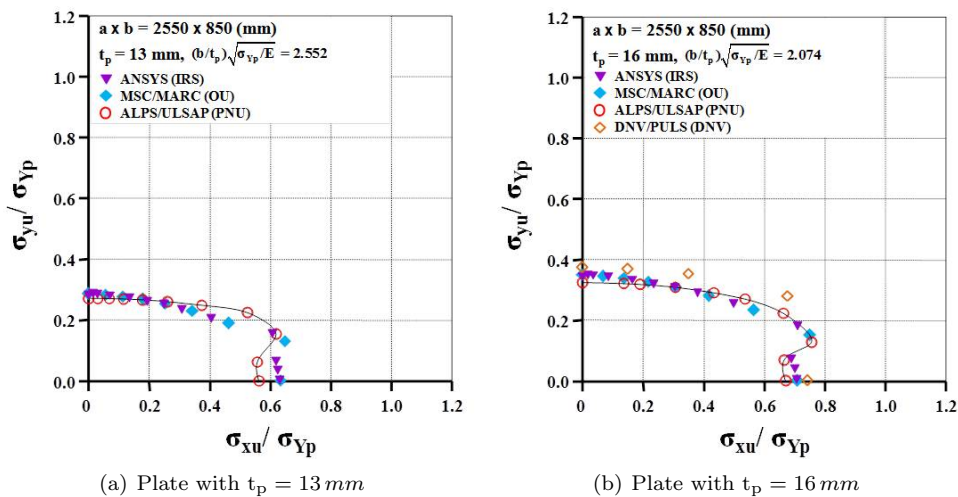


Figure 16: Results of benchmark on unstiffened plates under biaxial compressive loads

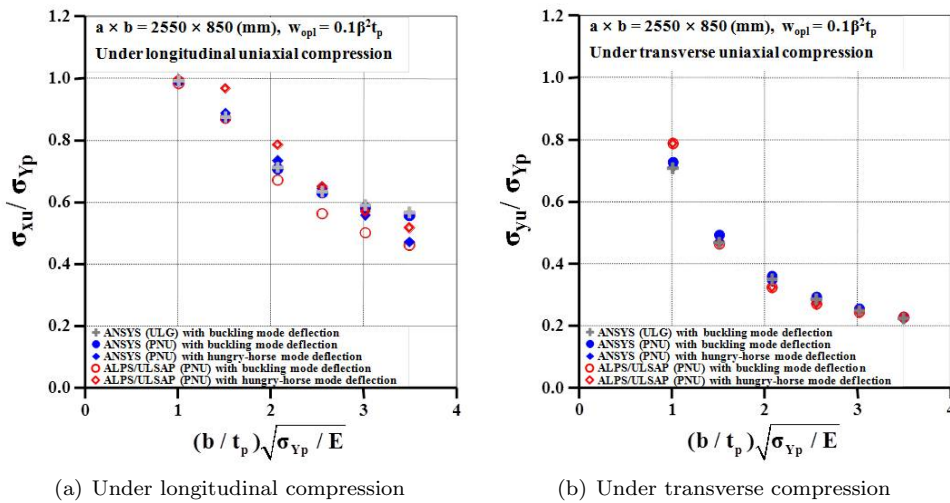


Figure 17: Effect of Initial Deflection

with buckling mode initial deflection when longitudinal compressive loads are predominant, but the effect of the initial deflection shape is small when predominantly transverse compressive loads are applied.

6.4.2 Stiffened Panels

In the following, the benchmark study results for stiffened panels are presented. ALPS/ULSAP method calculations provide the information for panel collapse modes, which are classified into six types, namely (Hughes and Paik, 2010)

- Mode I: overall collapse
- Mode II: plate collapse without distinct failure of stiffeners
- Mode III: beam-column type collapse of stiffeners with attached plating
- Mode IV: local buckling of stiffener web
- Mode V: torsional-flexural buckling (tripping) of stiffeners
- Mode VI: gross yielding

Panel A

Figure 18 represent the results of the benchmark studies on Panel A under longitudinal or transverse compressive loads, respectively, in which the types and dimensions of stiffeners are varied. Figures 19 show the ultimate strength of stiffened panels under longitudinal or transverse compressive loads, respectively, as a function of the column slenderness ratio. Figures 20–22 represent the results for Panel A under biaxial compressive loads with varied stiffener types and dimensions, where σ_{yeq} is the equivalent yield stress and r = radius of gyration for the stiffener with attached plating.

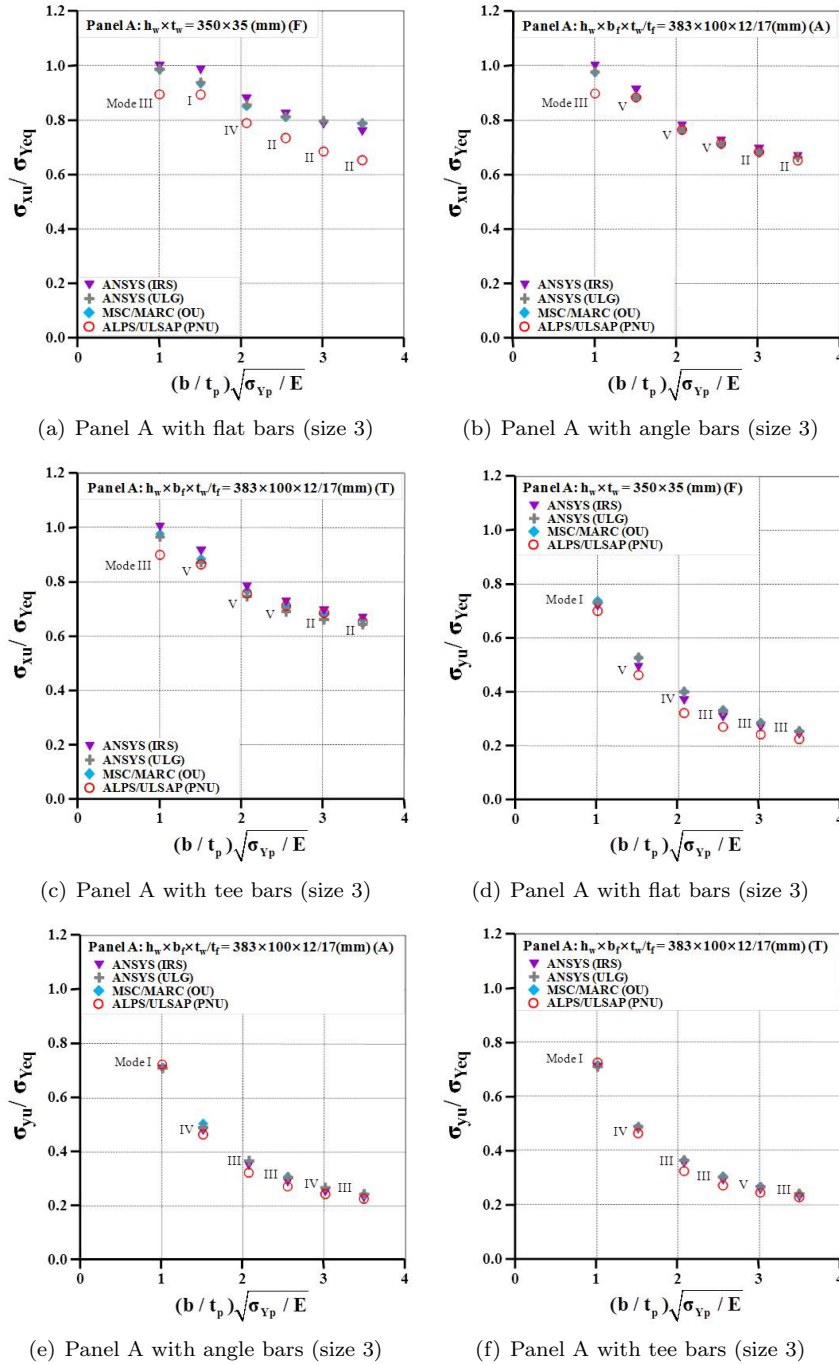


Figure 18: Results of Panel A under longitudinal or transverse compressive loads

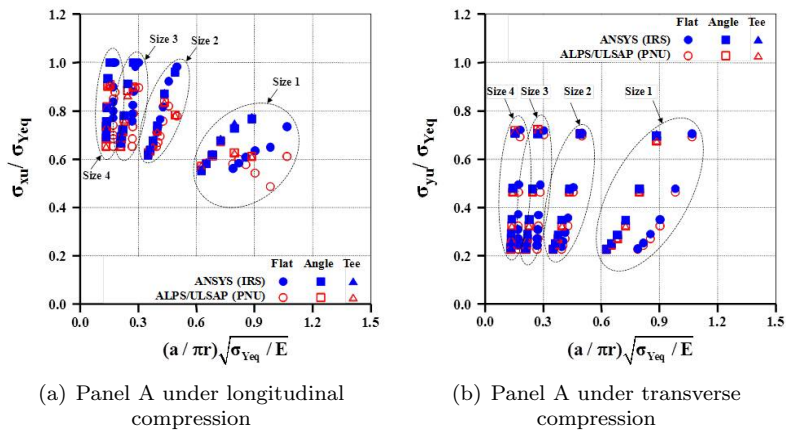


Figure 19: Ultimate strength of stiffened panels under longitudinal or transverse compressive loads

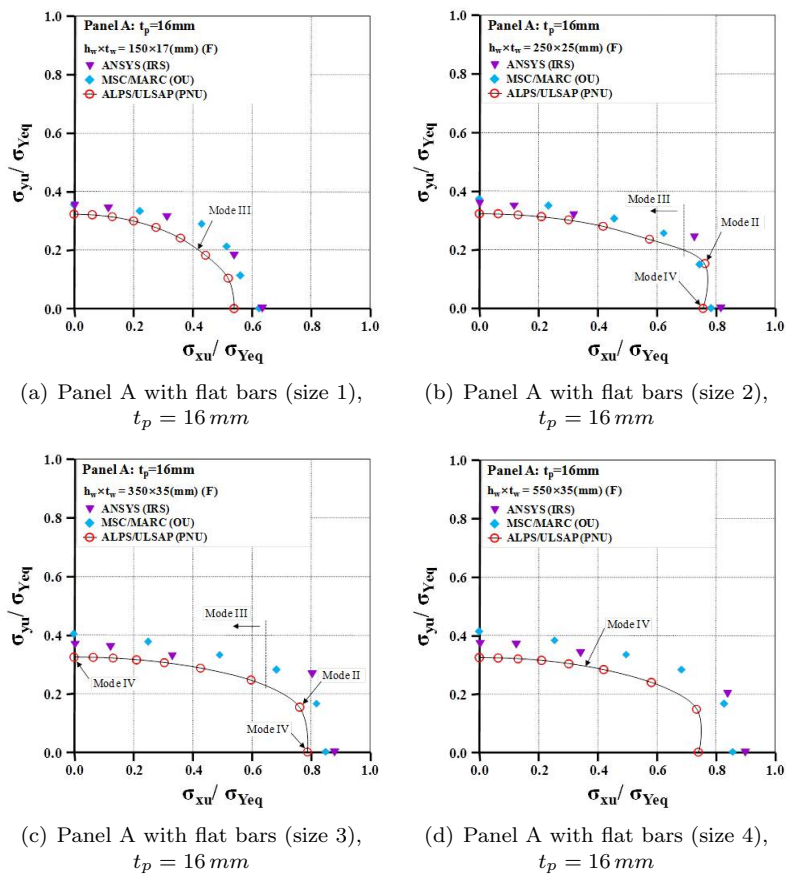
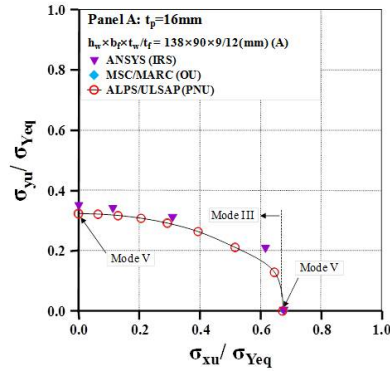
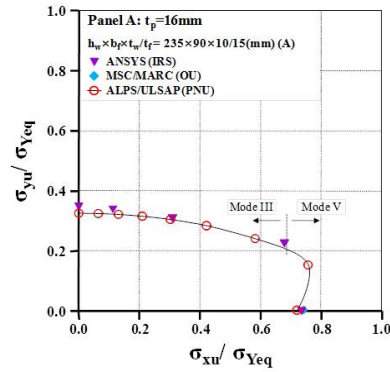


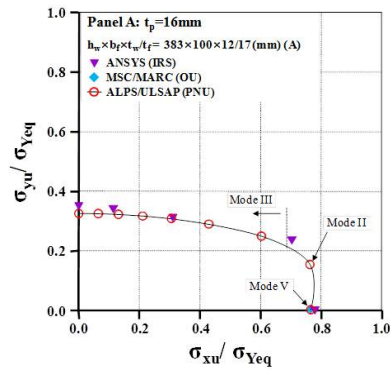
Figure 20: Results for Panel A under biaxial compressive loads with varied stiffener types and dimensions



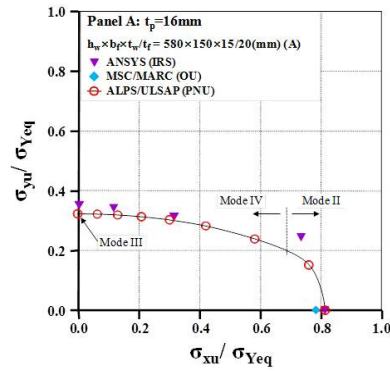
(a) Panel A with angle bars (size 1),
 $t_p = 16 \text{ mm}$



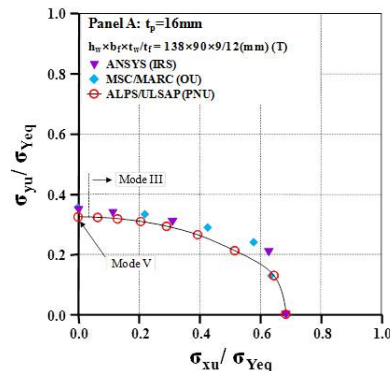
(b) Panel A with angle bars (size 2),
 $t_p = 16 \text{ mm}$



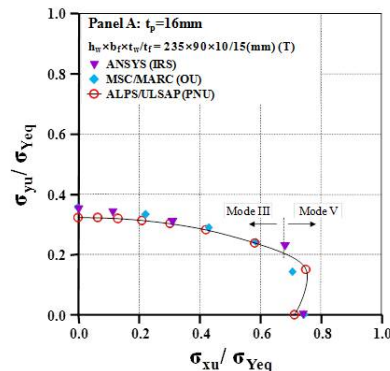
(c) Panel A with angle bars (size 3),
 $t_p = 16 \text{ mm}$



(d) Panel A with angle bars (size 4),
 $t_p = 16 \text{ mm}$



(e) Panel A with Tee bars (size 1),
 $t_p = 16 \text{ mm}$



(f) Panel A with Tee bars (size 2),
 $t_p = 16 \text{ mm}$

Figure 21: Results for Panel A under biaxial compressive loads with varied stiffener types and dimensions – continued

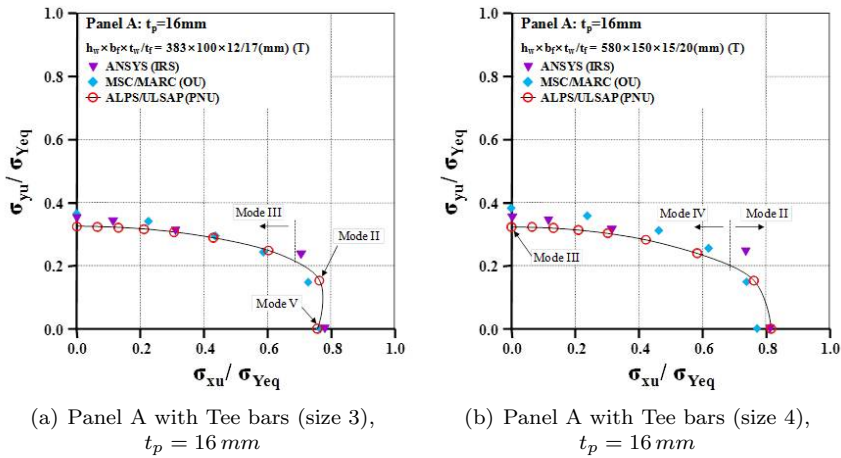


Figure 22: Results for Panel A under biaxial compressive loads with varied stiffener types and dimensions – continued

Panel C

Figures 23 and 24 represent the results of the benchmark studies on Panel C under longitudinal or transverse compressive loads, respectively, in which the types and dimensions of stiffeners are varied. Figure 25 show the ultimate strength of stiffened panels under longitudinal or transverse compressive loads, respectively, as a function of the column slenderness ratio. Figures 26 and 27 represent the results of benchmark studies for Panel A under biaxial compressive loads with varied stiffener types and dimensions, where σ_{Yeql} is the equivalent yield stress. It is found that the BV method is not applicable for some ranges of stiffener dimensions. Also, the Abaqus method applied by NTUA significantly overestimates the ultimate strength in some cases. This is due to the fact that the Abaqus models by NTUA adopted the one bay/one span model where the sideways distortions of stiffeners at the locations of transverse frames are not allowed, and subsequently the panel ultimate strength can be overestimated as discussed with Figure 12.

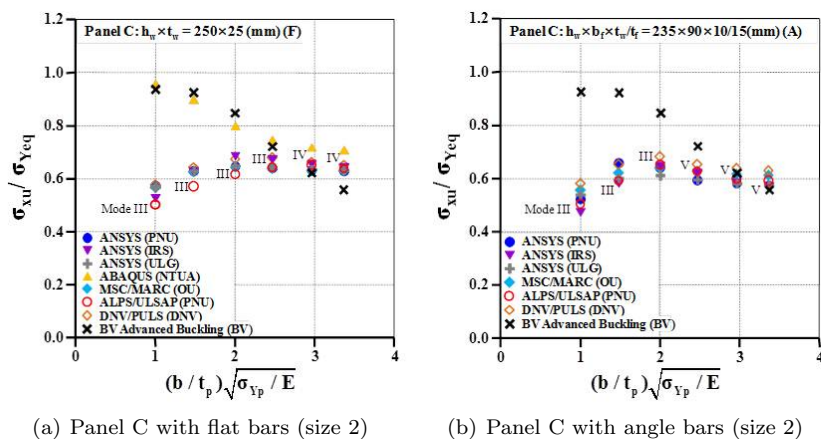


Figure 23: Results of studies on Panel C under longitudinal compressive loads

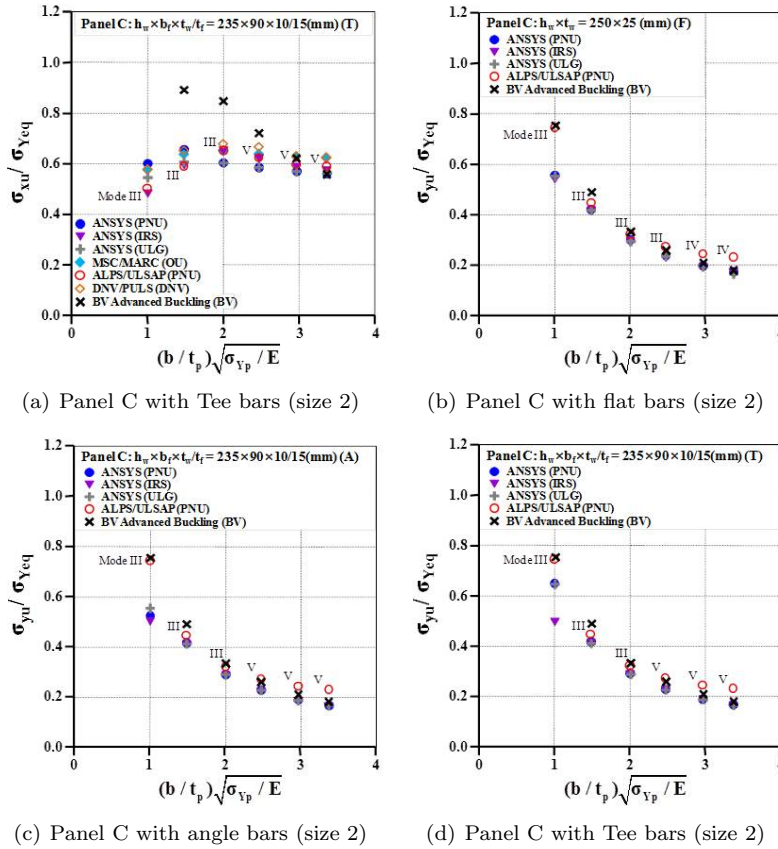


Figure 24: Results of studies on Panel C under longitudinal or transverse compressive loads

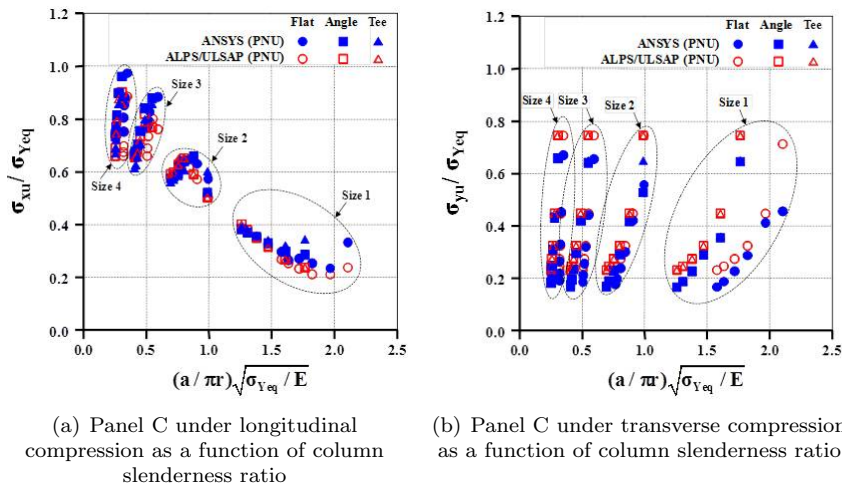


Figure 25: Ultimate strength of stiffened panels under longitudinal or transverse compressive loads

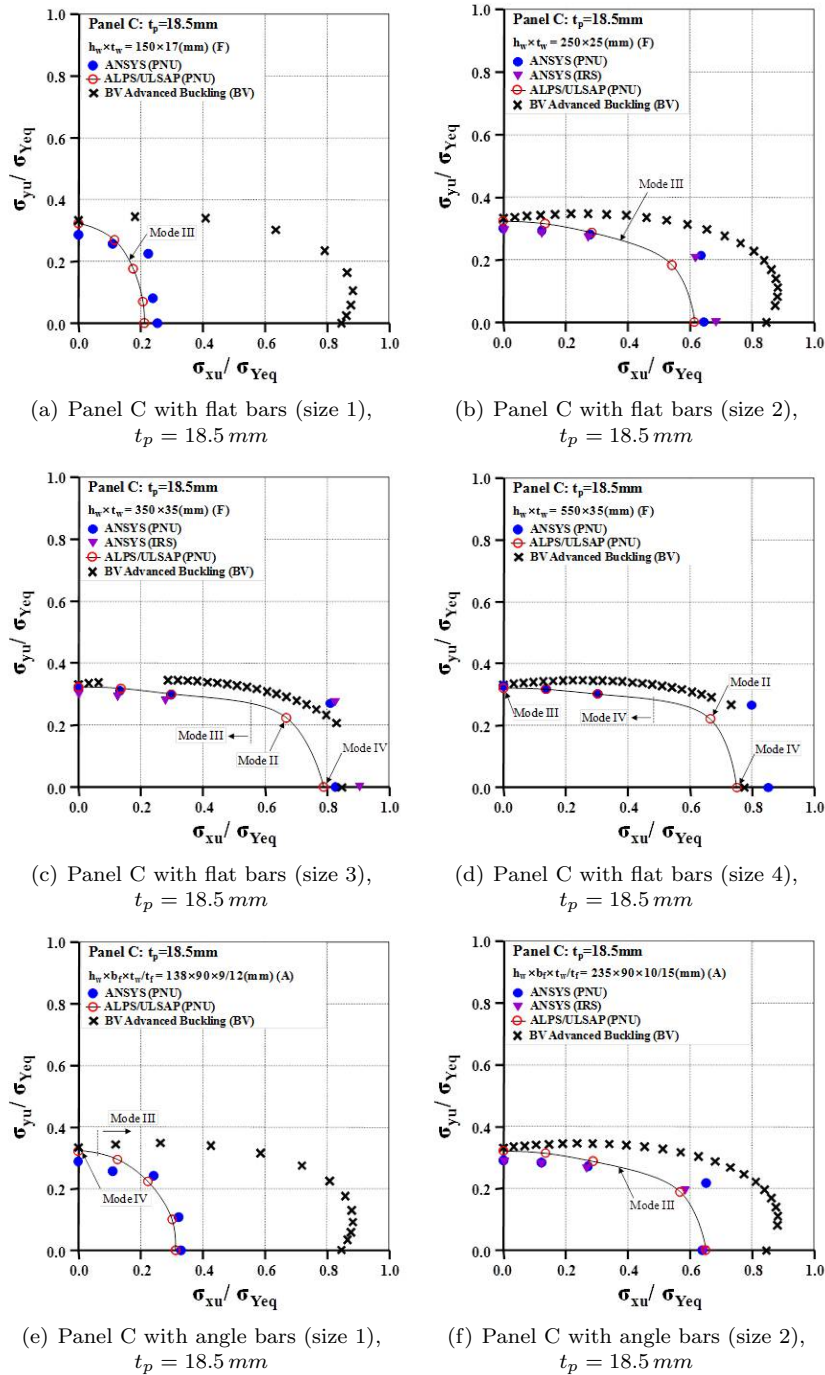
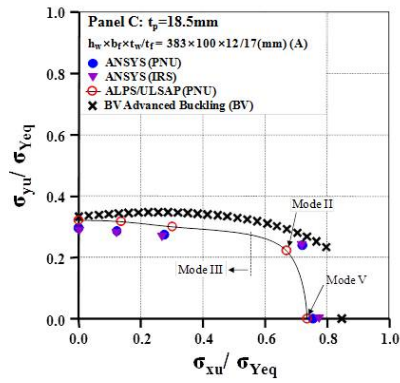
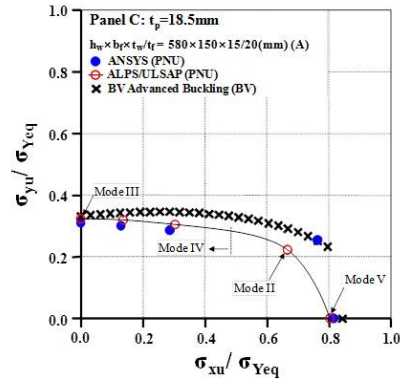


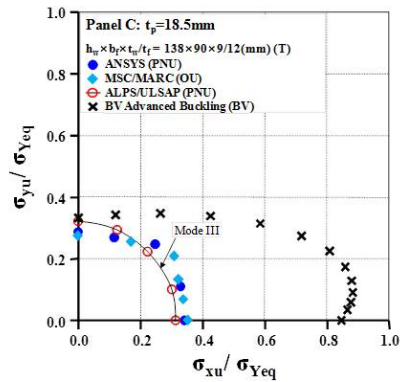
Figure 26: Results of studies for Panel C under biaxial compressive loads



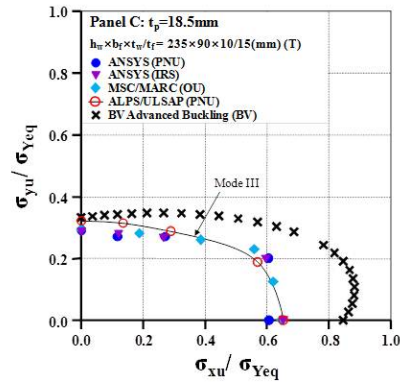
(a) Panel C with angle bars (size 3),
 $t_p = 18.5 \text{ mm}$



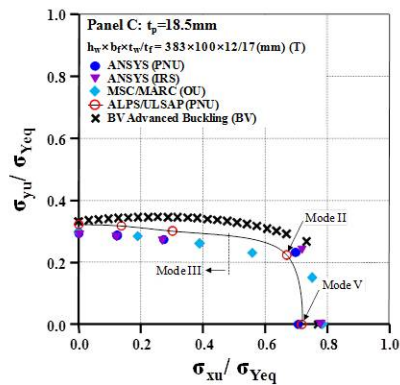
(b) Panel C with angle bars (size 4),
 $t_p = 18.5 \text{ mm}$



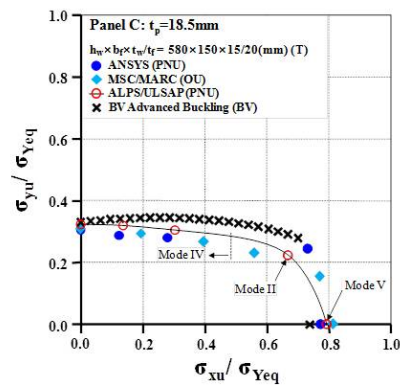
(c) Panel C with Tee bars (size 1),
 $t_p = 18.5 \text{ mm}$



(d) Panel C with Tee bars (size 2),
 $t_p = 18.5 \text{ mm}$



(e) Panel C with Tee bars (size 1),
 $t_p = 18.5 \text{ mm}$



(f) Panel C with Tee bars (size 2),
 $t_p = 18.5 \text{ mm}$

Figure 27: Results of studies for Panel C under biaxial compressive loads – continued

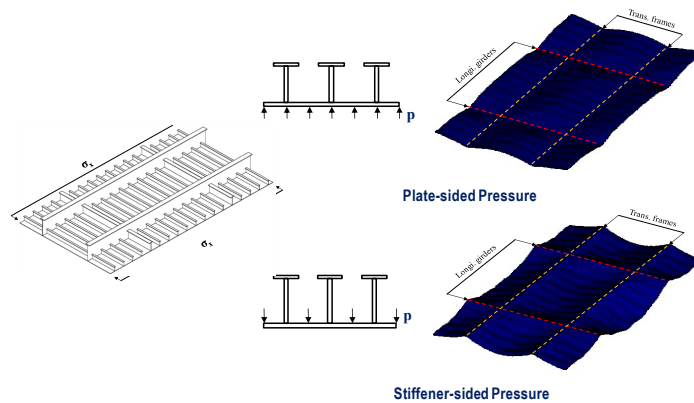


Figure 28: Plate-sided pressure and stiffener-sided pressure

Effect of Lateral Pressure Loads

Two types of pressure loads are considered in terms of loading direction, namely plate-sided pressure and stiffener-sided pressure (see Figure 28). Figure 29 shows the effect of lateral pressure on the ultimate strength of Panel C under longitudinal compressive loads with varied stiffener types and dimensions.

Effect of Plate Initial Deflection

To investigate the effect of initial distortions on panel ultimate strength, the magnitude and shape of initial distortions for plates and stiffeners are varied. Figure 31 shows the effect of initial distortions. In Figure 31, Case A is with the buckling mode initial deflection; Case B with a hungry-horse mode initial deflection and with the magnitude as referred in Japanese shipyards with the fabrication tolerance of Japanese Shipbuilding Quality Standards in plate thickness of 6 mm; and Case C with a hungry horse-mode initial deflection whose magnitude is same to Case A with the buckling mode. It is found from Figure 31 that the initial deflection of Case A, widely used in the literature, significantly underestimate the ultimate strength of the stiffened panel

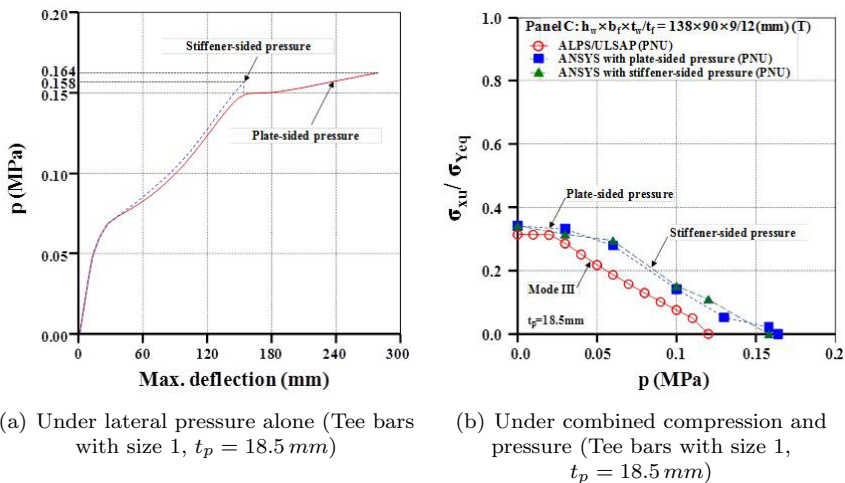


Figure 29: Effect of lateral pressure on the ultimate strength of Panel C under longitudinal compressive loads

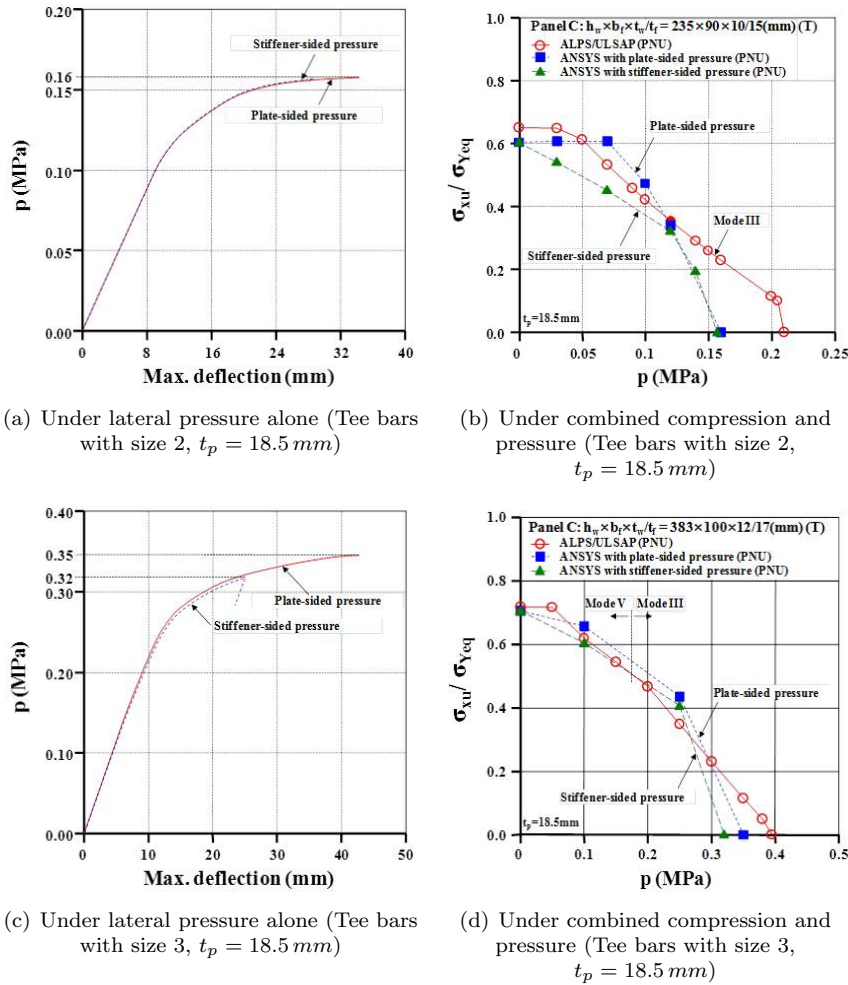


Figure 30: Effect of lateral pressure on the ultimate strength of Panel C under longitudinal compressive loads – continued

with the initial deflection of Case B, which has more realistic shape and magnitude. In this regard, a systematic analysis of modeling uncertainty is highly required when Case A is going to be applied.

Effect of Welding Residual Stresses

To investigate the effect of welding residual stresses, the following residual stresses were considered.

- Welding residual stress in plating:

$$\sigma_{rcx} = \begin{cases} -0.05\sigma_{Yp} & \text{for slight level} \\ -0.15\sigma_{Yp} & \text{for average level} \\ -0.3\sigma_{Yp} & \text{for severe level} \end{cases} \quad \text{where } \sigma_{Yp} = 313.6 \text{ MPa}$$

- Welding residual stress in stiffeners:

$$\sigma_{rcx} = -0.15\sigma_{Ys}, \text{ where } \sigma_{Yp} = 313.6 \text{ MPa}$$

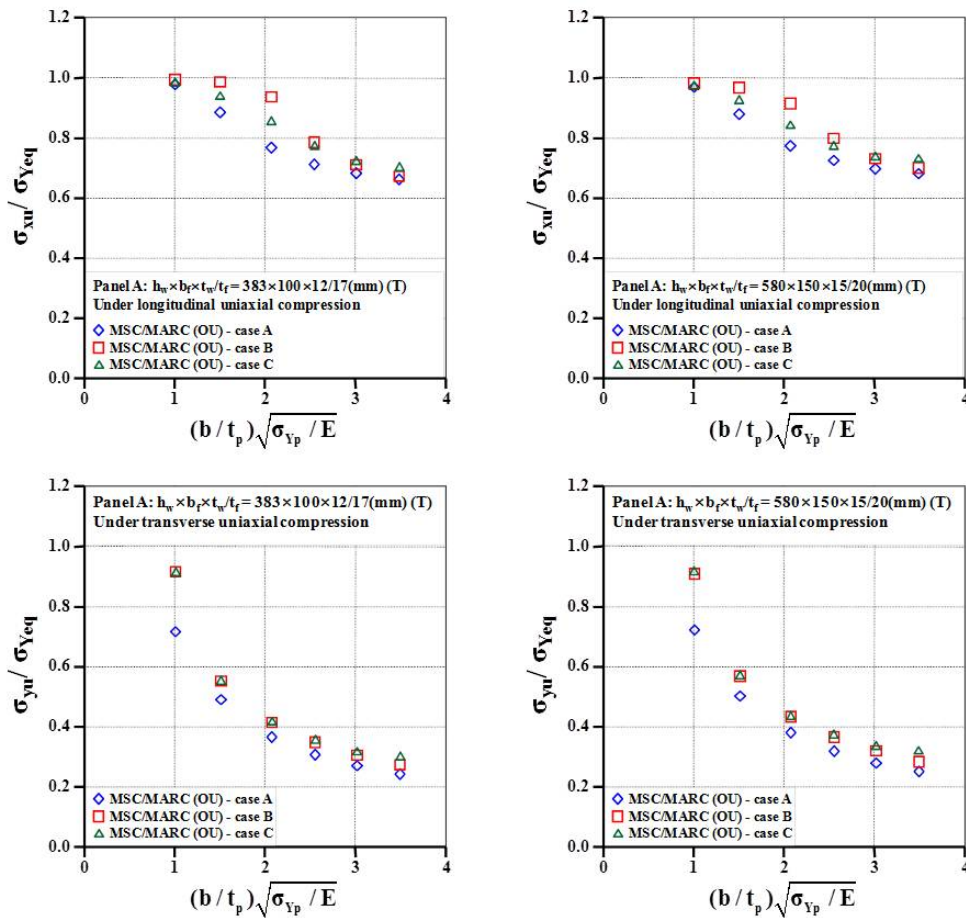


Figure 31: Ultimate strength of Tee-stiffened panels (Panel A) on the effect of initial deflection under longitudinal or transverse compression

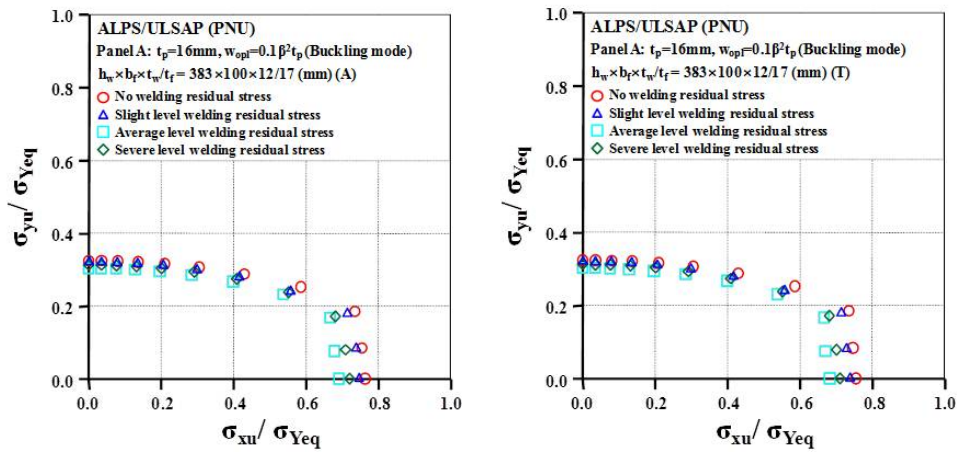
- Initial deflection: buckling mode initial deflection with an average level

Figure 32 represents the effect of welding residual stresses on the ultimate strength of Panel A or C under biaxial compressive loads, respectively, showing that the effect of residual stresses is small under predominantly transverse compressive loads. This is because the welding residual stresses in the transverse direction were not presumed in the present study. However, support members are attached by welding in the transverse direction as well as in the longitudinal direction, and thus the effect of welding residual stresses on a panel's ultimate strength even under predominantly transverse compressive loads can also be significant (Paik and Thayamballi, 2003; Paik and Sohn, 2012).

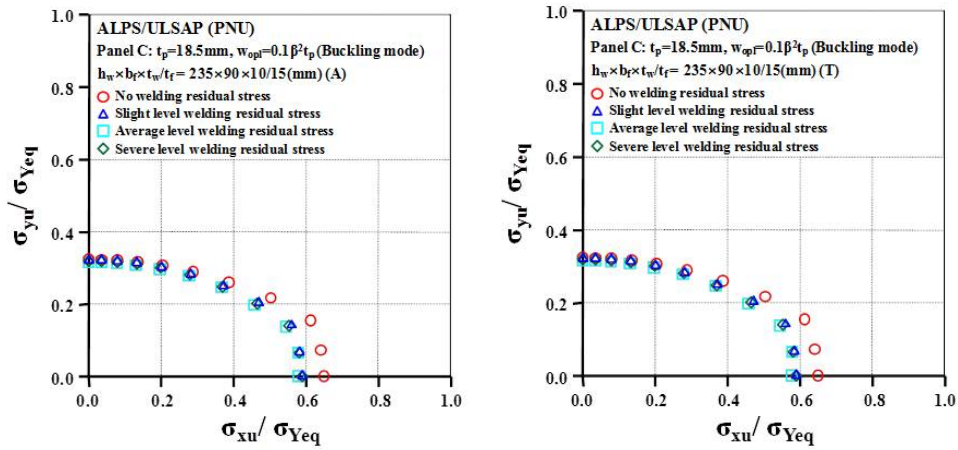
6.4.3 Hull Girders

Under Vertical Bending Moments

Figures 33 and 34 shows the progressive collapse behaviour of various ship hulls under vertical bending moments. Table 12 summarizes ultimate hull girder strengths obtained by each candidate method for six types of ship hulls under hogging and sagging moments. It is found that the CSR method results differ by different working organizations. This may be due to the different modelling techniques including hard corner



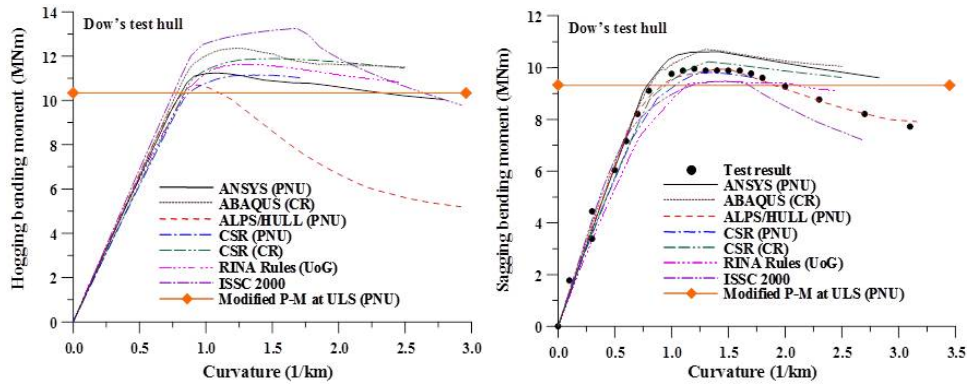
(a) Panel A with angle bars (size 3), $t_p = 16 \text{ mm}$ (b) Panel A with tee bars (size 3), $t_p = 16 \text{ mm}$



(c) Panel C with angle bars (size 2), $t_p = 18.5 \text{ mm}$ (d) Panel C with tee bars (size 2), $t_p = 18.5 \text{ mm}$

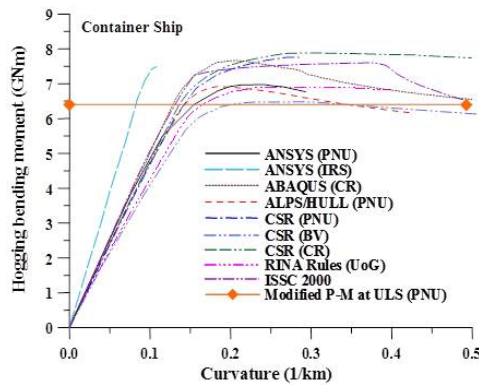
Figure 32: Effect of welding residual stresses on the ultimate strength of Panel A or C under biaxial compressive loads

elements adopted by the different working organizations, among others. However, it is important to realize that the modelling techniques can significantly affect the resulting computations. If the modelling techniques are inadequate, then the results could be totally wrong. Furthermore, it is recognized that there are still a lot of uncertainties in terms of predicting hull girder's ultimate strength.

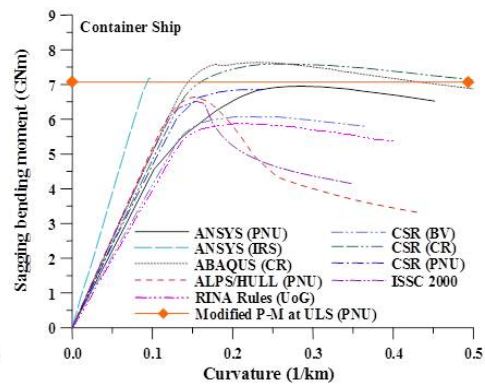


(a) Progressive collapse behaviour of Dow's test hull under hogging moment

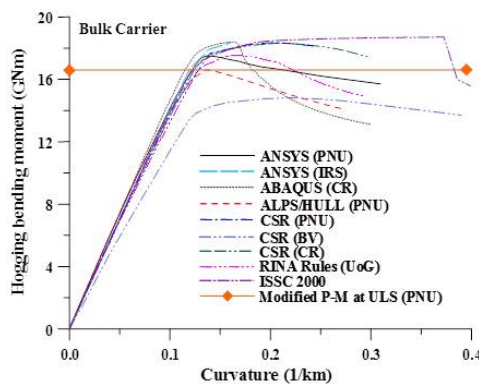
(b) Progressive collapse behaviour of Dow's test hull under sagging moment



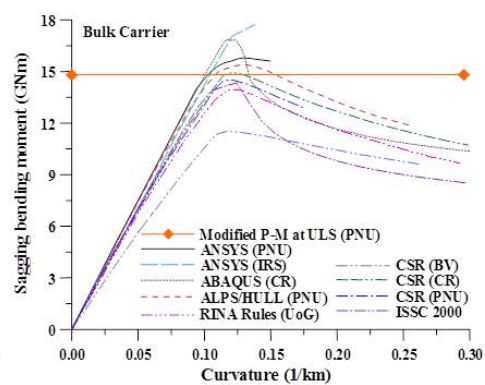
(c) Progressive collapse behaviour of container ship hull under hogging moment



(d) Progressive collapse behaviour of container ship hull under sagging moment

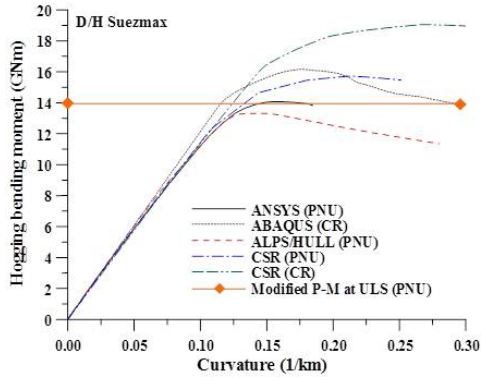


(e) Progressive collapse behaviour of bulk carrier hull under hogging moment

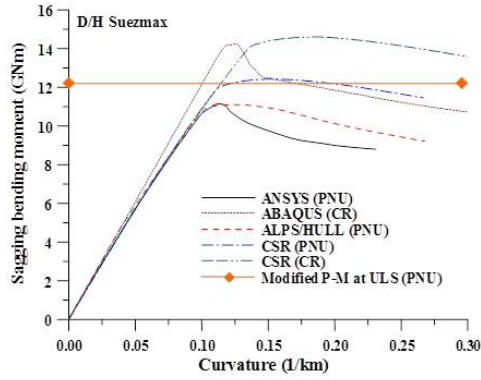


(f) Progressive collapse behaviour of bulk carrier hull under sagging moment

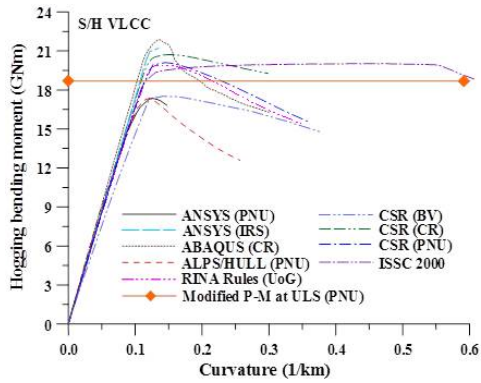
Figure 33: Progressive collapse behaviour of various ship hulls under vertical bending moments



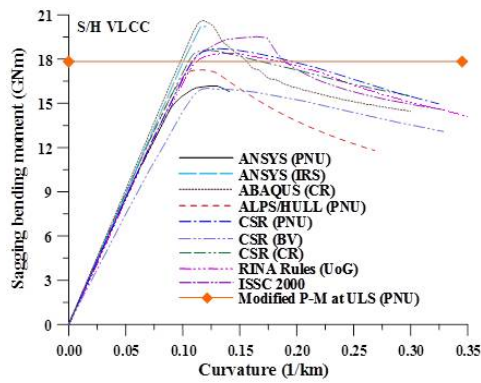
(a) Progressive collapse behaviour of Suezmax class double hull tanker hull under hogging moment



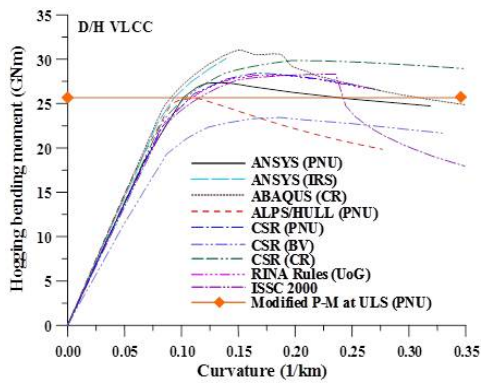
(b) Progressive collapse behaviour of Suezmax class double hull tanker hull under sagging moment



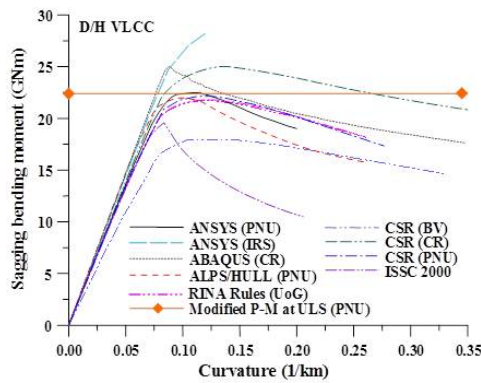
(c) Progressive collapse behaviour of single hull VLCC hull under hogging moment



(d) Progressive collapse behaviour of single hull VLCC hull under sagging moment



(e) Progressive collapse behaviour of double hull VLCC hull under hogging moment



(f) Progressive collapse behaviour of double hull VLCC hull under sagging moment

Figure 34: Progressive collapse behaviour of various ship hulls under vertical bending moments

Table 12: Summary of ultimate hull girder strengths obtained by each candidate method for six types of ship hulls under hogging and sagging moments

| Method | Dow's test hull (MNm) | | Container (GNm) | | Bulk carrier (GNm) | | D/H Suezmax (GNm) | | S/H VLCC (GNm) | | D/H VLCC (GNm) | |
|---------------------|-----------------------|--------|-----------------|-------|--------------------|--------|-------------------|--------|----------------|--------|----------------|--------|
| | Hog. | Sag. | Hog. | Sag. | Hog. | Sag. | Hog. | Sag. | Hog. | Sag. | Hog. | Sag. |
| ANSYS (PNU) | 11.235 | 10.618 | 6.969 | 6.951 | 17.500 | 15.800 | 14.066 | 11.151 | 17.355 | 16.179 | 27.335 | 22.495 |
| ANSYS (ISR) | - | - | 7.490 | 7.176 | 18.326 | 17.726 | - | - | 21.200 | 20.210 | 30.106 | 28.175 |
| ABAQUS (CR) | 12.357 | 10.708 | 7.664 | 7.631 | 18.396 | 16.855 | 16.160 | 14.258 | 21.860 | 20.625 | 31.006 | 24.995 |
| ALPS/-HULL (PNU) | 10.698 | 9.940 | 6.916 | 6.635 | 16.602 | 15.380 | 13.308 | 11.097 | 17.335 | 17.263 | 25.594 | 21.967 |
| CSR (BV) | - | - | 6.476 | 6.068 | 14.822 | 11.521 | - | - | 17.500 | 16.029 | 23.431 | 17.941 |
| CSR (CR) | 11.890 | 10.220 | 7.879 | 7.589 | 18.338 | 14.921 | 19.045 | 14.605 | 20.708 | 18.593 | 29.847 | 25.014 |
| CSR (PNU) | 11.149 | 9.825 | 7.758 | 6.851 | 18.360 | 14.500 | 15.714 | 12.420 | 20.102 | 18.712 | 28.423 | 22.130 |
| RINA Rules (UoG) | 11.624 | 9.454 | 6.859 | 5.898 | 17.482 | 13.952 | - | - | 19.836 | 18.468 | 28.202 | 21.696 |
| ISSC (2000) Rigo(1) | 13.261 | 9.475 | 7.600 | 6.513 | 18.714 | 14.340 | - | - | 18.460 | 17.900 | 28.312 | 19.573 |
| Modified P-M (PNU) | 10.338 | 9.329 | 6.400 | 7.077 | 16.576 | 14.798 | 13.965 | 12.213 | 18.701 | 17.825 | 25.667 | 22.390 |
| Test (Dow, 1991) | - | 9.64 | - | - | - | - | - | - | - | - | - | - |

Note: Estimated applied bending moment of S/H VLCC at collapse in hogging = 17.94GNm (ISSC, 2000)

Effect of Initial Distortions

Figure 35 and 36 shows the effect of plate initial deflection on the progressive collapse behaviour of a Suezmax class double hull tanker hull or a double hull VLCC hull. It is found that the effect of initial distortions on the ultimate hull girder strength is small as long as the magnitude of initial distortions is less than an average level.

Effect of Residual Stresses

Figure 37 shows the effect of welding residual stresses on the progressive collapse behaviour of a Suezmax class double hull tanker hull or a double hull VLCC hull. It is found that the effect of welding residual stresses of plates on ultimate hull girder strength is small.

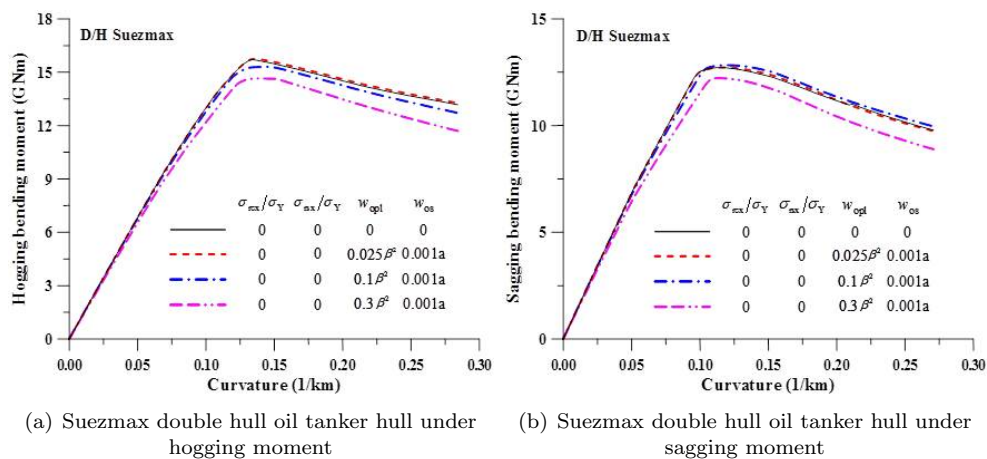


Figure 35: Effect of plate initial deflection on the progressive collapse behaviour

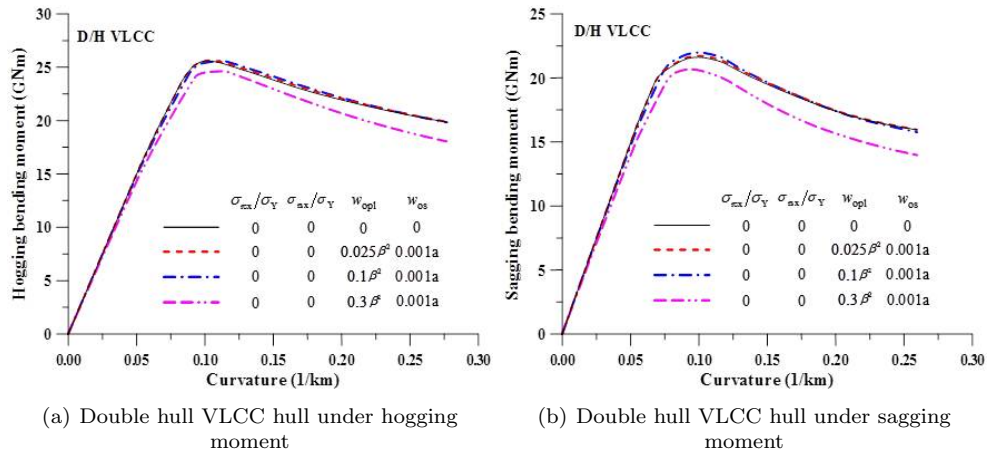


Figure 36: Effect of plate initial deflection on the progressive collapse behaviour – continued

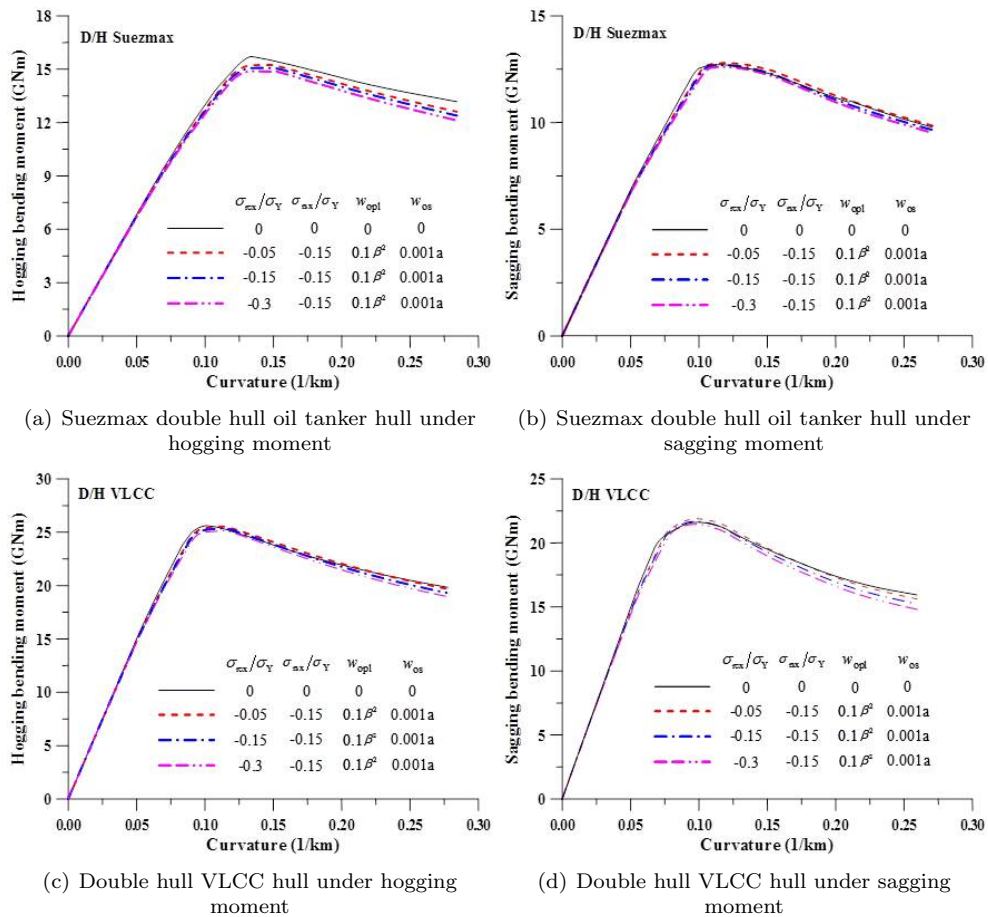


Figure 37: Effect of welding residual stresses on the progressive collapse behaviour

7 CONCLUSION AND RECOMMENDATIONS

It is now well recognized that ultimate strength is a much better basis for structural design and safety assessment than the traditional allowable working stress. This is because the realistic safety margin of a structure can not be determined as long as the ultimate strength remains unknown. It is therefore required to calculate the ultimate strength of both structural members and system structures accurately and efficiently. In recent years, useful methods have been developed for this purpose. However, it is realized that there are still a lot of technical challenges associated with various factors affecting the ultimate strength behaviour as discussed in Section 2.2. A comprehensive benchmark study with various candidate methods has been undertaken in the Committee, observing that some methods are considered to be mature enough to apply in daily practice of structural design and safety assessment but a great attention should be paid in conjunction with possible uncertainties due to modelling techniques as well as inherent aspects.

Despite significant recent advancements in ultimate strength evaluation procedures and the availability of increasingly more powerful computation means, final results can still be affected by large uncertainties that must at least be identified and then possibly estimated. Indeed, the description of the practical aspects of calculations in Section 4 is aimed at identifying uncertainties and highlighting the difficulties that prevent correct and consistent analyses.

Physical aspects, i.e., uncertainties affecting input variables, such as material properties, definition of geometries, etc., have been widely studied in recent years, and reliability analyses account for such aspects by properly considering the statistical analysis of involved variables. Even if reliability analyses cannot be applied in daily design practice, useful results can be obtained for rules calibration. While the process is not fully completed, it is believed that the trend is clear and that the harmonization process of classifying society rules confirms it.

The estimation of model uncertainties is much more difficult because the comparative (and trustworthy) term is not always clear and defined enough to obtain information about the approximation in ultimate strength calculations. In fact, this estimate involves engineering judgment in the definition of the structures' limit states and abilities to properly idealize them according to the available theoretical and numerical structural models (i.e., beam theory, plate theory, FEM, etc.). Quantitative estimates of model uncertainties are also complex because interactions among various aspects often cannot be considered by current calculation procedures.

Ageing effects have recently been noted in a more explicit and transparent way by classification societies' rules, and again the trend is towards a deeper and wider analysis of such aspects in ships' structural designs. Even if the implementation of ageing effects in the calculations is still in progress, as several effects and relevant interactions with other effects are still empirically accounted for (e.g., local and global corrosion), statistical and reliability analyses are of great help.

In addition, actual data about ageing effects are rather hard to collect and sometimes not available. However, a few of the numerical studies conducted recently are starting to analyse ageing effects and their interactions (e.g., the effect of local corrosion and pitting on the ultimate strength of misaligned components).

In short, the abovementioned limitations can be defined as "technology transfer" problems and it should be recognized that if not correctly faced, important research achievements cannot be successfully implemented in ship design and technical management.

8 ACKNOWLEDGEMENTS

The Committee is pleased to acknowledge P. Rigo and A. Bayatfar of University of Liege, Belgium, who made a great contribution to the benchmark studies even if they are not members of the Committee.

9 REFERENCES

- ABS (2004). Guide for buckling and ultimate strength assessment for offshore structures, American Bureau of Shipping, Houston, USA.
- ABS (2009). Guide for building and classing floating production installations, American Bureau of Shipping, Houston, USA.
- ABS (2010). Guide for building and classing floating offshore liquefied gas terminals, American Bureau of Shipping, Houston, USA.
- ABS (2011a). Guide for building and classing drillships, American Bureau of Shipping, Houston, USA.
- ABS (2011b). Rules for building and classing steel vessel, American Bureau of Shipping, Houston, USA.
- Ahmmad M.M. and Sumi Y. (2010). Strength and deformability of corroded steel plates under quasi-static tensile load, *Journal of Marine Science and Technology*, Vol. 15, pp.1-15.
- Amani M., Edlund B.L.O. and Alinia M.M. (2011). Buckling and post-buckling behaviour of unstiffened slender curved plates under uniform shear, *Thin-Walled Structures*, Vol. 49, pp.1017-1031.
- Amante D.A. and Estefen S.F. (2011). Buckling strength of damaged stiffened panels, *Proceedings of the 30th International Conference on Ocean, Offshore and Arctic Engineering (OMAE 2011)*, Rotterdam, Netherlands, OMAE2011-49650.
- Amante D.A., Rossetto R.M. and Estefen S.F. (2010). Strength loss of SS platform column due to ship collision, *Proceedings of the 29th International Conference on Ocean, Offshore and Arctic Engineering (OMAE2010)*, Shanghai, China, OMAE2010-20680.
- Amlashi H.K.K., Hørte T., Steen E. and Kippenes J. (2010). Probabilistic assessment of stiffened panel strength: An interactive tool using PROBAN and PULS, *Proceedings of the 29th International Conference on Ocean, Offshore and Arctic Engineering (OMAE2010)*, Shanghai, China, OMAE2010-21178.
- Amlashi H.K.K. and Moan T. (2008). Ultimate strength analysis of a bulk carrier hull girder under alternate hold loading condition – A case study, Part 1: Nonlinear finite element modelling and ultimate hull girder capacity, *Marine Structures*, Vol. 21, pp. 327-352.
- Amlashi H.K.K. and Moan T. (2009). Ultimate strength analysis of a bulk carrier hull girder under alternate hold loading condition – A case study, Part 2: Stress distribution in the double bottom and simplified approaches, *Marine Structures*, Vol. 22, pp. 522-544.
- Amlashi H.K.K. and Moan T. (2011). A proposal of reliability-based design formats for ultimate hull girder strength checks for bulk carriers under combined global and local loadings, *Journal of Marine Science and Technology*, Vol. 16, pp. 51-67.
- API (2004). Bulletin on design of stability design of cylindrical shells, API Bulletin 2U, 3rd Edition, American Petroleum Institute, USA.
- Bardi F.C., Tang H., Kulkarni M. and Yin X. (2011). Structural analysis of cryogenic flexible hose, *Proceedings of the 30th International Conference on Ocean, Offshore and Arctic Engineering (OMAE2011)*, Rotterdam, Netherlands, OMAE2011-50238.

- Bayatfar A., Matagne J. and Rigo P. (2011). Influence of transverse cracks on ultimate strength of a steel plate under compression, *Proceedings of the 30th International Conference on Ocean, Offshore and Arctic Engineering (OMAE2011)*, Rotterdam, Netherlands, OMAE2011-49919.
- Benson S., Downes J. and Dow R.S. (2009). Ultimate strength characteristics of aluminium plates for high speed vessels: Analysis and Design of Marine Structures, Guedes Soares and Das (eds), Taylor & Francis, London, UK, pp. 121-131.
- Benson S., Downes J. and Dow R.S. (2010). A semi analytical method to predict the ultimate strength and collapse behaviour of orthogonally stiffened panels, *Proceedings of the 11th International Symposium on Practical Design of Ships and Other Floating Structures (PRADS 2010)*, Rio de Janeiro, Brazil, pp. 1091-1101.
- Benson S., Downes J. and Dow R.S. (2011). Ultimate strength characteristics of aluminium plates for high-speed vessels, *Ships and Offshore Structures*, Vol.6, Nos. 1-2, pp.67-80.
- Błachut J. and Ifayefunmi O. (2010). Plastic buckling of conical shells, *Journal of Offshore Mechanics and Arctic Engineering*, Vol. 132, pp. 041401 (11 pages).
- Brubak L., Helleland J. and Steen E. (2009). Approximate post-buckling analysis of imperfect stiffened plates with a free edge, *Proceedings of the 3th International Conference on Computational Methods in Marine Engineering (MARINE 2009)*, Trondheim, Norway.
- BV (2010). Rules for the classification of offshore units NR 445.D1 DT R03 E, Bureau Veritas, Paris, France.
- BV (2011). Rules for the classification of steel ships NR 467.B2 DT R05 E, Bureau Veritas, Paris, France.
- Chaithanya P.P., Das P.K., Crow A. and Hunt S. (2010). The effect of distortion on the buckling strength of stiffened panels, *Ships and Offshore Structures*, Vol. 5, No. 2, pp. 141-153.
- Chen Q., Marley M. and Zhou J. (2011). Remaining collapse capacity of corroded pipelines, *Proceedings of the 30th International Conference on Ocean, Offshore and Arctic Engineering (OMAE 2011)*, Rotterdam, Netherlands, OMAE2011-49054.
- Chen Q. and Moan T. (2010). Material softening effect on ultimate strength of stiffened aluminium panels, *Proceedings of the 29th International Conference on Ocean, Offshore and Arctic Engineering (OMAE 2010)*, Shanghai, China, OMAE2010-20979.
- Cho S.R., Hyun H.S., Koo J.B., Doh H.M. and Chon Y.K. (2011). Robust ultimate strength formulation for stiffened plates subjected to combined loads, *Advances in Marine Structures*, Guedes Soares and Fricke (eds), Taylor & Francis, London, UK, pp. 99-108.
- Collette M.D. (2011). Rapid analysis techniques for ultimate strength predictions of aluminium structures, *Advances in Marine Structures*, Guedes Soares and Fricke (eds), Taylor & Francis, London, UK, pp. 109-117.
- Daley C. and Bansal A. (2009). Discussion of plastic capacity of plating subject to patch loads, *Analysis and Design of Marine Structures*, Guedes Soares and Das (eds), Taylor & Francis, London, UK, pp. 113-120.
- Daniel I. M. (2007). Failure of composite materials, *Journal of Strain*, Vol. 43, pp.4-12.
- Das P.K., Subin K.K. and Pretheesh P.C. (2011). A revisit on design and analysis of stiffened shell structures for offshore applications, *Proceedings of the 3rd International Conference on Marine Structures (MARSTRUCT 2011)*, Hamburg, Germany, pp. 119-131.
- Dawood M., Taylor E. and Rizkalla S. (2010). Two-way bending behavior of 3-D

- GFRP sandwich panels with through-thickness fiber insertions, *Composite Structures*, Vol. 92, pp. 950-963.
- DNV (2010a). DNV-RP-C201, Buckling strength of plated structures, Det Norske Veritas, Oslo, Norway.
- DNV (2010b). DNV-RP-C202, Buckling strength of shells, Det Norske Veritas, Oslo, Norway.
- DNV (2010c). DNV-CN30-1, Buckling strength analysis of bars and frames, and spherical shells, Det Norske Veritas, Oslo, Norway.
- Dow R.S. (1991). Testing and analysis of a 1/3-scale welded steel frigate model, *Proceedings of the 2nd International Conference on Advances in Marine Structures*, Vol.2, Scotland, May.
- Estefen S.F., Roseeto R.M. and Lourenco M.I. (2010). Failure analysis of wing tank panels on a bulk carrier, *Proceedings of the 11th International Symposium on Practical Design of Ships and Other Floating Structures (PRADS 2010)*, Rio de Janeiro, Brazil, pp.1144-1153.
- Estefen T.P., Trovado L.C. and Estefen S.F. (2007). Structural behaviour of Suezmax tanker under extreme bending moment, *Proceedings of the 10th International Symposium on Practical Design of Ships and Other Floating Structures (PRADS 2007)*, Houston, USA, pp.731-740.
- Frank D., Klanac A., Kniep M., Polić D. and Ehlers S. (2011). Optimization system for design of laser-welded steel-sandwich structures, *Proceedings of the 11th International Symposium on Practical Design of Ships and Other Floating Structures (PRADS 2010)*, Rio de Janeiro, Brazil, pp.1079-1087.
- Frieze P.A., Abbatisa M., Vallascas M. and Paik J.K. (2011). A benchmark study of ISO-18072-2 on the stiffened panel ultimate strength, *Proceedings of the 30th International Conference on Ocean, Offshore and Arctic Engineering 2011*, Rotterdam, Netherlands, OMAE2011-50152.
- Fujikubo M., Harada S, Yao T., Khedmati M.R. and Yanagihara D. (2005). Estimation of ultimate strength of continuous stiffened panel under combined transverse thrust and lateral pressure, Part 2: Continuous stiffened panel, *Marine Structures*, Vol. 18, pp.411-417.
- Fujikubo M. and Kaeding P. (2002). New simplified approach to collapse analysis of stiffened plates, *Marine Structures*, Vol.15, pp. 251-283.
- Gaiotti M., Rizzo C.M., Branner K. and Berring P. (2011). Finite elements modeling of delaminations in composite laminates, *Proceedings of the 3rd International Conference on Marine Structures (MARSTRUCT 2011)*, Hamburg, Germany.
- Gannon L.G., Liu Y., Pegg N. and Smith M. (2009). Effect of welding sequence on residual stress and distortion in flat-bar stiffened plates, *Marine Structures*, Vol. 23, pp. 385-404.
- Gannon L.G., Pegg N.G., Smith M.J., and Liu Y. (2011). Shakedown of welding-induced residual stresses and effect on stiffened plate strength and behaviour, *Proceedings of the 3rd International Conference on Marine Structures (MARSTRUCT 2011)*, Hamburg, Germany, pp.141-149.
- Gao C., Pei Z., Yasuoka A., Tanaka S., Okazawa S., Alie Z.M., Iijima K., Fujikubo M. and Yao T. (2011). Collapse analysis of double bottom structures considering shear, lateral pressure and welding residual stress, *Proceedings of the 21st International Society of Offshore and Polar Engineers (ISOPE 2011)*, Hawaii, USA, Vol. 4, pp. 902-909.
- Garbatov Y., Tekgoz M. and Guedes Soares C. (2011). Uncertainty assessment of the

- ultimate strength of a stiffened panel, *Proceedings of the 3rd International Conference on Marine Structures (MARSTRUCT 2011)*, Hamburg, Germany.
- GL (2011a). GL rules and guidelines 2011, I Ship technology – Part 1 Seagoing ships – Chapter 1 Hull structures Section 3 Design principles – F Proof of buckling strength (GL I-1-1;3-f), Germanischer Lloyd SE, Germany.
- GL (2011b). GL rules and guidelines 2011, I Ship technology – Part 1 Seagoing ships – Chapter 1 Hull structures, Section 5 Longitudinal strength C Section moduli, moment of inertia, shear and buckling strength, 8 Ultimate load calculation of the ship's transverse section (GL I-1-1;5-C;8), Germanischer Lloyd SE, Germany.
- Goplen S., Fyrileiv O., Grandal J.P. and Børsheim, L. (2011). Global buckling of pipe-in-pipe: structural response and design criteria, *Proceedings of the 30th International Conference on Ocean, Offshore and Arctic Engineering 2011*, Rotterdam, Netherlands, OMAE2011-49960.
- Gordo J.M. (2011). Effect of initial imperfection on the strength of restrained plates, *Proceedings of the 30th International Conference on Ocean, Offshore and Arctic Engineering 2011*, Rotterdam, Netherlands, OMAE2011-49161.
- Gordo J.M. and Guedes Soares C. (2008). Experimental evaluation of the behaviour of a mild steel box girder under bending moment, *Ships and Offshore Structures*, Vol.3, No.4, pp.347-358.
- Gordo J.M. and Guedes Soares C. (2009). Tests on ultimate strength of hull box girders made of high tensile steel, *Marine Structures*, Vol.22, No.4, pp.770-790.
- Gordo J.M. and Guedes Soares C. (2011). Compressive tests on stiffened panels of intermediate slenderness, *Thin-Walled Structures*, Vol.49, pp.782-794.
- Gresnigt A.M. and Karamanos S.A. (2009). Local buckling strength and deformation capacity of pipes, *Proceedings of the 19th International Society of Offshore and Polar Engineers (ISOPE 2009)*, Osaka, Japan, Vol.4, pp.212-224.
- Harada M. and Fujikubo M. (2002). Estimation of buckling and ultimate strength of rectangular plate with cutout, *Proceedings of the 12th International Society of Offshore and Polar Engineers (ISOPE 2002)*, Kita-Kyushu, Japan, Vol.4, pp.630-635.
- Harada M. and Shigemi T. (2006). Research on uncertainties in ultimate longitudinal strength of cross section of ship's hull based on nonlinear FEM, *Proceedings of the 3rd International ASRANet Colloquium (ASRANet 2006)*, Glasgow, UK.
- Henaio A., Carrera M., Miravete A. and Castejon L. (2010). Mechanical performance of through-thickness tufted sandwich structures, *Composite Structures*, Vol. 92, pp.2052-2059.
- Hilberink A., Gresnigt A.M. and Sluys L.J. (2010). Liner wrinkling of lined pipe under compression: A numerical and experimental investigation, *Proceedings of the 29th International Conference on Ocean, Offshore and Arctic Engineering (OMAE 2010)*, Shanghai, China, OMAE2010-20285.
- Hilberink A., Gresnigt A.M. and Sluys L.J. (2011). Mechanical behaviour of lined pipe during bending: Numerical and experimental results compared, *Proceedings of the 30th International Conference on Ocean, Offshore and Arctic Engineering (OMAE 2011)*, Rotterdam, Netherlands, OMAE 2011- 9434.
- Hinton M. J., Kaddour A. S. and Soden P. D. (2004). Failure criteria in fibre reinforced polymer composites, *The world-wide failure exercise*, Elsevier, Amsterdam, Netherlands.
- Huang Z.M. (2004). A bridging model prediction of the ultimate strength of composite

- laminates subjected to biaxial loads, *Composite Science and Technology*, Vol. 64, pp. 395-448.
- Hughes O.F. and Paik J.K. (2010). *Ship structural analysis and design*, Society of Naval Architects and Marine Engineers, New Jersey, USA.
- IACS (2010a). Common structural rules for double hull oil tankers, International Association of Classification Societies, London, UK.
- IACS (2010b). Common structural rules for bulk carriers, International Association of Classification Societies, London, UK.
- Ifayefunmi O. and Błachut J. (2011). The effect of shape, thickness and boundary imperfection on plastic buckling of cones, *Proceedings of the 30th International Conference on Ocean, Offshore and Arctic Engineering (OMAE 2011)*, Rotterdam, Netherlands, OMAE2011-49055.
- Islam M.R. and Sumi Y. (2011). Geometrical effects on strength and deformability of corroded steel plates, *Proceedings of the 3rd International Conference on Marine Structures (MARSTRUCT 2011)*, Hamburg, Germany, pp.151-159.
- ISO (2007). ISO 18072-1 Ships and marine technology – ship structures – Part 1: General requirements for their limit state assessment, International Organization for Standardization, Geneva, Switzerland.
- ISSC (2000). Report of Specialist Committee IV.2 Ultimate Hull Girder Strength, *Proceedings of the 14th International Ship and Offshore Structures Congress (ISSC 2000)*, Edited by H. Ohtsubo and Y. Sumi, Nagasaki, Japan, Vol.2, pp.321-391.
- Ivanov L.D. (2009). Challenges and possible solutions of the time-variant reliability of ship's hull girder, *Ships and Offshore Structures*, Vol. 4, No. 3, pp. 215-228.
- Jiang X. and Guedes Soares C. (2011). Ultimate capacity behaviour of pitted mild steel plates under biaxial compression, *Proceedings of the 30th International Conference on Ocean, Offshore and Arctic Engineering (OMAE 2011)*, Rotterdam, Netherlands, OMAE2011-49980.
- Jiao R. and Kyriakides S. (2009). Ratcheting, wrinkling and collapse of tubes under axial cycling, *International Journal of Solids and Structures*, Vol.46, pp.2856–2870.
- Jiao R. and Kyriakides S. (2011a). Ratcheting and wrinkling of tubes due to axial cycling under internal pressure: Part I experiments, *International Journal of Solids and Structures*, Vol.48, pp.2814–2826.
- Jiao R. and Kyriakides S. (2011a). Ratcheting and wrinkling of tubes due to axial cycling under internal pressure: Part II analysis, *International Journal of Solids and Structures*, Vol.48, pp.2827–2836.
- Joshi N. and Muliana A. (2010). Deformation in viscoelastic sandwich composites subject to moisture diffusion, *Composite Structures*, Vol. 92, pp. 254-264.
- Kaddour A.S. and Hinton M.J. (2005). The launch of WWFE-II: Benchmarking of 3D strength and damage theories for polymer fibre composites, *Proceedings of the 15th International Committee on Composite Materials (ICCM 2005)*, Durban, South Africa.
- Kaddour A.S., Hinton M.J., Smith P.A. and Li S. (2007). Damage theories for polymer fibre composites: The third world failure exercise (WWFE-III), *Proceedings of the 16th International Committee on Composite Materials (ICCM 2007)*, Kyoto, Japan.
- Khedmati M.R., Bayatfar A. and Rigo P. (2010a). Post-buckling behaviour and strength of multi-stiffened aluminium panels under combined axial compression and lateral pressure, *Marine Structures*, Vol. 23, pp. 39-66.
- Khedmati M.R., Rastani M. and Ghavami K. (2009a). Ultimate strength and ductility

- characteristics of intermittently welded stiffened plates, *Journal of Constructional Steel Research*, Vol. 65, pp.599-610.
- Khedmati M.R., Zareei M.R. and Rigo P. (2009b). Sensitivity analysis on the elastic buckling and ultimate strength of continuous stiffened aluminium plates under combined in-plane compression and lateral pressure, *Thin-Walled Structures*, Vol. 47, pp. 1232-1245.
- Khedmati M.R., Zareei M.R. and Rigo P. (2010b). Empirical formulations for estimation of ultimate strength of continuous stiffened aluminium plates under combined in-plane compression and lateral pressure, *Thin-Walled Structures*, Vol. 48, pp. 274-289.
- Kim U.N., Choe I.H. and Paik J.K. (2009). Buckling and ultimate strength of perforated plate panels subject to axial compression: experimental and numerical investigations with design formulations, *Ships and Offshore Structures*, Vol. 4, No.4, pp. 337-361.
- Kippenes J., Notaro G., Amlashi H. and Steen E. (2010). Ultimate strength of cape-size bulk carrier under alternate hold loading, *Proceedings of the 11th International Symposium on Practical Design of Ships and Other Floating Structures (PRADS 2010)*, Rio de Janeiro, Brazil, pp. 1114-1122.
- Laš V., Zemčík R., Kroupa T. and Kottner R. (2008). Failure prediction of composite materials, *Bulletin of Applied Mechanics*, Vol. 4, No. 14, pp. 81-87.
- Lassen T., Meling T.S. and Eide A.L. (2010). Ultimate strength and fatigue durability of steel reinforced rubber loading hoses, *Proceedings of the 29th International Conference on Ocean, Offshore and Arctic Engineering (OMAE 2010)*, Shanghai, China, OMAE2010-20236.
- Lehman E. (2009). Discussion on Report of Committee III.1: Ultimate strength, *Proceedings of the 16th International Ship and Offshore Structures Congress (ISSC 2009)*, Vol. 3, pp.121-131.
- Li X., Chen Y.F. and Su C.L. (2011). Burst capacity estimation of pipeline with colonies of interacting corrosion defects, *Proceedings of the 30th International Conference on Ocean, Offshore and Arctic Engineering (OMAE 2011)*, Rotterdam, Netherlands, OMAE2011-49918.
- Lie S. T. and Yang Z. M. (2011). Plastic collapse loads of cracked square hollow section T-, Y-, and K-joints, *Journal of Offshore Mechanics and Arctic Engineering*, Vol.133, 021601.
- Limam A., Lee L.H., Corona E. and Kyriakides S. (2010). Inelastic wrinkling and collapse of tubes under combined bending and internal pressure, *International Journal of Mechanical Science*, Vol.52, pp.637-647.
- Liu C. J., Nijhof A. H. J., Ernst L. J. and Marissen R. (2010). A new ultimate strength model of notched composite laminates - including the effects of matrix failure, *Journal of Composite Materials*, Vol. 44, No. 11.
- Liu Z. and Amdahl J. (2009). Residual strength of damaged stiffened panel on double bottom ship, *Proceedings of the 2nd International Conference on Marine Structures (MARSTRUCT 2009)*, Lisbon, Portugal, pp. 163-171.
- Loose T. (2008). Schweissverzug, Schweisseigenstressungen and Schalenstabilität, *Stahlbau*, Vol.77, pp.111-119.
- MacKay J.R., Keulen F. and Smith M.J. (2011). Quantifying the accuracy of numerical collapse predictions for the design of submarine pressure hulls, *Thin-Walled Structures*, Vol. 49, pp. 145-156.
- Merino, H.E.M., Sousa, J.R.M., Magluta, C. and Roitman, N. (2010). Numerical

- and experimental study of a flexible pipe under torsion, *Proceedings of the 29th International Conference on Ocean, Offshore and Arctic Engineering (OMAE 2010)*, Shanghai, China, OMAE2010-20902.
- Misirlis K., Downes J. and Dow R.S. (2010). Assessment of the ultimate compressive strength for FRP plates with geometrical imperfections, *Proceedings of the 11th International Symposium on Practical Design of Ships and Other Floating Structures (PRADS 2010)*, Rio de Janeiro, Brazil, pp.1102-1113.
- Neto A.G., Martins C.A., Pesce C.P., Meirelles C.O.C., Malta E.R., Neto T.F.B. and Godinho C.A.F., (2010). Burst Prediction of Flexible Pipes, *Proceedings of the 29th International Conference on Ocean, Offshore and Arctic Engineering (OMAE 2010)*, Shanghai, China, OMAE2010-20414.
- Newbury B.D. (2010). The third ISOPE strain-based design symposium - A review, *Proceedings of the 20th International Society of Offshore and Polar Engineers (ISOPE 2010)*, Beijing, China, Vol.4, pp.383-393.
- Nogueira V.P.P. and Netto, T.A., (2010). A simple alternative method to estimate the collapse of flexible pipes, *Proceedings of the 29th International Conference on Ocean, Offshore and Arctic Engineering (OMAE 2010)*, Shanghai, China, OMAE2010-20692.
- Notaro G., Kippenes J., Amlashi H., Russo M. and Steen E. (2010). Residual hull girder strength of ships with collision or grounding damages, *Proceedings of the 11th International Symposium on Practical Design of Ships and Other Floating Structures (PRADS 2010)*, Rio de Janeiro, Brazil, pp.941-951.
- Okasha N.M. and Frangopol D.M. (2010). Efficient method based on optimization and simulation for the probabilistic strength computation of the ship hull, *Journal of Ship Research*, Vol. 54, No.4, pp. 244-256.
- Özgülç O. and Barltrop N.D.P. (2008). Analysis on the hull girder ultimate strength of a bulk carrier using simplified method based on an incremental-iterative approach, *Journal of Offshore Mechanics and Arctic Engineering*, Vol. 130, p. 021013.
- Paik J.K. (2009). Residual ultimate strength of steel plates with longitudinal cracks under axial compression-nonlinear finite element method investigations, *Ocean Engineering*, Vol. 36, pp.266-276.
- Paik J.K. (2011). Recent advances and future trends on ship and offshore technologies, *Proceedings of the 4th International Conference on Computational Methods in Marine Engineering (MARINE 2011)*, Lisbon, Portugal.
- Paik J.K., Kim B.J., Sohn J.M., Kim S.H., Jeong J.M. and Park J.S. (2012b). On buckling collapse a fusion-welded aluminium stiffened plate structure: An experimental and numerical study, *Journal of Offshore Mechanics and Arctic Engineering*, Vol.134, pp.021402-021409.
- Paik J.K., Kim D.K., Lee H.S. and Shim Y.L. (2012a). A method for analyzing elastic large deflection behaviour of perfect and imperfect plates with partially rotation-restrained edges, *Journal of Offshore Mechanics and Arctic Engineering*, Vol.134, pp.021603-021614.
- Paik J.K., Kim D.K., Park D.H., Kim H.B., Mansour A.E. and Caldwell J.B. (2011a). Modified Paik-Mansour formula for ultimate strength calculations of ship hulls, *Proceedings of the 3rd International Conference on Marine Structures (MARSTRUCT 2011)*, Hamburg, Germany, pp. 187-202.
- Paik J.K., Kim S.J., Kim D.H., Kim D.C., Frieze P.A., Abbattista M., Vallascas M. and Hughes O.F. (2011b). Benchmark study on use of ALPS/ULSAP method to determine plate and stiffened panel ultimate strength, *Proceedings of the 3rd*

- International Conference on Marine Structures (MARSTRUCT 2011)*, Hamburg, Germany, pp.169-186.
- Paik J.K., Lee J.M. and Ko M.J. (2003). Ultimate strength of plate elements with pit corrosion wastage, *Journal of Engineering for Maritime Environment*, Vol. 217, pp.185-200.
- Paik J.K. and Melcher R.E. (ed) (2008). Condition assessment of aged structures, CRC Press, New York, USA.
- Paik J.K. and Pedersen P.T. (1996). A simplified method for predicting ultimate compressive strength of ship panels, *International Shipbuilding Progress*, Vol.43, No.434, pp.139-157.
- Paik J.K. and Seo J.K. (2009a). Nonlinear finite element method models for ultimate strength analysis of steel stiffened-plate structures under combined biaxial compression and lateral pressure actions - Part I: Plate elements, *Thin-Walled Structures*, Vol. 47, pp. 1008-1017.
- Paik J.K. and Seo J.K. (2009b). Nonlinear finite element method models for ultimate strength analysis of steel stiffened-plate structures under combined biaxial compression and lateral pressure actions - Part II: Stiffened panels, *Thin-Walled Structures*, Vol. 47, pp. 998-1007.
- Paik J.K. and Sohn J.M. (2012c). Effects of welding residual stresses on high tensile steel plate ultimate strength: nonlinear finite element method investigations, *Journal of Offshore Mechanics and Arctic Engineering*, Vol.134, pp.021401 (6 pages).
- Paik J.K. and Thayamballi A.K. (2003). Ultimate limit state design of steel-plated structures, John Wiley & Sons, Chichester, UK.
- Paik J.K. and Thayamballi A.K. (2007). Ship-shaped offshore installations: Design, building, and operation, Cambridge University Press, Cambridge, UK.
- Pan B.B., Cui W.C., Shen Y.S. and Liu T. (2010). Further study on the ultimate strength analysis of spherical pressure hulls, *Marine Structures*, Vol. 23, pp. 444-461.
- Park J.S., Chun M.S. and Suh Y.S. (2011). Development of advanced designed formulation to estimate the buckling/ultimate strength of curved plates, *Proceedings of the 3rd International Conference on Marine Structures (MARSTRUCT 2011)*, Hamburg, Germany, pp. 203-211.
- Park J.S., Fujikubo M., Iijima K. and Yao T. (2009). Prediction of the secondary buckling strength and ultimate strength of cylindrically curved plate under axial compression, *Proceedings of the 19th International Society of Offshore and Polar Engineers (ISOPE 2009)*, Osaka, Japan, Vol. 4, pp.740-747.
- Pei Z., Gao C., Tanaka Y., Tanaka S., Okazawa S., Iijima K., Fujikubo M. and Yao T. (2011). Collapse analysis of container ship model under combined bending and torsion applying idealized structural unit method, *Proceedings of the 21st International Society of Offshore and Polar Engineers (ISOPE 2011)*, Hawaii, USA, Vol. 4, pp. 894-901.
- Pei Z., Keiji Nakamaru K., Tanaka S., Okazawa S., Fujikubo M. and Yao T. (2010a). Development of isoparametric ISUM plate element, *Proceedings of the 20th International Society of Offshore and Polar Engineers (ISOPE 2010)*, Beijing, China, Vol. 4, pp. 781-788.
- Pei Z., Takami T., Gao C., Fu J., Tanaka Y., Iijima K., Fujikubo M. and Yao T. (2010b). Development of ISUM shear plate element and its application to progressive collapse analysis of plates under combined loading, *Proceedings of the 20th In-*

- ternational Society of Offshore and Polar Engineers (ISOPE 2010)*, Beijing, China, Vol. 4, pp. 773-780.
- Pesce C.P., Martins C.A., Neto A.G., Fajarra A.L.C., Takafuji F.C.M., Franzini G.R., Barbosa T., Godinho C.A.F. (2010). Crushing and wet collapse of flowline carcasses: A theoretical-experimental approach, *Proceedings of the 29th International Conference on Ocean, Offshore and Arctic Engineering (OMAE 2010)*, Shanghai, China, OMAE2010-20423.
- Piscopo V. (2010). Refined buckling analysis of rectangular plates under uniaxial and biaxial compression, *World Academy of Science, Engineering and Technology*, Vol. 71, ISSN1307-6892, pp.528-535.
- Piscopo V. (2011). Refined buckling analysis of plates under shear and uniaxial compression, *Proceedings of 14th International Maritime Association of the Mediterranean (IMAM 2011)*, Genoa, Italy.
- Puskar F.J., Westlake H.S., O'Connor P.E. and Bucknell J.R. (2006). The development of a recommended practice for structural integrity management (SIM) of fixed offshore platforms, *Proceedings of Offshore Technology Conference (OTC 2006)*, Houston, USA, OTC 18332.
- Qian X., Choo Y.S., van der Vegte G.J. and Wardenier J. (2009). Evaluation of the new IIW CHS strength formulae for thick-walled joints, *Tubular Structures XII*, edited by Shen, Z.Y., Chen Y.Y. and Zhao X.Z., pp.271-279.
- Rabiul Islam M. and Sumi Y. (2011). Geometrical effects on strength and deformability of corroded steel plates, *Proceedings of the 3rd International Conference on Marine Structures (MARSTRUCT 2011)*, Hamburg, Germany.
- Reany J. and Grenestedt J.L. (2009). Corrugated skin in a foam core sandwich panel, *Composite Structures*, Vol. 89, pp. 345-355.
- RINA (2011). Rules for the classification of steel ships, Registro Italiano Navale, Genova, Italy.
- Rizzo C.M., Figari M., Cervetto D. and Boote D. (2002). Ultimate strength of a ship: rule requirements and reliable assessment, *Proceedings of 13th International Maritime Association of the Mediterranean (IMAM 2002)*, Crete, Greece.
- Rizzuto E., Teixeira A. and Guedes Soares C. (2010). Reliability assessment of a tanker in damage conditions, *Proceedings of the 11th International Symposium on Practical Design of Ships and Other Floating Structures (PRADS 2010)*, Rio de Janeiro, Brazil, pp.1446-1458.
- Romanoff J., Laakso A. and Varsta P. (2009). Improving the shear properties of web-core sandwich structures using filling material, *Proceedings of the 2nd International Conference on Marine Structures (MARSTRUCT 2009)*, Lisbon, Portugal, pp. 133-138.
- Romanoff J., Naar H. and Varsta P. (2011). Interaction between web-core sandwich deck and hull girder of passenger ship, *Proceedings of the 11th International Symposium on Practical Design of Ships and Other Floating Structures (PRADS 2010)*, Rio de Janeiro, Brazil, pp. 1071-1078.
- Ruan D., Lu G.X. and Wong Y.C. (2010). Quasi-static indentation tests on aluminum foam sandwich panels, *Composite Structures*, Vol. 92, pp. 2039-2046.
- Saad-Eldeen S., Garbatov Y. and Guedes Soares C. (2011). Experimental assessment of the ultimate strength of a box girder subjected to severe corrosion, *Marine Structures*, Vol. 24, pp. 338-357.
- Saeidifar M., Sadeghi S.N. and Saviz M.R. (2010). Analytical solution for the buckling of rectangular plates under uni-axial compression with variable thickness and

- elasticity modulus in the y-direction, *Journal of Mechanical Engineering Science*, Vol. 224, No. 1, pp. 33-41.
- Schleyer G., Underwood N., Do H.M., Paik J.K. and Kim B.J. (2011). On the simplified analysis of square plates with holes, *Proceedings of the 30th International Conference on Ocean, Offshore and Arctic Engineering (OMAE 2011)*, Rotterdam, Netherlands, OMAE2011-49134.
- Seo J.K., Kim B.J., Ryu H.S., Ha Y.C. and Paik J.K. (2011). Validation of the equivalent plate thickness approach for ultimate strength analysis of stiffened panels with non-uniform plate thickness, *Thin-Walled structures*, Vol. 49, pp. 753-761.
- Shu Z. and Moan T. (2011). Reliability analysis of a bulk carrier in ultimate limit state under combined global and local loads in the hogging and alternate hold loading condition, *Marine Structures*, Vol. 24, pp. 1-22.
- Silva J.E., Garbatov Y. and Guedes Soares C. (2011). Ultimate strength assessment of aging steel plates subjected to random non-uniform corrosion wastage, *Proceedings of the 3rd International Conference on Marine Structures (MARSTRUCT 2011)*, Hamburg, Germany, pp. 213-220.
- Sousa, J.R.M., Viero P.F., Magluta, C. and Roitman, N. (2010). An experimental and numerical study on the axial compression response of flexible pipes, *Proceedings of the 29th International Conference on Ocean, Offshore and Arctic Engineering (OMAE 2010)*, Shanghai, China, OMAE2010-20856.
- Suneel Kumar M., Alagusundaramoorthy P. and Sundaravadivelu R. (2007). Ultimate strength of square plate with rectangular opening under axial compression, *Journal of Naval Architecture & Marine Engineering*, Vol. 4, pp. 15-26.
- Sun H. and Wang X. (2005a). Buckling and ultimate strength assessment of FPSO structures, *Trans. Society of Naval Architects and Marine Engineers*, Vol. 113, pp. 634-656.
- Sun H. and Wang X. (2005b). Procedure for calculating hull girder ultimate strength of ship structures, *Marine Systems & Ocean Technology*, Vol. 1, No. 3, pp.137-143.
- Taczala M. (2009). Approximate method for evaluation of stress-strain relationship for stiffened panel subject to tension, compression and shear employing the finite element approach, *Proceedings of the 2nd International Conference on Marine Structures (MARSTRUCT 2009)*, Lisbon, Portugal, pp. 155-161.
- Tanaka Y., Ando T., Anai Y., Yao T., Fujikubo M. and Iijima K. (2009). Longitudinal strength of container ships under combined torsional and bending moments, *Proceedings of the 19th International Society of Offshore and Polar Engineers (ISOPE 2009)*, Osaka, Japan, Vol.4, pp.748-755.
- Theobald M.D., Langdon G.S., Nurick G.N., Pillay S., Heyns A. and Merrett R.P. (2010). Large inelastic response of unbonded metallic foam and honeycomb core sandwich panels to blast loading, *Composite Structures*, Vol. 92, pp. 2465-2475.
- Tsuru E., Agata J. and Shinohara Y. (2010). The potential limit of compressive and tensile strain considering thermal aging and manufacturing strength range, *Proceedings of the 20th International Society of Offshore and Polar Engineers (ISOPE 2010)*, Beijing, China, Vol.4, pp.502-509.
- Ueda Y. and Yao T. (1985). The influence of complex initial deflection modes on the behaviour and ultimate strength of rectangular plates in compression, *Journal of Constructional Steel Research*, Vol. 5, No. 4, pp. 265-302.
- van der Vegte G.J. and Makino Y. (2010). Further research on chord length and boundary conditions of CHS T- and X-joints, *Advanced Steel Construction*, Vol. 6, pp.897-890.

- van der Vegte G.J., Wardenier J., Qian X.D. and Choo Y.S. (2010). Re-evaluation of the moment capacity of CHS joints, *Proceedings of Institution of Civil Engineers - Structures and Buildings*, Vol.163, pp.439-449.
- van der Vegte G.J., Wardenier J., Zhao X.L. and Packer J.A. (2009). Evaluation of new CHS strength formulae to design strengths, *Tubular Structures XII*, edited by Shen Z.Y., Chen Y.Y. and Zhao X.Z., pp.313-322.
- Vasilikis D. and Karamanos S.A. (2011). Buckling of clad pipes under bending and external pressure, *Proceedings of the 30th International Conference on Ocean, Offshore and Arctic Engineering (OMAE 2011)*, Rotterdam, Netherlands, OMAE2011-49470.
- Vhanmane S. and Bhattacharya B. (2011). Ultimate strength analysis of ship hull girder under random material and geometric properties, *Journal of Offshore Mechanics and Arctic Engineering*, Vol. 133, pp. 031602-031609.
- Wang F., Cui W.C. and Paik J.K. (2009). Residual ultimate strength of structural members with multiple crack damage, *Thin-Walled Structures*, Vol. 47, pp. 1439-1446.
- Wang G., Lee A., Ivanov L., Lynch T.J., Serratella C. and Basu R. (2008). A statistical investigation of time-variant hull girder strength of aging ships and coating life, *Marine Structures*, Vol. 21, pp. 240-256.
- Wang G., Sun H., Peng H. and Uemori R. (2009). Buckling and ultimate strength of plates with openings, *Ships and Offshore Structures*, Vol. 4, No. 1, pp. 43-53.
- Wang X., Sun H., Wang X., Wang Z. and Thayamballi A. (2010). Comparison study of various buckling and ultimate strength assessment criteria of stiffened panels in offshore structures, *Proceedings of the 29th International Conference on Ocean, Offshore and Arctic Engineering (OMAE 2010)*, Shanghai, China, OMAE2010-21053.
- Wang X., Yao T., Fujikubo M. and Basu R. (2011). Methodologies on hull girder ultimate strength assessment of FPSOs, *Journal of Offshore Mechanics and Arctic Engineering*, Vol. 133, pp. 031603-031608.
- Wardenier J., van der Vegte G.J., Makino Y. and Marshall P.W. (2009). Comparison of the new IIW (2008) CHS joint strength formulae with those of the previous IIW (1989) and the new API (2007), *Tubular Structures XII*, edited by Shen Z.Y., Chen Y.Y. and Zhao X.Z., pp.281-291.
- Witkowska M. and Guedes Soares C. (2009). Ultimate strength of stiffened plates with local damage on the stiffener, *Proceedings of the 2nd International Conference on Marine Structures (MARSTRUCT 2009)*, pp. 145-154.
- Xu M. and Guedes Soares C. (2011a). Comparison of numerical results with experiments on ultimate strength of short stiffened panels, *Proceedings of the 3rd International Conference on Marine Structures (MARSTRUCT 2011)*, Hamburg, Germany, pp. 221-228.
- Xu M. and Guedes Soares C. (2011b). Comparison of numerical results with experiments on the ultimate strength of long stiffened panels, *Proceedings of the 30th International Conference on Ocean, Offshore and Arctic Engineering (OMAE 2011)*, Rotterdam, Netherlands, OMAE2011-50294.
- Xu M. and Guedes Soares C. (2011c). Numerical study of the effect of geometry and boundary conditions on the collapse behaviour of short stiffened panels, *Proceedings of the 3rd International Conference on Marine Structures (MARSTRUCT 2011)*, Hamburg, Germany, pp. 229-237.
- Xu W., Iijima K. and Fujikubo M. (2011a). Hydro-elastoplasticity approach to ship's hull girder collapse behaviour in waves, *Proceedings of the 3rd International Conference on Marine Structures (MARSTRUCT 2011)*, Hamburg, Germany, pp. 239-247.

- Xu W., Iijima K. and Fujikubo M. (2011b). Investigation into post-ultimate strength behaviour of ship's hull girder in waves by analytical solution, *Proceedings of the 30th International Conference on Ocean, Offshore and Arctic Engineering (OMAE 2011)*, Rotterdam, Netherlands, OMAE2011-49617.
- Yang S.H., Chien H.L., Chou C.M., Tseng K.C. and Lee Y.J. (2011). A study on the dynamic buckling strength of containership's bow structures subjected to bow flare impact force, *Proceedings of the 3rd International Conference on Marine Structures (MARSTRUCT 2011)*, Hamburg, Germany, pp. 249-255.
- Yao T., Fujikubo M., Iijima K. and Pei Z. (2009). Total system including capacity calculation- Applying ISUM/FEM and loads calculation for progressive collapse analysis of ship's hull girder in longitudinal bending, *Proceedings of the 19th International Society of Offshore and Polar Engineers (ISOPE 2009)*, Osaka, Japan, Vol. 4, pp. 748-755.
- Yao T. and Nikolov P.I. (1991). Progressive collapse analysis of a ship's hull under longitudinal bending, *Journal of Society of Naval Architects of Japan*, Vol. 170, pp. 449-461.
- Ye Q., He Y., Jin W.L. and Qu Y. (2011). Assessment of ultimate strength of semi-submersible platform using nonlinear finite element method, *Proceedings of the 30th International Conference on Ocean, Offshore and Arctic Engineering (OMAE 2011)*, Rotterdam, Netherlands, OMAE2011-49415.
- Yoon J.W., Bray G.H., Valente R.A.F. and Childs T.E.R. (2009). Buckling analysis for an integrally stiffened panel structure with a friction stir weld, *Thin-Walled structures*, Vol. 47, pp. 1608-1622.
- Yoon S.H. and Lee D.G. (2011). Design of the composite sandwich panel of the hot pad for the bonding of large area adhesive films, *Composite Structures*, Vol. 94, pp. 102-113.
- Zhang S. and Khan I. (2009). Buckling and ultimate capability of plates and stiffened panels in axial compression, *Marine Structures*, Vol. 22, pp. 791-808.
- Zhao X.L., Wardenier J., Packer J.A. and van der Vegte G.J. (2010). Current static design guidance for hollow-section joints, *Proceedings of Institution of Civil Engineers - Structures and Buildings*, Vol.163, pp.361-373.
- Zhou Y.X. and Huang Z.M. (2008). A modified ultimate failure criterion and material degradation scheme in bridging model prediction for biaxial strength of laminates, *Journal of Composite Materials*, Vol. 42, pp. 2123-2141.

